IDENTIFICATION OF NOVEL GENETIC ALTERATIONS IN THE PROGRESSION OF LUNG AND ORAL CANCER

by

CATHIE GARNIS

B.Sc., The University of British Columbia, 2000

A THESIS SUBMITTED IN PARTIAL FULFILMENT OF
THE REQUIREMENTS FOR THE DEGREE OF

DOCTOR OF PHILOSOPHY

in

THE FACULTY OF GRADUATE STUDIES

(Pathology and Laboratory Medicine)

THE UNIVERSITY OF BRITISH COLUMBIA

April 2005

ABSTRACT

The major etiological factor for oral and lung cancer is tobacco and both diseases have poor survival and high recurrence rates. In order to facilitate early diagnosis and lay the groundwork for new treatment strategies, we must determine the genetic alterations that drive these diseases. Due to the genomic instability associated with late stage tumors, early causal genetic changes will be best identified by studying both premalignant lesions and invasive tumors. The overall objective of this thesis is to identify genetic alterations that are associated with the progression of lung and oral cancer and to further assess if these changes are of biological importance. This will help to identify candidate genes for use as diagnostic markers and/or therapeutic targets. The first genome-scanning technique used was a PCR-based technique: RAPD-PCR. From this analysis we cloned and localized 15 recurrent alterations in the lung and oral samples. Two of these alterations, 13q14 and 8q22, were further fine mapped using microsatellite analysis to reveal two candidate genes: *AKAP220* and *ST7*. The remaining regions identified with RAPD-PCR were then fine-mapped by comparative genomic hybridization (CGH) using a bacterial artificial chromosome (BAC) array. We called this array the regional array as it contained 26 selected regions as well as complete coverage of chromosome arms 1p, 3p, and 5p. This methodology identified numerous novel regions of alteration and highlighted the value of the premalignant lesion: we found that there were fewer alterations in the premalignant lesions as well as some discrete changes that were masked in the later stage samples. We expanded this approach by using a new CGH array that covers the entire genome and have profiled various histopathological

stages in both oral and lung cancer. This new tool is ideal for novel gene discovery as no prior knowledge of regions is required. Whole genome profiling of different histopathological stages for both oral and lung cancer has given us insight into the genetic alterations associated with the progression of these diseases. While oral and lung cancer share some similarities, such as the early loss of chromosome 3p and 9p, there are also some drastic differences. By combining high resolution CGH tiling arrays with precious pre-invasive material we have for the first time produced a comprehensive view of oral and lung pre-invasive lesion genomes. In doing this, we have identified numerous recurrent novel genetic alterations and have shown the biological relevance of these alterations through expression analysis. In the future these candidates will serve as potential diagnostic makers and therapeutic targets.

TABLE OF CONTENTS

LIST OF TABLES

LIST OF FIGURES

ABBREVIATIONS

AFLP – amplified fragment length polymorphism
AI – allelic imbalance
AP-PCR – arbitrarily primed PCR
BAC – bacterial artificial chromosome
BLAST – basic local alignment search tool
BLAT – basic local alignment tool
CGH – comparative genomic hybridization
CIS – carcinoma in situ
CT – computed tomography
FISH – fluorescent in situ hybridization
HNSCC – head and neck squamous cell carcinoma
LM – linker mediated
LOH – loss of heterozygosity
Mbp – mega base pair
MRA – minimal region of alteration
NA – not available
NCBI – National Center for Biotechnology Information
NSCLC – Non-small cell lung carcinoma
OPL – oral premalignant lesions
OSCC – oral squamous cell carcinoma
PCR – polymerase chain reaction
RAPD – randomly amplified polymorphic DNA
RT-PCR – reverse transcriptase PCR
SCC - squamous cell carcinoma
SCLC – small cell lung carcinoma
SD – standard deviation
SDS – sodium dodecyl sulfate
SKY – spectral karyotyping
SMRT – sub megabse resolution tiling
SNP- single nucleotide polymorphism
UCSC – University California Santa Cruz
WLB – white light bronchoscopy

ACKNOWLEDGEMENTS

There are a number of individuals who have contributed to the work described in this thesis. I would like to acknowledge my fellow lab members, Bradley P. Coe, Corisande Baldwin, Jonathan J. Davies, and Timon Buys who were invaluable in putting together the manuscripts describing this work. I would also like to thank Jennifer (C-Toe) Campbell and Emily Vucic for their technical assistance and for making me laugh everyday, the BAC array production group for providing me with arrays, members of the Rosin Lab for LOH analysis and for providing clinical material for the oral cancer projects, Dr. Jean LeRiche, Chris Dawe, and Arek Siwoski for their help in microdissecting the CIS lung lesions and Drs. Calum MacAulay and Stephen Lam for their assistance with the lung cancer projects. I would also like to thank Laura Jane Henderson and Timon Buys for their amazing editing skills. I also would like to thank all of my friends and family, especially Timon, for their love and support and of course a very special thanks to my supervisor Dr. Wan Lam for believing in me, supporting me, and (of course) feeding me!

1. BACKGROUND

1.1 Epithelium

The epithelium covers or lines body surfaces, cavities, and tubes and serves a wide range of functions including selective diffusion, absorption/secretion, protection, and containment. Epithelial cells are attached to each other by cell junctions which allow cell cross talk and metabolite exchange. All epithelia are supported by a basement membrane that separates the epithelium from the underlying tissue. Because the epithelium does not contain blood vessels, all oxygen and metabolites are received from adjacent tissue.

Epithelium is sub-classified on the basis of the number of cell layers and the morphology of the surface cells. A single layer of cells is termed "simple", while numerous layers are referred to as "stratified". A single layer of cells is "pseudostratified" when all cells are attached to the basement membrane but not all cells reach the surface. With respect to morphological divisions, flat surface cells are referred to as "squamous" while cells of equal height and width are termed "cuboidal" and cells of greater height are called "columnar" (Burkitt et al., 1993; Eroschenko, 2000)(Figure1).

1.2 Oral Epithelium

Major structures in the oral cavity include the lips, teeth, tongue, oral mucosa, and any associated salivary glands. The main functions of the oral cavity include speech,

facial expressions, sensory reception, digestion, and breathing. The entire oral cavity is lined by a mucous membrane called the oral mucosa. The epithelial portion of the oral mucosa is stratified squamous and tends to be keritinized in areas that are prone to friction (Burkitt et al., 1993; Eroschenko, 2000).

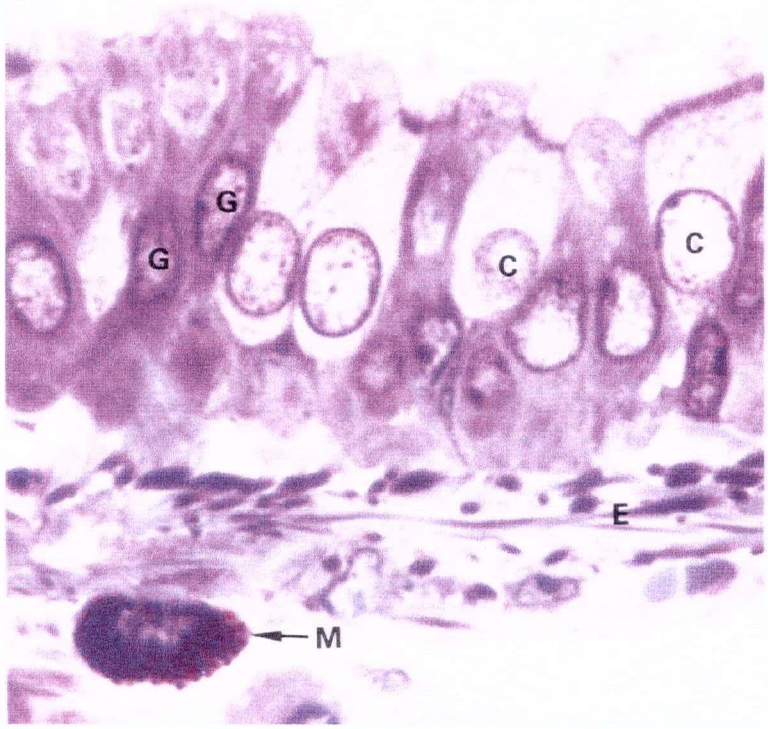

Figure 1. Bronchial Epithelium. Micrograph of the bronchial epithelium stained with toludine blue. (C) Ciliated Cells. (G) Goblet Cells. (E) Elastin. (M) Mast Cells (Burkitt et al., 1993).

1.3 Respiratory Epithelium

The respiratory system consists of two lungs and numerous air passages. Conducting passages consist of solid air passages both inside and outside the lung and are responsible for bringing air to the lungs (Figure 2). Respiratory passages exist solely within the lung and are the site of gas exchange. The upper respiratory tract consists of the nasal cavity, paranasal sinuses, and nasopharynx. It is primarily involved in filtering, humidifying, and adjusting the temperature of inspired air. This portion of the respiratory tract is lined with pseudostratified columnar epithelium with numerous goblet cells. The lower respiratory tract begins at the larynx and proceeds to the trachea before dividing into numerous smaller airways: left and right primary bronchi divide into secondary bronchi, then tertiary bronchi, then bronchioles, then through a series of transitional airways (these are involved in gaseous exchange), then into dilated spaces called alveolar sacs, and, finally, into the alveoli (Burkitt et al., 1993; Eroschenko, 2000).

Each type of airway has its own characteristic structural features but the transition is gradual. Generally, the airways are pliable tubes lined with respiratory mucosa containing variable amounts of muscle and cartilage. The diameter of the air passage becomes progressively smaller and there is also a gradual decrease in the height of the lining of the epithelium, the amount of cilia, and the number of goblet cells in the tubes.

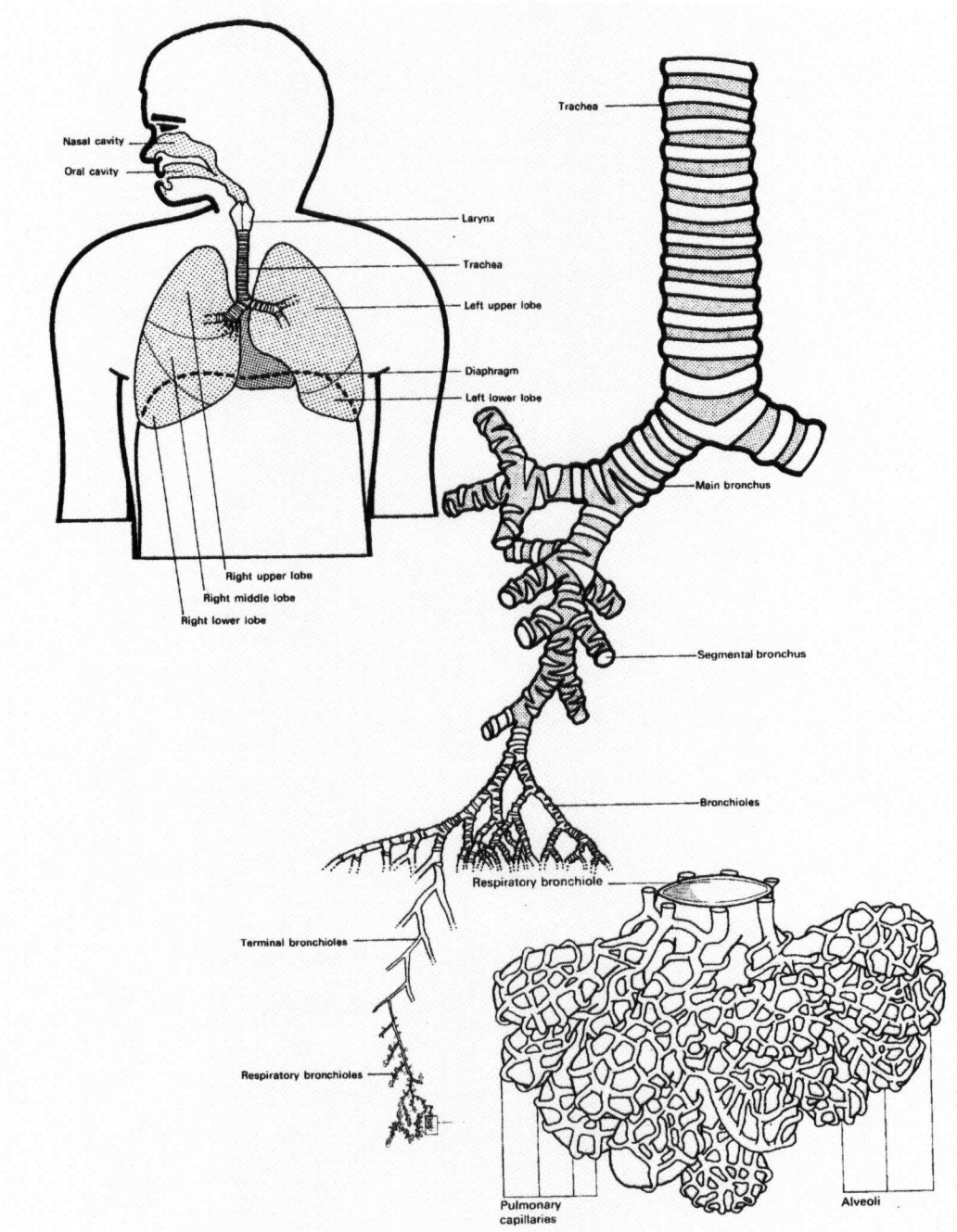

Figure 2. Structure of the Respiratory System (Burkitt et al., 1993).

1.4 Oral Cancer

Oral cancer is among the ten most common cancers worldwide and, in parts of Asia and Latin America, it is the most common cancer (http://www.oralcdx.com/store/index.aspx). The incidence of this disease is increasing in developing countries (Macfarlane et al., 1994; Parkin et al., 1999). Head and neck squamous cell carcinoma (HNSCC) accounts for about 3% of all malignancies with an estimated 37,200 new cases and 11,000 deaths in the United States. The main etiological factors are tobacco and alcohol use and, to a lesser extent, nutrition, occupation, viral infection, and poor dentition (Jemal et al., 2003; Maier et al., 1991). Oral cancer has a poor prognosis and a high rate of recurrence. Second primary tumors are estimated to occur at an annual rate of 3-10% and are significant threats to long term survivors (Sturgis and Miller, 1995). The survival rate for second primary tumor patients is less than 5 years (Brunin et al., 1999; Silverman and Gorsky, 1990). Despite therapeutic advances in treatment, overall survival rate has not changed in the last 2 decades, presumably due to the development of the secondary tumors.

Oral cancer progresses through various histopathological stages, from hyperplasia, various stages of dysplasia, carcinoma in situ, and finally invasive tumor (Figure 3). There are two types of precancerous oral lesions: leukoplakia and erythroplakia (red patches). Both show varying degrees of dysplastic change. In general, erythroplakia contains more severe dysplasia and is more likely to progress. Leukoplakia, however, comprises the biggest group of precancerous lesions (Shafer and Waldron, 1975).

Oral leukoplakia is a white-plaque mucosal lesion that confers increased risk for the development of squamous cell carcinoma (SCC). 5-15% of oral white patches are classified as dysplasia (Suarez et al., 1998). Of these, only 15-20% develop into carcinoma (Lumerman et al., 1995). Treatment for oral leukoplakia is removal via surgery or laser. However, because histology is of limited prognostic value, therapeutic intervention is considered only where there is evidence of transition to carcinoma in situ or carcinoma. Hence, there is a need for the identification of molecular targets that predict outcome from the early pre-invasive lesions (Zhang et al., 1997a).

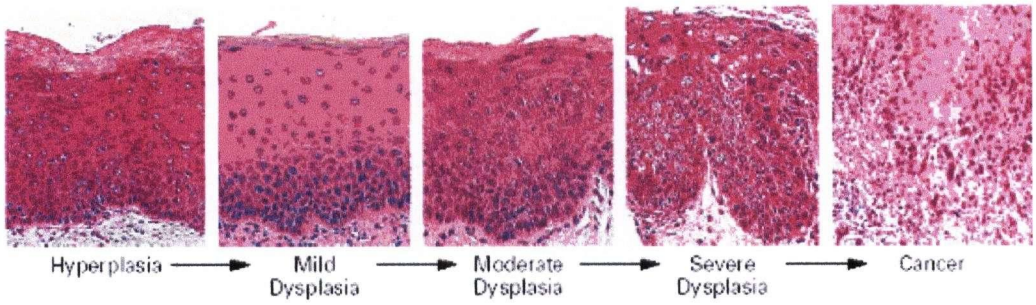

Figure 3. Histopathological Progression of Squamous Cell Oral Carcinoma (Lippman and Hong, 2001).

1.5 Lung Cancer

Lung cancer is the leading cause of cancer-related deaths in industrialized countries. As in oral cancer, the major etiological factor is tobacco use (Ahsan and Thomas, 2004). While the rate of lung cancer incidence has decreased slightly for men in the United States over the past decade, the mortality rate for women diagnosed with lung cancer continues to increase. Smoking cessation alone will not alleviate the burden of lung cancer on the health care system since ex-smokers are still at an elevated risk for developing the disease (Doll, 1981).

There are two major types of lung cancer: small-cell lung cancer (SCLC) and non-small cell lung cancer (NSCLC). SCLC accounts for approximately 20% of all lung cancers. It is characterized by its origin in large central airways and histological composition of sheets of small cells with little cytoplasm. SCLCs are tumors of neuroendocrine origin and they are very aggressive, metastazing early. Prognosis for SCLC is poor. NSCLC can be further classified into three different subtypes: squamous cell carcinoma, adenocarcinoma and large cell carcinoma. Large cell carcinoma represents 10-20% of bronchogenic tumors. These tumors lack diagnostic features to suggest their diagnosis prior to biopsy and they tend to grow rapidly and metastasize early.

Adenocarcinoma is the most common type of lung cancer, accounting for 30-35% of all cases (http://www.lungcanceronline.org/info/types.html). Over the past 30 years, the frequency of adenocarcinomas has increased, while SCC incidence has decreased. Adenocarcinoma is the most common cause of lung cancer in women and non-smokers. The majority of adenocarcinomas occur at the periphery of the lung and, as a result, are

often asymptomatic until later in the progression of the disease.

SCC accounts for approximately one third of all cases of bronchogenic carcinomas. Unlike adenocarcinoma, it is strongly linked with a history of cigarette smoking. Most SCCs arise centrally from either the main, lobar, or segmental bronchi and their central location tends to produce symptoms at an earlier stage than tumors located peripherally. Histological and cytological studies have shown that a series of changes occur over many years and represent a morphologic progression to bronchogenic carcinoma. Early changes include a loss of the ciliated columnar epithelium, basal cell hyperplasia, and the formation of a low columnar epithelium without cilia. These changes are followed by a squamous metaplasia. As cellular atypia develops and advances there is progression, like oral cancer, through mild, moderate and severe dysplasia, to carcinoma in situ, and finally to invasive carcinoma which is capable of widespread metastasis (Figure 4)(Minna et al., 2002).

The poor prognosis for lung cancer patients (overall 5 year survival rate is 14%) is attributed to multiple factors including: 1) the lack of sensitive methods for early diagnosis, 2) the development of metastases when primary tumors are still small, and 3) the absence of systemic therapies capable of dealing with micrometastatic disease with great efficacy (Travis et al., 1995).

Patients with early stage lung cancer show the best response to therapies and exhibit the greatest survival rate compared to patients with the advanced stage disease. However, with current screening techniques, 65% of patients present with advanced stage disease at the time of diagnosis. Hence new methods for early detection and diagnosis are necessary.

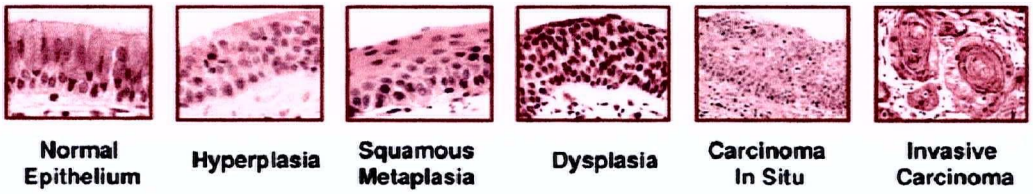

Figure 4. Histopathological Progression of Squamous Cell Lung Cancer (Minna et al., 2002).

Management of lung cancer patients is dictated by disease subtype (SCLC vs NSCLC) and also tumor size, location, and stage. Both traditional X-ray and computed tomography (CT) radiographical imaging analyses are commonly used to visualize abnormalities in the chest. Numerous studies have demonstrated that CT provides superior detection of early stage and small size lung cancer (1 mm compared to 10 mm) (McWilliams et al., 2002). Sone et al. reported that X-rays fail to detect up to 77% of cancers that were detected by CT analysis (Sone, 2000). However, this improved sensitivity is associated with a high rate of false positives and may not have the resolution required to detect pre-invasive cancers in the central airways (Kakinuma et al., 1999).

White light bronchoscopy (WLB) is the most common tool used for detecting early stage cancers in the central airways. However, because these lesions are small and often lack characteristics that would make them visible on white-light bronchoscopy (WLB), they are frequently not observed with this method. Fluorescence bronchoscopy and the development of the Laser-induced fluorescence endoscopy (LIFE)-Lung device facilitates the identification of premalignant lesions (Palcic et al., 1991). LIFE was developed to detect high-grade (moderate to severe) dysplasia and CIS by tissue autofluorescence. Several studies have compared the diagnostic specificity and sensitivity of the LIFE bronchoscope and WLB with respect to pre-invasive and early invasive lesions. Most of these studies report a higher sensitivity for the LIFE bronchoscopy but with lower specificity (Kennedy et al., 2000).

Screening of sputum samples for malignant cells has been instrumental in identifying malignancies in patients with a high risk of developing lung cancer. Controlled trials sponsored by the NCI show that both chest radiography as well as

sputum cytology can detect pre-symptomatic, early stage carcinoma. While resectability and survival rates were found to be higher in the study groups than the control groups these improvements did not lead to a reduction in overall mortality (Fontana et al., 1986; Melamed and Flehinger, 1984). Although the average specificity of sputum cytology for lung cancer diagnosis is high, the sensitivity is low and therefore there is a need for new techniques/biomarkers that can detect early pre-invasive lung cancer (Bocking et al., 1992).

1.6 Field Cancerization and Multi-step Process

Tumors of the aerodigestive tract have been proposed to reflect a field cancerization process whereby the whole tissue is exposed to carcinogenic abuse and as a result is at greater risk for multi-step tumor development (Farber, 1984; Ha and Califano, 2003). Field cancerization was proposed by Slaughter et al. in the 1950s to account for their observation of multifocal SCC in the oral cavity (Slaughter et al., 1953). There is an abundance of evidence to support this including the frequent occurrence of synchronous primary and subsequent secondary tumors that exhibit dissimilar histologies as well as distinct genetic signatures in these tissues (Chung et al., 1993; Scholes et al., 1998).

Tumorigenesis occurring in these tissues is believed to be a multi-step process where tumors originate from a progression of genetic or epigenetic changes in a monoclonal fashion (Ruddon, 1995). The statistical model for the multi-step process

suggests that 6-10 different genetic events are required to create a malignant cell (Renan, 1993; Steen, 2000). There are three basic principles of the multi-step process:

1) neoplasms are the result of tumor supressor gene inactivation and/or proto-oncogene activation,

2) there exists a defined order of genetic events leading to the development of a tumor phenotype, and

3) variations on the order of genetic events are possible because it is ultimately the net accumulation of genetic alterations that determines the tumor phenotype (Fearon and Vogelstein, 1990).

1.7 Current Genomic Scanning Techniques

To identify the genetic alterations associated with the progression of lung and oral cancer a number of techniques have been used. Gene discovery has been greatly facilitated by molecular cytogenetic technologies identifying chromosomal regions associated with various stages and outcomes. Furthermore, high throughput, genome wide approaches and the complete sequencing of the human genome have accelerated the large-scale discovery of cancer-related genes and pathways (Baak et al., 2003).

To date, genomic and proteomic efforts have been primarily directed at the study of tumors (Garnis et al., 2004a). The relatively limited literature on genetic studies of earlier stage cancers is attributable to challenges associated with accessing premalignant specimens and the fact that genome wide analysis would require quantities of material far exceeding the size of the minute specimens obtained.

Current methods for genome wide detection of genetic alterations in tumors fall into three main categories: (1) molecular cytogenetic evaluation of chromosomal aberrations and re-arrangements, (2) DNA polymorphism analysis for detecting loss of heterozygosity (LOH) or allelic imbalance (AI), and (3) comparative genomic hybridization (CGH) approaches for identifying segmental copy number changes.

1.7.1. Molecular Cytogenetics

Cytogenetic approaches are designed to detect aberrations and rearrangements under direct examination of chromosomes and chromosomal targets. G-banding, fluorescence in situ hybridization (FISH), and spectral karyotyping (SKY) are the commonly used methods (Bayani and Squire, 2002b; Roylance, 2002). G-banding is often used in clinical settings for the analysis of leukemia and is best suited to detect large chromosomal aberrations, namely structural or numeric changes (Zhao et al., 2001). This method evaluates stained metaphase chromosome spreads to identify rearrangements and gain or loss of chromosome bands. One of the most comprehensive databases of cytogenetic information for various tumor types is the Mitelman Database of Chromosome Aberrations in Cancer (Mitelman et al., 2003).

FISH has helped bridge the gap between molecular genetics and classical cytogenetics. This technology uses specific DNA probes of known chromosomal location to evaluate alterations at a specific locus on a cell-by-cell basis (Macoska et al., 2000). Gain, loss, and splitting of hybridization signals on metaphase or interphase chromosomes reflect duplication, deletion, and translocation events respectively (Trask, 1991). FISH is useful in fine-mapping genetic alterations in very small specimens such

as premalignant lesions since it does not require microdissection. With the development of fluorochromes that fluoresce at different wavelengths, multicolor FISH (M-FISH) has enabled the examination of multiple loci in the same experiment (Gray et al., 1991).

SKY uses 24 different probe sets to virtually paint each chromosome a different color. This technique involves the simultaneous excitation of multiple fluorochromes and the use of an interferometer to determine the profile at each pixel (Bayani and Squire, 2002a).

Although whole genome cytogenetic techniques are limited to the identification of intrachromosomal rearrangements and breakpoint determination, they have been the preferred techniques for detailed karyotypic assessment of structural chromosome aberrations (Bayani and Squire, 2002a).

1.7.2 Assessing LOH Using Microsatellite Markers

Microsatellite analysis uses simple sequence repeat polymorphisms as markers for detecting LOH. A polymerase chain reaction (PCR) using primers flanking a repeat should yield two signals corresponding to the two heterozygous alleles. When the signal intensity ratio of the tumor alleles differs from that of the normal alleles, AI or LOH is inferred. It should be noted that microsatellite analysis can not distinguish between deletion or amplification. Additional experiments such as fluorescence in situ hybridization (FISH) are required to distinguish between these events. An example of mapping of LOH at the chromosome scale was the use of 28 markers spanning chromosome 3p to determine three distinct regions of alteration in NSCLC (Wistuba et al., 2000). In addition, microsatellite analysis is commonly used for fine mapping

minimal regions of LOH. However, this approach is limited by the availability of polymorphic markers in the chromosomal regions of interest. For microdissected, minute premalignant specimens, DNA yield is an additional limitation since each marker requires at least five nanograms of DNA per assay (Zhang et al., 1997a). Therefore, although genome wide allelotyping has been applied to early stage cancer, efforts have been largely focused on tumors and cell lines where material is not limiting (Li et al., 2002; Maitra et al., 2001; Simpson et al., 2003; Wistuba et al., 2002).

Single nucleotide polymorphisms (SNPs) are another source of DNA markers used in identifying LOH. SNPs are common in the human genome and in some instances their variation can be correlated to disease behaviour (Kallioniemi, 2001; Wang et al., 1998). The through-put of this approach is greatly enhanced by parallel analysis of multiple loci on microarrays. For example, GeneChip® arrays from Affymetrix® have enabled simultaneous tracking of approximately 1,500 SNPs (Lindblad-Toh et al., 2000). The large number of SNPs examined would compensate for the fact that not all loci will be informative (heterozygous). The recently released "Mapping 10K Array" tracks greater than 10,000 SNPs distributed throughout the genome should increase the information content of an array hybridization experiment (Matsuzaki et al., 2004).

Unlike microsatellite or SNP analyses, amplified fragment length polymorphism (AFLP)-based approaches require no previous knowledge of polymorphisms. Fingerprinting techniques such as random amplification of polymorphic DNA (RAPD) or arbitrarily primed PCR (AP-PCR) use short primers of 10 to 20 nucleotides to amplify multiple fragments randomly distributed throughout the genome. The PCR products are then separated by electrophoresis to display up to dozens of anonymous DNA

polymorphisms (Figure 5)(Siwoski et al., 2002; Welsh and McClelland, 1990; Williams et al., 1990). It has been applied to a variety of tumor types to study genomic instability, to identify novel DNA amplifications and deletions, and to assess changes in methylation state (Arribas et al., 1997; de Juan et al., 1998; Navarro and Jorcano, 1999; Odero et al., 2001; Scarpa et al., 2001; Viswanathan et al., 2003; Yamada et al., 2000). The recently developed methylation-sensitive AFLP (MS-AFLP) technology allows for an unbiased assessment of epigenetic changes in a subset of methylation sites throughout the genome (Yamamoto et al., 2001; Yamashita et al., 2003). However, the use of RAPD patterns in predicting prognosis has not yet been widely used.

1.7.3 Comparative Genomic Hybridization

Comparative Genomic Hybridization (CGH) detects segmental DNA copy number changes. Differentially labeled tumor DNA and control normal DNA are co-hybridized to a metaphase chromosome spread, producing an average fluorescence ratio profile at approximately 20 Mbp resolution (Pinkel et al., 1998). Copy number changes in a variety of cancers – and to a lesser extent, premalignant lesions – have been detected using this method (Kashiwagi and Uchida, 2000; Kiechle et al., 2000; Kirchhoff et al., 1999; Kirchhoff et al., 2001; Marchio et al., 2001; Oga et al., 2002; Tachdjian et al., 2000). While CGH provides a profile of the entire genome, the resolution is limited and therefore it is difficult to determine the identity of specific gene alterations. CGH is often used in conjunction with FISH in order to fine-map alterations to the gene level. As

CGH has become a more widely used method, profile databases have been assembled for public access such as http://www.progenetix.net/ and http://amba.charite.de/cgh/.

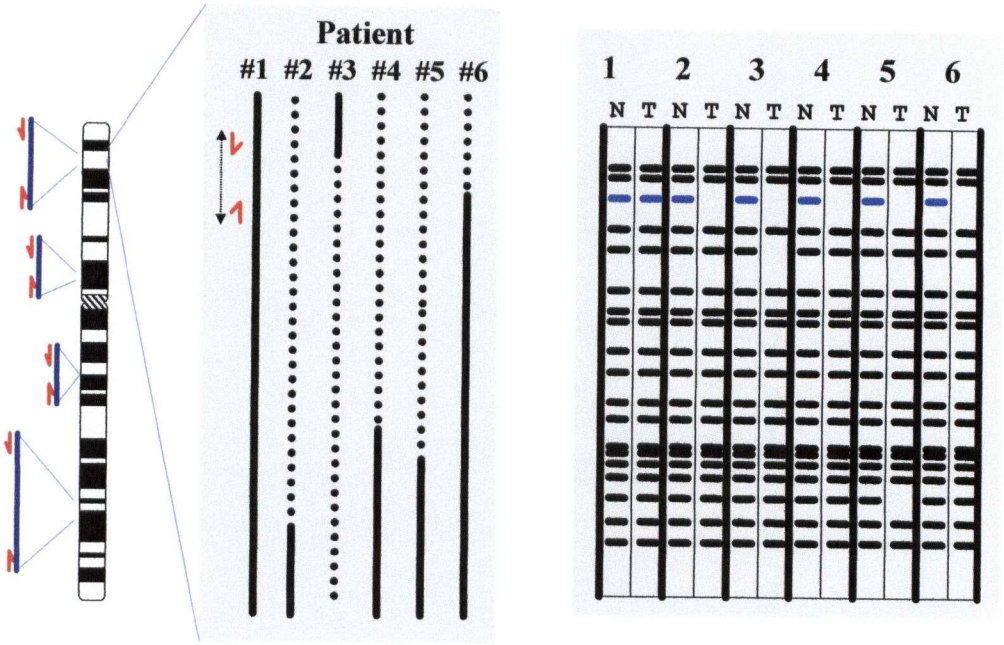

Figure 5. Schematic Representation of Randomly Amplified Polymorphic DNA PCR Analysis of Tumor DNA. Panel A shows chromosome with multiple binding sites for selected primers (red arrows). Panel B is a representation of a given locus in six different patients. Patient 1 contains both primer sites, patients 2, 4, and 5 contain neither sites, and patients 3 and 6 contain only one of the primer sites. Solid line represents normal chromosome, while the dotted line represents regions of chromosomal loss. Panel C displays the DNA fingerprints for paired normal and tumor DNA from these six individuals. The blue bands correspond to fragments indicated in Panel B (Garnis et al., 2004a).

1.7.4 Array Based CGH

Until recently, localized deletion mapping using microsatellite markers has represented the highest resolution method available to identify potential tumor suppressor genes. However, new approaches based on the use of genomic microarrays have been developed. To achieve higher resolution, Pollack et al. made use of cDNA microarrays for analyzing genomic DNA derived probes (Lucito et al., 2003; Pollack et al., 2002). However this approach is hampered by suboptimal hybridization which arises because the genomic DNA probe that is used has introns that are absent in the spotted cDNA target. As mentioned above, the recent development of SNP arrays has greatly facilitated deletion detection. However, the resolution of SNP arrays is currently limited to approximately 10,000 SNPs. One would expect that only a subset of these loci will be informative (heterozygous). Another technology called representational oligonucleotide microarray analysis (ROMA) provides a means of detecting genetic alterations in cancer tissue using a high density oligonucleotide array to profile subtractive hybridization products generated through representational differential analysis (Lisitsyn and Wigler, 1993; Lucito et al., 2003).

Complementary to these array-based CGH techniques, bacterial artificial chromosome (BAC) array CGH allows the detection of segmental copy number changes (Pinkel et al., 1998). BAC array CGH is similar to conventional chromosomal CGH except that it uses segments of human DNA as hybridization targets instead of a metaphase spread of chromosomes (Albertson and Pinkel, 2003; Ishkanian et al., 2004; Pinkel et al., 1998; Solinas-Toldo et al., 1997). Hybridization onto such arrays overcomes the low resolution that limits conventional CGH. As with conventional CGH,

total genomic DNA from a tumor and a normal cell population are differentially labeled and co-hybridized onto an array. The ratio of the fluorescence intensities on each DNA spot on the array is proportional to the copy number of the corresponding sequence.

High resolution arrays allow for the delineation of amplification and deletion boundaries in a single experiment. These arrays have been instrumental in detailed analysis of specific chromosomal regions (Albertson, 2003; Bruder et al., 2001; Garnis et al., 2004b; Garnis et al., 2004c; Garnis et al., 2004d; Garnis et al., 2004e). High resolution analysis of entire chromosome arms for segmental copy number alterations is made possible with whole chromosome or chromosome arm BAC arrays (Buckley et al., 2002; Garnis et al., 2003).

The application of this technology for genome wide profiling was first described by Snijders et al., who used 2460 marker BACs and P1 clones to generate an array with clones positioned at ~1.4 Mbp intervals (Snijders et al., 2001). Arrays of similar resolution have been reported by other groups (Chung et al., 2004; Greshock et al., 2004). This technology has been applied to analyze cell lines and tumors from lymphoma, bladder, breast, prostate, and kidney (Albertson, 2003; Kraus et al., 2003; Paris et al., 2003; Sanchez-Izquierdo et al., 2003; Veltman et al., 2003; Wilhelm et al., 2002)

Further advancement of this technology to tiling resolution of the whole genome has eliminated the need for inferring continuity between marker BACs. This was achieved by using an ordered set of 32,433 BAC clones that provide full coverage of the genome, allowing the profiling of the entire genome in a single experiment (Ishkanian et al., 2004).

1.8 Genetic Alterations in Lung and Oral Cancer

The molecular alterations associated with lung and oral cancers are mainly due to oncogene activation and/or tumor suppressor gene inactivation leading to deregulation of cell proliferation. Oncogenes are altered growth-promoting regulatory genes that govern cell signal transduction pathways and mutation of these genes leads to either overproduction or increased function of the resulting protein while tumor suppressor genes are "gatekeepers" of cellular proliferation. They can either inhibit cell growth or promote cell death. Mutations in a number of tumor suppressor genes as well as oncogenes are common to both cancer types. These include *RAS*, *MYC*, *CyclinD1 (CCND1)*, *Epidermal Growth Factor Recepter (EGFR)*, *TP53*, *Cyclin Dependent Kinase Inhibitor 2A* (*CDKN2A*), and *Fragile Histidine Triad* (*FHIT*).

1.8.1 Oncogenes

The RAS family includes three closely related genes *HRAS*, *KRAS*, and *NRAS*, each encoding a 21-kDa guanosine-triphosphate (GTP)-binding protein that attaches to the inside of the cell membrane and transduces molecular signals to the nucleus. Mutation in RAS causes the protein to lose its capability to hydrolyze GTP resulting in the permanent active state of the *RAS* protein and continued growth signal transduction. Common *RAS* mutations occur as single point mutations at codons 12, 13, or 61 occurring in 20-30% of adenocarcinomas and 15-20% of squamous carcinomas (Gazdar et al., 1994; Sekido et al., 1998; Sugio et al., 1994). In head and neck squamous cell

carcinoma (HNSCC), *RAS* mutations have been identified in less than 5% of patients from the Western world (Yarbrough et al., 1994) however, 35% *H-RAS* mutations have been described in patients from India (Saranath et al., 1991).

MYC family members (*CMYC*, *NMYC*, and *LMYC*) encode for a transcription factor activated by the RAS signaling pathway. Overexpression of *MYC* changes the regulation of many genes and contributes to malignant transformation. The frequency of *MYC* amplification and/or overexpression in HNSCC varies from 9-48% while the reports for lung cancer are 8% (Richardson and Johnson, 1993; Yin et al., 1991).

Cyclin D1, located at 11q13, encodes a critical cell cycle regulatory protein that drives the cell cycle from the G1 to the S phase of the cell cycle. Cyclin D1 binds a cyclin dependent kinase, CDK4 or CDK6, and phosphorylates and inactivates Rb resulting in the release of bound E2F resulting in cell cycle progression. Amplification of the 11q13 region has been reported in 70% of primary HNSCC (Bockmuhl et al., 1998) and overexpression has been observed in 39-64% of cases (Akervall et al., 1997; Michalides et al., 1997). Additionally, overexpression in HNSCC correlates with shorter time to recurrence and with higher stage disease, lymph node involvement, and reduced overall survival (Fracchiolla et al., 1995; Michalides et al., 1995). Similarly in lung cancer ~70% of tumors showed overexpression of *Cyclin D1* and this overexpression has also been linked with prognosis (Gugger et al., 2001; Lingfei et al., 1998).

EGFR is a member of the receptor tyrosine kinase family which has several extracellular growth factor ligands including EGF and TGF alpha. *EGFR* regulates epithelial proliferation and differentiation. Its activation induces autophosphorylation resulting in downstream activation of *RAS*. Amplification and overexpression are

frequently observed in oral and lung cancers, especially squamous cell lung cancer (Franklin et al., 2002; Grandis and Tweardy, 1993). Alterations affecting *EGFR* have recently been a hot topic in the literature. Two different groups separately reported that certain mutations in the *EGFR* gene in lung tumors can predict a patient's response to the tyrosine kinase inhibitor drug, Iressa, that targets *EGFR* (Lynch et al., 2004; Paez et al., 2004).

1.8.2 Tumor Suppressor Genes

TP53, located at 17p13, encodes a 53 kDa nuclear phosphoprotein that maintains genome stability and regulates cell cycle progression, cellular differentiation, DNA repair, and apoptosis (Levine, 1997). *TP53* is also the most frequently mutated tumor suppressor gene (TSG) in human maliganancy (Wallace-Brodeur and Lowe, 1999). Somatic mutations of *TP53* commonly affect exons 5-8 which encode a DNA-binding domain. In both HNSCC and lung cancer alterations of *TP53* are believed to be early events (Boyle et al., 1993; Forgacs et al., 2001). Mutations in 60% of HNSCC have been reported (Hainaut et al., 1998). Smoking and tobacco chewing causes *TP53* alteration in the early stages of HNSCC development and higher levels of *TP53* mutant expression correlates with an increased risk secondary tumors (Shin et al., 1996; van Oijen et al., 1999). Similarly, mutations of *TP53* are observed in 51% of squamous cell lung carcinomas. Approximately 70-80% of the somatic mutations of *TP53* found in lung cancer are missense and prolong the half life of the *TP53* protein (Casey et al., 1996).

CDKN2A, located at 9p21.3, is central in controlling the G1-S phase transition of the cell cycle. *CDKN2A* arrests cells in G1 phase by leading to hyperphosphorylation of *RB*, the active growth suppression form. *CDKN2A* has been reported to be mutated in numerous cancer types (Ohtani et al., 2004; Raschke et al., 2005). Mutations including homozygous deletion, point mutations, and epigenetic alterations such as hypermethylation have been observed in 30-70% of NSCLC (Sekido et al., 1998). Similarly, in HNSCC methylation is also a mechanism of inactivation of *CDKN2A* as well as homozygous deletion, being observed in 50% of cases (Merlo et al., 1995; Reed et al., 1996).

Allele loss involving chromosome arm 3p is one of the most frequent and earliest known genetic events in HNSCC and lung cancer pathogenesis and may affect several potential tumor suppressor gene regions. For both oral and lung cancer, multiple discountinuous regions of allelic loss support the idea that there are multiple TSGs on this chromosome arm (Uzawa et al., 2001; Zabarovsky et al., 2002). It is evident that several genes residing on 3p are important for the development of these cancers however, it is still uncertain exactly how many candidate genes exist on chromosome 3p and exactly what role they play in the development of the disease. One gene residing on chromosome 3p that has been implicated in both cancer types is *FHIT*. *FHIT*, located at 3p14.2, is also the location to the most common fragile site in the human genome, FRA3B. The *FHIT* gene, a member of the histidine triad gene family, is a target of tyrosine phosphorylation by the SRC protein kinase (Pekarsky et al., 2004).

1.9 Rationale

Despite the advances in technology over the last decade, survival rates for both oral and lung cancer remain poor. In order to increase the survival rate of these cancer patients detection at the earlier stages of disease, prediction of secondary lesions, and discovery of new therapies is necessary. In order to accomplish this, a better understanding of the progression of the disease is required. Due to the high genomic instability associated with tumor genomes, alterations and/or genes critical to cancer progression will most likely be identified by analyzing the pre-invasive lesions.

1.10 Hypothesis and Objective

1.10.1 Overall Objective

The overall objective of this thesis is to identify genetic alterations that are associated with the progression of lung and oral cancer and to associate these changes with biological importance in order to identify suitable candidates for potential use as diagnostic markers and or therapeutic targets.

1.10.2 Hypotheses

1. Certain genetic events occur at specific stages in tumorigenesis.

2. Due to the high level of genomic instability associated with late stage tumors, changes present in the pre-invasive lesions may be masked by later events.

3. Only a small percentage of dysplastic lesions progress to invasive carcinoma, therefore, we expect few changes to be present in the dysplastic samples. Those changes that are present may not be important for driving the disease or may not be sufficient on their own to drive progression.

4. Genetic alterations that are important for disease progression will appear at the carcinoma in situ stage, as the majority of these lesions will progress.

5. If a pathway is important to the progression of the disease it is likely that more than one component of that pathway will be altered.

2. MATERIALS AND METHODS

2.1 Oral Sample Selection and Microdissection

Formalin-fixed paraffin-embedded samples were retrieved from the archive of the Oral Biopsy Service of British Columbia and histological diagnoses were confirmed by two oral pathologists. Serial sections from each biopsy were stained with haematoxylin and eosin, and microdissected. All lesions were meticulously microdissected under the supervision of Dr. L. Zhang. Connective tissue from each specimen was submitted as controls. Microdissection and DNA extractions were performed as previously described by Zhang et al. (Zhang et al., 1997b). Briefly, the dissected tissues were placed in sodium dodecyl sulfate/proteinase K at 48°C and spiked twice a day for 72 hours with fresh proteinase K. Genomic DNA was extracted with phenol-chloroform and precipitated with ethanol. DNA was quantified fluorometrically using Picogreen (Molecular Probes, Eugene, OR). Patient information is listed in Appendix 1. Collection and use of all samples was approved by the institution ethics board.

2.2 Lung Sample Selection and Microdissection

The detection and capture of minute precancerous and cancerous bronchial lesions has been facilitated by the development of fluorescence bronchoscopy technology (McWilliams et al., 2002). The isolation of carcinoma in situ (CIS) specimens was

guided by use of the LIFE-Lung device by Dr. S. Lam (Lam et al., 2000). Formalin-fixed paraffin-embedded CIS tissue blocks were retrieved from the Cancer Imaging Collection at the British Columbia Cancer Agency and diagnoses were confirmed by a lung pathologist. In addition, formalin-fixed and frozen lung tumor specimens (for DNA profiling and gene expression analysis, respectively) were provided by Dr. James Hogg, St. Paul's Hospital, Vancouver, B.C. Serial sections of the archival material were cut and stained with methyl green. Manual microdissection of the CIS lesions as well as invasive tumors were performed by myself and others.

Scraped tissue was digested in digestion buffer (10 mM Tris-HCl pH8, 1 mM EDTA pH 8.0, 0.5% sodium dodecyl sulfate (SDS), and 50 mM NaCl) at 55°C for 72 hours with fresh proteinase K being added every 24 hours. DNA was extracted two times with phenol chloroform and precipitated with ethanol. DNA was quantified using the Nanodrop ND-1000 Spectrophotometer (Nano Drop Technologies). Patient information is listed in Appendix 1. Collection and use of all samples was approved by the institution ethics board.

2.3 RNA Extraction

Microdissected frozen tissue was placed in GITC solution (4 M guanidine isothiocyanate, 0.02 M sodium citrate, 0.5% sarcosyl), and 3.5 µl of beta mercaptoethanol was added for each ml of GITC solution used. Extraction was performed using equal volumes of acidic phenol. Aqueous layer was collected and

ethanol precipitated. Frozen lung tissue was collected from St. Paul's Hospital and RNA was extracted using the TRIzol Reagent (Invitrogen).

2.5 RAPD PCR

RAPD-PCR fingerprints were generated from pairs of pre-invasive oral and lung specimens (or tumor) and normal DNA from each patient. A positive control (human genomic DNA) and a negative control (no DNA template) were used for each experiment. Ten picomoles of each primer (17/19: 5'-GACGCCGCTT-3' and 5'-CGCCTAATGC-3' or 33/34: 5'-CGTACGGCTG-3' and 5'-CACGTGACGT-3') were radiolabeled with 2 μCi of γ^{32}P ATP (6000 Ci/mmol; Amersham Pharmacia Biotech) using T4 polynucleotide kinase (MBI Fermentas, Burlington, ON) at 37°C for 1 hour, and inactivated at 95°C for 5 minutes. RAPD-PCR reactions were performed in a 10 μl volume containing 2 ng of template DNA, 2.5 U of recombinant Taq DNA polymerase, 200 μM of each dNTP, 10 mM Tris-Cl, pH 8.3, 50 mM KCl, 2 mM $MgCl_2$, and 0.001% gelatin. All reactions were performed in a PTC-100 thermal cycler (MJ Research, Waltham, MA) for 45 cycles of 94°C for 1 minute, 35°C for 1 minute, and 72°C for 2 minutes. The PCR products from sets of 20 paired normal and tumor samples were resolved on 8% non-denaturing acrylamide gels (38 acrylamide: 1 N', N'-methylene-bis-acrylamide) in 100 mM Tris-borate-EDTA buffer, pH 8 for 3 hours at 800V. Dried gels were imaged by autoradiography. Gain or loss of signals was identified by pairwise comparison of RAPD-PCR fingerprints (Siwoski et al., 2002). Signal alterations that occurred in multiple samples were selected for further analysis.

2.6 Cloning

DNA from excised bands was amplified in 20 µl reactions using 0.25 pmol of each primer:

5'-ACAAGCTTCTGCAGGACGCCGCTT-3'and

5'-ACGAATTCGGATCCCGCC TAATGC-3' or

5'ACAAGCTTCTGCAGCGTACGGCTG-3' and

5'-ACGAATTCGGATCCCACGTGACGT-3'

(these primers are identical to the primers used for the RAPD-PCR reactions except they also have *BamHI* or *Pst*1 recognition site), Taq DNA polymerase, and buffer (Promega, Madison, WI). Since the RAPD-PCR bands were created using a combination of two primers there are three possible terminal sequences for each band. Therefore to amplify the DNA from the excised band three reactions are required: primer 1 with itself, primer 2 with itself, and a combination of primer 1 and primer 2. Amplification was performed as follows: 2 cycles (94°C, 1 minute; 35°C, 1 minute; 72°C, 2 minutes) and then 30 cycles at 94°C; 40 seconds; 62°C , 40 seconds, 72°C , 40 seconds). PCR product was resolved on an agarose gel to determine the correct restriction enzyme needed for cloning. 5 µl of the amplified DNA was digested with *BamHI* and *Pst*1. The digestion product was gel-purified on a 5% polyacrylamide gel. DNA was eluted form the gel piece with water at room temperature. The digested DNA was ligated to pBlueScript SK vector overnight at 16 degrees and transformed into ElectroMAX DH10B Cells (Invitrogen, Burlington, ON)

by electroporation. Cells were plated on LB plates containing ampacillin, X-Gal, and IPTG and grown at 37°C overnight.

Colonies containing an insert appeared white while those with no insert appeared blue. To confirm the insert size a minimum of ten white colonies were selected for colony PCR. This reaction contained 1X PCR buffer (50 mM KCl, 10 mM Tris-HCl pH 9, 0.1% Triton X-100), 0.25 mM d NTPs, 2 U recombinant Taq polymerase, 5 pmol each of M13 -47 and -48 primers, and 2 mM $MgCl_2$. The reaction was as follows: 94 °C for 3 minutes, 30 cycles of 94°C for 45 seconds, 40°C for 45 seconds, and 72°C for 45 seconds. The final product was resolved on an agarose gel. Those colonies with the expected insert size were fingerprinted to determine if all colonies contained the same sequence. The colony fingerprint reactions contained 1X nucleotide stock (0.5M dNTPs, 0.5 mM ddGTP), 1X buffer (10 mM Tris pH8, 50 mM KCl, 1.5 mM $MgCl_2$), 0.5 pmol γ ^{32}P ATP labeled T7 primer (0.34 pmol γ ^{32}P ATP, 1X PNK buffer, and 0.5 pmol T7 primer incubated at 37°C for 1 hour followed by 65°C for 5 minutes), 2.5 U recombinant Taq polymerase, and 1 μg RNase A. The colony fingerprints reaction occurred at 94°C for 3 minutes followed by 30 cycles of 94°C for 1 minute, 40° C for 1 minute, and 72°C for 1 minute.

One representative colony was selected for DNA purification. Colony was inoculated into 2 ml of LB broth containing ampicillan and grown overnight at 37°C with constant agitation. Cells were collected by centrifugation and the supernatant was discarded. Cells were resuspended in 100 μl TE (10 mM Tris HCl pH 8, 1 mM EDTA) and 200 μl of lysis buffer (1% SDS, 0.2 M NaOH) was added and placed on ice for 10 minutes. 150 μl of 3 M KOAc was added, and centrifuged at 4°C for 10 minutes. The

supernatant was collected and ethanol precipitated. Samples were resuspended in 100 µl TE and 1 µl of RNase was added. After 30 minutes, equal volumes of phenol were added, the sample centrifuged, and the aqueous layer collected. This was followed by another ethanol precipitation. The final product was resuspended in TE.
Plasmid DNA was sequenced using the ABI Prism at the Nucleic Acids Protein Service (NAPS) Unit at the University of British Columbia.

2.7 Localization of Clones to Chromosomal Loci

Sequences obtained from NAPS were used to localize the alteration to the human genome. NCBI standard nucleotide-nucleotide BLAST (blastn) at www.ncbi.nlm.nih.gov and the University of California at Santa Cruz (UCSC) genome BLAT search (www.ucsc.genome.edu) matched the sequences to the human genome by nucleotide alignment.

2.8 Microsatellite Analysis

Some of the regions defined by RAPD-PCR analysis were verified and fine mapped using microsatellite analysis. Markers in the region close to the RAPD alteration were determined using map information provided by the Ensembl system (http://www.ensembl.org) and UCSC (http://genome.cse.ucsc.edu/index.html). Markers with high degree of heterozygosity based on the GDB Human Genome Database

(www.GDB.org) were chosen (Table 1). The protocol used for microsatelite analysis is described in Zhang *et al.* and all LOH reactions were performed in the laboratory of Dr. Miriam Rosin (Zhang et al., 1997a). After PCR amplification, PCR products were separated on denaturing polyacrylamide gels and visualized by autoradiography. For informative cases, AI was inferred when the signal ratio of the 2 alleles, differed in the normal samples by at least 50%. Samples showing AI were subjected to repeat analysis after a second independent amplification whenever the quantity of DNA was sufficient.

2.9 Regional Array CGH Construction

The first BAC array constructed was a test case for the whole genome array that would soon follow. This first array, termed the regional array, consisted of 26 regions selected from areas of interest as defined by the literature as well as regions discovered through RAPD analysis. In addition full chromosome arm coverage was selected for 1p (642 BAC clones spanning 1p11.2 to 1p36.33), 3p (535 BAC clones spanning chromosome arm 3p from 3p12.3 to 3p26.3), and 5p (491 BAC clones spanning 5p11 to 5p15.33). In total 2770 BAC clones were present on the regional array. The choice of these clones was based on their location on the human physical map (http://genome.wustl.edu) and their map location was verified using the UCSC Human Genome Browser (http://www.genome.ucsc.edu). These clone lists are available publicly at http://www.bccrc.ca/cg/ArrayCGH_Group.html.

Table 1. Microsatellite Markers Used For LOH Analysis

Primer Name	Location	Size (bp)
D3S1234	3p14.2	121
D3S1228	3p14.1	84
D3S1300	3p14.2	241
IFNA	9p21.3	NA
D9S171	9p21.3	177
D9S1748	9p21.3	159
D9S1751	9p21.3	170
D8S267	8q22.3	NA
D8S1459	8q22.3	132
D8S506	8q22.2	127
D8S545	8q22.3	187
D8S1814	8q22.3	212
D8S1844	8q22.3	190
D8S556	8q22.3	163
D8S1830	8q23.1	187
D8S1793	8q24.1	147
RH30616	8q22.3	195
D13S263	13q14.11	149
D13S1297	13q14.11	163
D13S1227	13q14.11	124

2.9.1 BAC DNA Preparation and Fingerprint Verification

DNA extraction, digestion, and electrophoresis for the 1p and 5p subsets were performed at the Genome Sciences Center as outlined by Marra et al. (Marra et al., 1997). BAC clones for the remaining region array were obtained from glycerol stocks of the RPCI-11 library (Osoegawa et al., 2001). Each BAC clone was streaked onto an LB agar plate containing 12.5 μg /ml chloramphenicol and incubated overnight at 37°C. A single colony was selected and placed into 50 ml LB broth containing 12.5 μg/ μl chloramphenicol and placed in a shaker overnight at 37°C. DNA extraction for all other clones were performed using a Clontech NucleoBond Nucleic Acid Purification Kit. A fingerprint for each clone was generated by *Hind*III restriction enzyme digest. This fingerprint was used to verify the clone identity by matching it to an electronic image band pattern available on Fingerprinted Contigs (FPC), which is now available at www.genome.arizona.edu/fpc/.

2.9.2 Amplified Fragment Pool Synthesis

To obtain sufficient amounts of BAC DNA for spotting isolated DNA required amplification. In order to do this linkers acting as primer sites for PCR were ligated onto *Mse*I digested BAC DNA. At least 10 ng of DNA from each clone was digested with 5 U of *Mse*I (New England BioLabs) in 4 μl of NEB2 10X buffer and 0.4 μl of 100X bovine serum albumin in a 40 μl reaction for 8 hours, followed by inactivation of the enzyme at 65°C for 10 minutes. 4 μl of the final digestion mixture was added to 4 μl T4 ligase buffer (NEB), 0.2 μl (80 U) T4 ligase, 27 μl of sterile water, and 2 μl of 100 μM of each

primer (5'- AGTGGGATTCCGCATGCTAGT- 3' and 5'- TAACTAGCATGC- 3'). Primers were annealed for 5 minutes at room temperature before adding to the ligation mixture. The reaction proceeded at 14°C overnight.

Amplification required two rounds of PCR. For the first round 2.5 µl of the ligation reaction was added to 48 µl of PCR mix containing 5 µl Promega buffer, 16 µl of 25 mM MgCl, 10 µl of 5 mM dNTPs, 0.2 µl of 100 µM LM *Mse*I long primer, 16 µl of ddH2O and 1 µl (5U) of Taq polymerase (Promega buffer B). Cycling conditions were as follows: 95°C for 3 minutes, 30 cycles of 95°C for 1 minute, 55°C for 1 minute, and 72°C for 3 minutes, followed by 72°C for 10 minutes. The second round of PCR was performed with 5 µl of a 1/20 dilution of PCR1 and cycled 35 times under the same conditions. The final product was precipitated with ethanol and resuspended in 20% DMSO solution.

2.9.3 BAC Array Printing

The amplified DNA was dissolved in a 20% DMSO solution, boiled for 10 minutes and re-arrayed for robotic printing. Each clone was spotted in triplicate with Stealth Micro Spotting Pins onto amine-coated slides (Telechem/ArrayIT SMP2.5, Sunnyvale, CA) using a VersArray ChipWriter Pro system (BioRad, Mississauga, ON). The clones were arranged to ensure that adjacent BACs on the tiling set were not placed next to each other on the array. In order to allow normalization of the hybridization signal intensities between dyes, linker mediated (LM) PCR-amplified normal male human genomic DNA samples (Novagen, Madison, WI) were spotted on the array 48

times. In addition, 96 randomly selected BACs distributed throughout the genome were included on this array as internal control spots in order to detect hybridization artifacts such as hybridization signal gradients. The DNA was then covalently bonded to the slides by baking and UV cross-linking. Slides were washed to remove unbound DNA.

2.9.4 Regional Array Probe Labeling

Test and male or female genomic reference DNA (100 ng each) were separately labeled using cyanine 5 and cyanine 3 dCTPs respectively. Labeling was performed using a Bioprime Labelling Kit (Invitrogen). Each sample was combined with 10 µl 2.5X random primers buffer and made up to 20 µl final volume with sterile water, placed at 100°C for 10 minutes and then placed immediately on ice. 40 U of Klenow, 2.5 µl of a 10X dNTP mixture (2 mM dATP, dGTP, dTTP, 0.5 mM dCTP), and 2 nmoles of either cyanine 5-labelled dCTP or cyanine 3-labelled dCTP were added (cyanine 5 for test DNA and cyanine 3 for reference DNA). Reactions were placed at 37°C for 18 hours. At this point the probes were combined and unincorporated nucleotides were removed by placing the combined material through a G-50 Sephadex column (Amersham). 100 µg of cot-1 DNA (Invitrogen) was added to the recovered material and the sample was precipitated with ethanol and placed in -20°C for 1 hour. The sample was centrifuged at maximum speed at 4°C for 10 minutes. The supernatant was removed, samples air dried, and resuspended in 28 µl of DIG Easy (Roche), 3.5 µl (20 µg/µl) sheared herring sperm DNA (Sigma-Aldrich), and 3.5 µl (100 µg/µl) yeast tRNA (Calbiochem), followed by denaturing at 85°C for 10 minutes and 37°C for 1 hour.

2.9.5 Regional Array Hybridization

The arrays were pre-hybridized with a solution containing 28 μl DIG Easy hybridization buffer (Roche), 4 μl (20 μg/μl) sheared herring sperm DNA, and 4 μl 10% BSA. The solution was applied to the slide and a 24 x 40 mm cover slip was placed on top. The slide was placed in an ArrayIT Array Hybridization Cassette with 10 μl of water. The sealed cassette was incubated at 45°C for 1 hour. The prehybridization solution was removed from the array by washing with dH_2O. Slides were dried by dipping into 100% isopropanol and air drying. The labeled probe was placed onto the slide with a cover slip on top. The slide was placed in a hybridization cassette with 10 μl of water to maintain humidity and placed at 45°C for 40 hours.

2.9.6 Regional Array Visualization and Normalization

A charged coupled device (CCD) based imaging system (Arrayworx eAuto, API, Issaquah, WA) was used to determine signal intensities of the cyanine 5/cyanine 3 channels. Images were analyzed with Softworx array analysis software. A scale factor based on the signal intensities of the aforementioned 48 human genomic DNA control spots on the array was used to normalize spot signal data for each channel. Standard deviations for each triplicate spot set were calculated. The array CGH profile was presented as a graph plotting normalized cyanine5/cyanine3 log2 signal ratios versus the relative tiling path position of the BAC clones. A log2 signal ratio of 0 at a spot

represents equivalent copy number between the sample and reference DNA. Quality control was applied to each batch of arrays synthesized. Normal DNA versus normal DNA hybridizations revealed spots with aberrant signal intensity and these were removed from the analysis. Spots which exhibited signal ratios outside of 3 standard deviations from 0 in these experiments were discarded, resulting in the establishment of a $\pm$ 0.2 log2 ratio threshold for defining regions of copy number increase and decrease. In addition, alterations had to have more than one consecutive BAC with copy number change to be scored as a region of alteration.

2.10 Sub Mega Base Resolution Tiling (SMRT) Array Construction

All clones for the Whole Genome SMRT array were selected, extracted, digested, and gel electrophoresed by the Genome Sciences Center. 32, 433 clones spanning the entire genome at 1.5 fold coverage were selected from the RPCI-11 BAC clone library (Krzywinski et al., 2004). The final solution was resuspended in MSP printing solution (Telechem). PCR products were denatured by boiling prior to robotic spotting. The entire set of 32,433 PCR products were spotted in triplicate onto two aldehyde-coated slides (Ishkanian et al., 2004).

2.10.1 Whole Genome SMRT Array Hybridization

The SMRT array hybridization protocol was similar to that of the regional arrays except, because the slide type was changed from an amine to an aldehyde slide, the pre-hybridization step was no longer required (See section 2.9.5).

2.10.2 Imaging and Analysis

SMRT arrays were scanned in the same manner as the regional arrays. Standard deviations (SD) for the triplicate spots were calculated. All spots with SDs > 0.075 or signal to noise ratios below 20 were removed from the analysis. Custom viewing software, SeeGH, was used to visualize all data as log2 ratio plots where each dot represents one BAC (Chi et al., 2004). Normalization occurred by global median normalization. The filtered, normalized data was run through a smoothing algorithm in the aCGHsmooth program using default settings except for "lambda" = 6.75 and "number of breakpoints in initial pool" = 100 for breakpoint detection (Jong et al., 2004a). The frequency of alteration for each BAC was then determined. For this, the smoothed data were typed as loss, normal, or gain. The values were averaged for each BAC and plotted in SeeGH Frequency Plot to visualize areas of recurrent deletion and amplification (Coe et al., submitted).

To compare multiple profiles, we used Java TreeView (version 1.0.3) to generate a colored gene copy number matrix (http://jtreeview.sourceforge.net). Intensities of red and green coloration indicate an increased or decreased log2 signal ratio for each clone respectively. Gray coloration indicates clones discarded due to high standard deviations

(SD) (>0.075) or signal to noise ratios. Each column represents a separate array CGH profile.

2.11 Gene Expression Analysis

2.11.1 cDNA Synthesis

RNA obtained from the microdissected frozen tissue was made into cDNA using the Invitrogen SuperScript II protocol. 1 ng – 5 μg of total RNA were added to 1 μl (500 ug/mL) oligo dT, 1 μl 10 mM dNTP mix (10 mM each of dATP, dCTP, dTTP, dGTP). The final mixture was made up to 12 μl with sterile water and was heated at 65°C for 5 minutes and then placed immediately on ice. 4 μl 5X First Strand Buffer, 2 μl 0.1 M DDT, and 1 ul RNaseOUT Recombinant Ribonuclease Inhibitor (40 U/ μl) were added and incubated at 42°C for 2 minutes. At this time 1 μl (200 U) of SuperScript II was added and the mixture was incubated at 42°C for 50 minutes. The reaction was inactivated by heating to 70°C for 15 minutes.

2.11.2 RT-PCR Analysis

For semi-quantitative RT-PCR, expression levels were determined by gene-specific PCR (primers are listed in Table 2). PCR consisted of 1 μl of the cDNA synthesized product being added to 2.5 μl 10X PCR buffer (200 mM Tris-HCL, 500 mM KCl), 0.75 μl 50 mM MgCl2, 0.5 μl 10 mM dNTP mix, 0.5 μl of each forward and reverse primer, 0.2 μl Taq polymerase (5 U/ μl), and 19.5 μl sterile water. PCR cycle

conditions were as follows: 1 cycle of 95°C, 1 minute; 30-35 cycles of (95°C, 30 seconds; 55°C – (X) depending on primers (see Table 2) for 30 seconds; 72°C, 1 minute) and a 10 minute extension at 72°C. PCR products were resolved on an eight percent polyacrylamide gel, stained with SYBR green (Roche, Laval, Que), imaged on a Molecular Dynamics Storm Phosphoimager model 860, and quantified using ImageQuant software (Molecular Dynamics, Piscataway, NJ).

Table 2. Primers Used For RT-PCR Analysis.

Gene Name	Forward Primer (5'-3')	Reverse Primer (5'-3')	Annealing Temp °C
GAPDH	ACCTACCAAATATGATGACATCA	CGCTGTTGAAGTCAGAGGA	55
Beta Actin	GATGTGGATCAGCAAGCA	GAAAGGGTGTAACGCAACT	55
AKAP220	TTGGTTACTTGTGCAGTGTT	ACTGTTACACAGTACAAGATCT	55
RANKL	TCGGCACTTGTGGAAAAACA	TGGCCACCAGGTGCCTTTCA	55
LRP12	ACTGTAGTTCACTGT	AGTTCAAGATGTGCT	55
DPYS	CACAGCCTTTCCATC	ACATTGTCAACCCAT	55
FOG2	CTGATGCAGCTCTGTCTAA	TACTTGCAGCATTGAGTTTA	55
TRIO	ACTGCTGAGCACAGCTCACT	TAGAGTTTGACCTATCCAGA	60
GDNF	CACTGACTTGGGTCTGGGCTAT	GTCTCAGCTGCATCGCAAG	55
LRP8	ATGTTGCGGAAAGGTAACCA	TGAGTAAGGTACTGTGCCAT	55
DVL1	CCCAACCCCTTGTGTCTGGT	GGTGGGACAGATGACAGGGT	59
NOTCH2	GCCAATCGAGACATCACAGA	CCCACAGATGACAGGTGAGA	56
EGFL3	AGTTGGACTGAGGACAGGTG	AGCCTGCAGACCTGAATCAG	59
JUN	AACCGCATCGCTGCCTCCAA	CAACTGCTGCGTTAGCATGA	55
WNT4A	ACATGCAACAAGACGTCCAA	TCATCGGCACGTGTGCAACT	53
REG4	GAACAAGCACTGTGTCGAGA	ATGAGCAGATTTAGCCAGGC	55
ADAM30	GGGTGTTTGCAACAACAGAA	TGGACACAACCCAAATTGAC	56

3. RESULTS: RAPD-PCR ANALYSIS

The work in this chapter has resulted in two manuscripts:

Garnis C, Rosin MP, Zhang L, Lam WL. Alteration of *AKAP220*, an upstream component of the Rb pathway, in oral carcinogenesis. *International Journal of Cancer*. In Press

Garnis C, Coe BP, Ishkanian A, Zhang L, Rosin MP, Lam WL. (2004) Novel regions of amplification on 8q distinct from the MYC locus and frequently altered in oral dysplasia and cancer. *Genes Chromosomes and Cancer* 39:93-8.

As lead author on these manuscripts the writing, data analysis and the majority of the experiments were done by me. Microsatellite analysis was performed in Dr. Rosin's laboratory at Simon Fraser University and data analysis was performed in part with the assistance of Bradley P. Coe.

Using a multitude of techniques to scan and fine-map the genomes of both lung and oral pre-invasive lesions and tumors, I have been able to identify numerous novel genetic alterations associated with the progression of these diseases. The first approach used was a PCR based screening technique, RAPD-PCR (Section 3.1). This approach yielded numerous differences between paired normal and either tumor or dysplastic lesions. Two of these alterations, one at 13q14 and the other at 8q22, were fine mapped to reveal candidate genes with altered expression. The remaining regions identified with RAPD-PCR were then fine-mapped by BAC array CGH. We called this array the regional array as it contained 26 selected regions as well as complete coverage of chromosome arms 1p, 3p, and 5p (Section 3.2). This technology allowed us to fine-map to < 1Mbp with one experiment. This approach yielded numerous novel regions and highlighted the value of studying the premalignant lesion. We expanded this approach by

using a new CGH array that covers the entire genome and have profiled various histopathological stages in both oral and lung cancer (Section 3.3).

3.1 Randomly Amplified Polymorphic DNA (RAPD) PCR

In order to identify novel genetic alterations in the progression of lung and oral cancers and to make the most use out of the limited material obtained from the pre-invasive lesions a genome wide scanning technique called RAPD-PCR was employed. This is a PCR based technique that uses arbitrarily designed (non specific) decanucleotide primers to create a DNA fingerprint of normal and tumor DNA from the same individual. Discrepancies in banding pattern from the normal DNA can be cloned and sequenced to localize the alteration to a specific chromosomal locus. This allows for unbiased screening across the entire genome (Figure 5).

Primers for this analysis were selected based on the number of bands the particular primer set produced. Two sets of primers (33 and 34 and 17 and 20 - see materials and methods), each producing approximately 25 bands, were selected. In total, 40 oral tumors and 40 lung CIS samples were analyzed. Two sets of gels, each consisting of 20 paired samples, were compared. A total of 15 recurrent alterations were successfully cloned and localized to a chromosome band. Results are summarized in Table 3. Figure 6 shows a summary of the chromosomal loci identified by RAPD PCR.

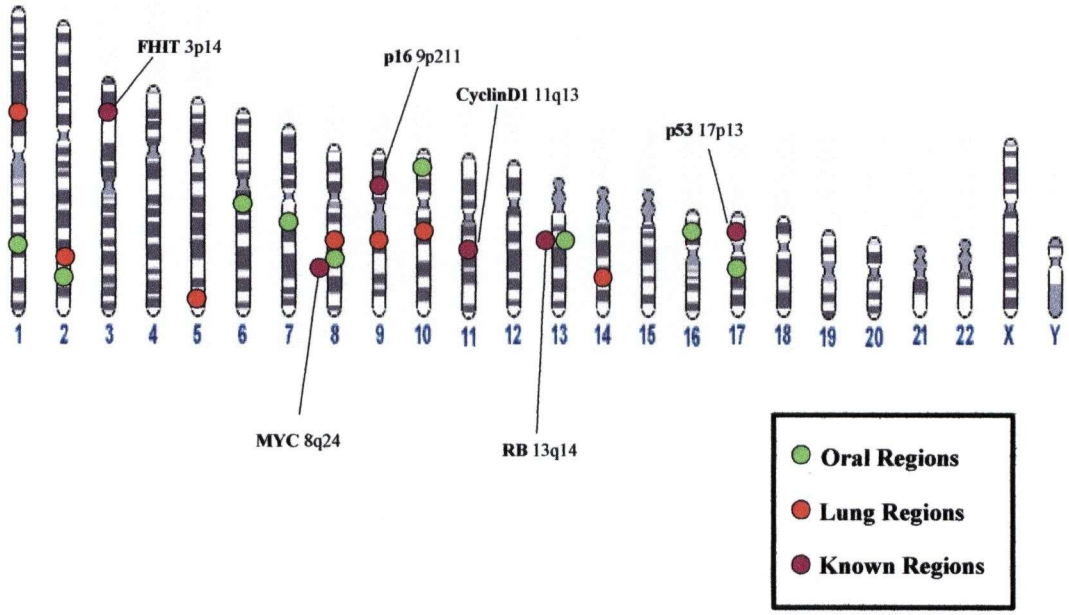

Figure 6. Summary of RAPD Regions

Table 3. Summary Of Regions Identified By RAPD-PCR.

ORAL Frequency of RAPD Cases	Fragment Size	Chromosome Location	BAC Matched	Accession
7:20	150	7q11.22	RP11-420H12	AC073330
2:20	270	10p12.2	RP11-108B14	AL157831
3:20	300	2q35	RP11-548N17	AC072062
5:20	400	chr17q12	RP11-4251O3	NA
5:20	395	1q25.2	RP11-114G14	AC069000
4:20	500	13q14.11	RP11-84N7	AL139328
3:20	510	6q11.22	RP11-26M18	AC025144
2:20	400	16p13.3	RP11-358F6	AC009041
4:20	185	8q22.3	RP11-171013	AC055117
LUNG Frequency of RAPD Cases	**Fragment Size**	**Chromosome Location**	**BAC Matched**	**Accession**
2:20	170	5q13	RP11-414A11	AC016640
2:20	190	9q32	RP11-9I6	NA
2:20	195	10q26.2	RP11-85C15	AL355529
3:20	150	14q32	RP11-336L21	AC023195
3:20	170	8q21	RP11-122C21	AC090190
7:20	200	10q26.2	RP11-290H6	AL691463

3.1.1 Fine mapping 13q14 RAPD alteration

Alterations involving 13q have been previously reported in oral and head and neck cancers (Gupta et al., 1999; Li et al., 1994; Maestro et al., 1996; Nawroz et al., 1994; Ogawara et al., 1998; Partridge et al., 2001; Sanchez-Cespedes et al., 2000; Yoo et al., 1994) and in cancers at other sites including liver, breast, ovary, larynx, lung, bladder, prostate, and the lymphoreticular system (Alers et al., 2001; Allen et al., 2002; Dong, 2001; Gras et al., 2001; Nishida et al., 2002; Selim et al., 2002; Sengelov et al., 2000; Sun et al., 1995; Vizcarra et al., 2001; Wada et al., 2000). The LOH studies suggest at least 3 separate regions of alteration: one centred around the retinoblastoma gene (*RB*) and candidate genes associated with chronic lymphocytic leukemia (CLL) and the others centromeric (e.g. around the *Breast Cancer Type 2* gene [*BRCA2*]) or telomeric to *RB* (Bullrich et al., 2001; Kitamura et al., 2000; Mabuchi et al., 2001; Wolf et al., 2001). My work describes the identification of a novel region of alteration that is frequently altered in both oral premalignant lesions (OPLs) and tumors. The minimal region contains two candidate genes, one of which, *AKAP220*, showed altered expression in tumors and may play an important role in driving the process of oral carcinogenesis.

As previously stated, upon BLAST search against Genebank, one of the recurrent alterations identified from the RAPD-PCR analysis of the oral tumors (Figure 7A) localized to human BAC clone RP11- 84N7 (AL139328) (http://www.ncbi.nlm.nih.gov/BLAST/). This BAC was localized to 13q14 by fingerprint alignment against the FPC database (http://www.genome.wustl.edu/gsc/) and by sequence alignment against the August 2001 release of the Human Genome Project

Working Draft (http://genome.cse.ucsc.edu). The RAPD-PCR alteration was confirmed to be at 13q14.11 by microsatellite analysis of the cases in which the alteration was initially identified. A marker, *D13S1297*, located 400 Kbp telomeric to the alteration was used to verify AI in 543T, 569T, 577T, and 385T. Three out of the 4 samples showed AI, with the fourth (385T) being non-informative. Figure 7B shows 2 examples.

To facilitate fine mapping we used FPC software to construct a BAC contig of this region containing RP11-84N07, which harbors the RAPD identified sequence. Figure 8 shows a 2 Mbp portion of this tiling path that later proved to contain the minimal region of alteration (MRA) (described below). The relative position of microsatellite markers and genes at 13q14 are shown in Figure 8. Marker positions were verified by BLAST against BACs in this tiling path.

To establish the MRA, we first examined a panel of 39 oral SCC cases for AI at *D13S1297*. Seventeen of the 31 informative cases showed alteration (a high frequency of 54%). We then evaluated *D13S263*, a neighboring microsatellite marker 1.6 Mbp centromeric to *D13S1297*. Thirteen of 33 informative cases showed AI (39%) (Figure 9A, top panel). For 4 of these samples (539T, 542T, 569T, 577T), the AI at *D13S1297* was flanked by retention at *D13S263*, suggesting the presence of a centromeric boundary at that locus. Further analysis with an additional marker, *D13S1227* (0.3 Mbp telomeric to *D13S1297*) revealed the other boundary in 2 cases (539T, 620T). Figure 9B shows two examples. These data support a 1.9 Mbp MRA spanning *D13S263* and *D13S1227* and including BACs RP11-157L14, RP11-322A14, RP11-84N7, RP11-215B13, RP11-366O17, RP11-127O12 (Figure 8).

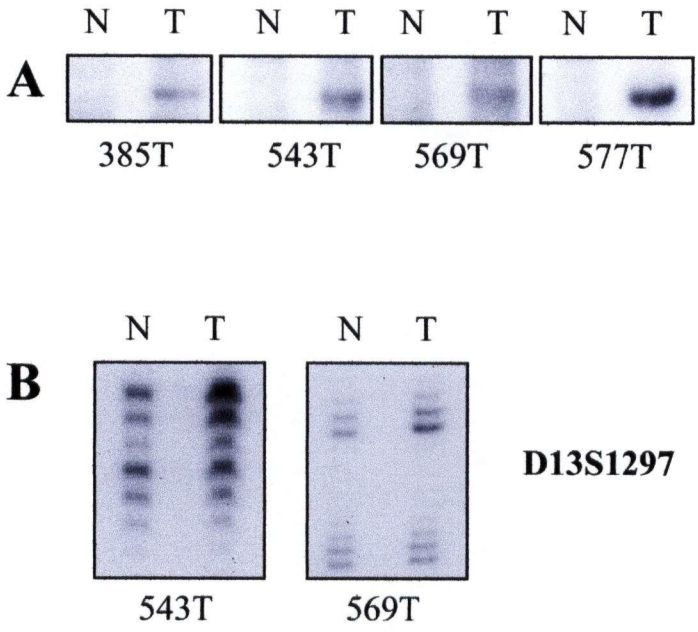

Figure 7. Novel Alteration at 13q14 as Detected by RAPD-PCR. (a) Gain of a ~400 Mbp band in 4 tumors. (b) Verification of allelic imbalance at *D13S1297* for 2 of the tumors showing the RAPD-PCR alteration: increase of the upper allele for 543T and 569T. N, normal and T, tumor.

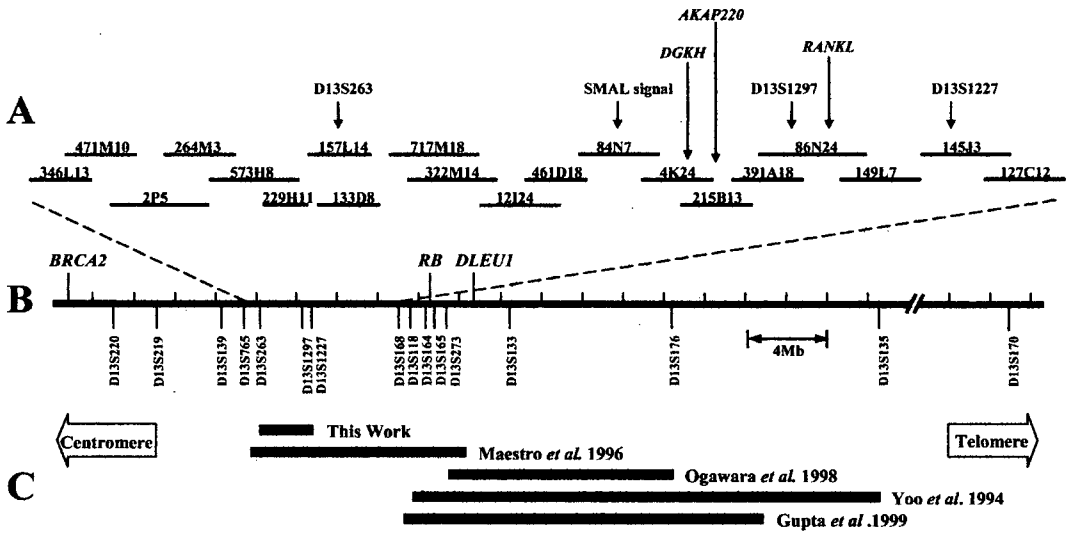

Figure 8. Physical Map Between *D13S220* and *D13S170*. (A) BAC contig spanning region between *D13S765* and *D13S168*. Microsatellite markers and genes within the minimal region of alteration have been placed onto corresponding BACs. (B) Relative position of microsatellite markers surounding the 13q14.11 region. *Dleu1* marks the location of a variety of BCMS and CLL splice forms. (C) Summary of the MRA previously reported in oral and head and neck cancer.

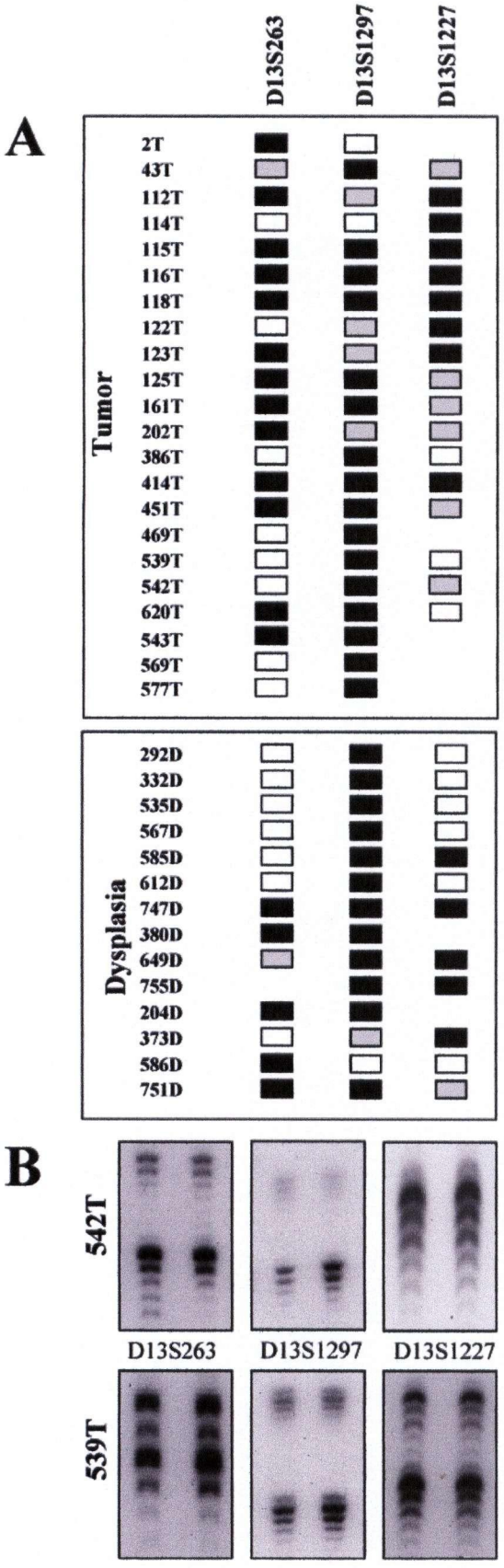

Figure 9. Definition of 13q14 MRA. (A) Summary of microsatellite analysis at 3 loci on chromosome 13q14.11 revealing the 1.9 Mbp MRA. Case numbers are indicated on the left. AI, black boxes; retention of heterozygosity, white boxes; NI, non-informative, shaded boxes. (B) Two examples of microsatellite analysis: 539T and 542T. For each panel normal is on the left and the tumor is on the right. Tumor 542 shows retention at *D13S263,* AI at *D131297*, and NI (not informative) at *D13S1227*. Tumor 539 shows retention at *D13S263,* AI at *D13S1297* and retention at *D13S1227*.

This MRA is distinct from regions previously described in the literature for head and neck SCCs and excludes *RB, DLeu*, and *BRCA2* (Figure 8B and C)(Gupta et al., 1999; Maestro et al., 1996; Yoo et al., 1994). Yoo et al. and Gupta et al. reported an MRA that included *RB* and extended telomerically (Gupta et al., 1999; Yoo et al., 1994). This region was further fine mapped to exclude *RB* by Ogawara et al. (Ogawara et al., 1998). Maestro et al. described a region that includes the *RB* locus but extends centromerically (Maestro et al., 1996). The location of the 1.9 Mbp MRA defined in this work to the aforementioned papers is indicated in Figure 8C. As shown on this Figure, *BRCA2* is 9 Mbp centromeric, the *DLeu* locus is ~6 Mbp telomeric and *RB* is 5 Mbp telomeric to the MRA.

We further determined whether there was any association of AI with histopathological progression of dysplasia from low-grade (mild or moderate, N=42) to high grade dysplasia (severe dysplasia or CIS, N=16) to invasive SCC (N=36). AI in this region was present in 9 of 32 informative low grade cases (28%), 9 of 14 high grade dysplasia (64%), and 22 of 36 SCCs (61%). This suggests that although this alteration is present in some low-grade lesions, the frequency increases significantly in high-grade premalignancy before the lesion becomes invasive (Figure 10).

We also compared the frequency of alteration at 13q14.11 to AI at two other regions: 3p14 (containing *FHIT*) and 9p21 (containing *CDKN2A*) using the microsatellite markers shown in Table 1. Alterations in these regions are early events, occurring frequently in low-grade dysplasia (Califano et al., 1996; Partridge et al., 2001; Rosin et al., 2000). As shown in Figure 10, there is a higher frequency of AI at these regions in low grade dysplasia than AI at 13q14.11, suggesting that AI at 3p14 and 9p21 occur

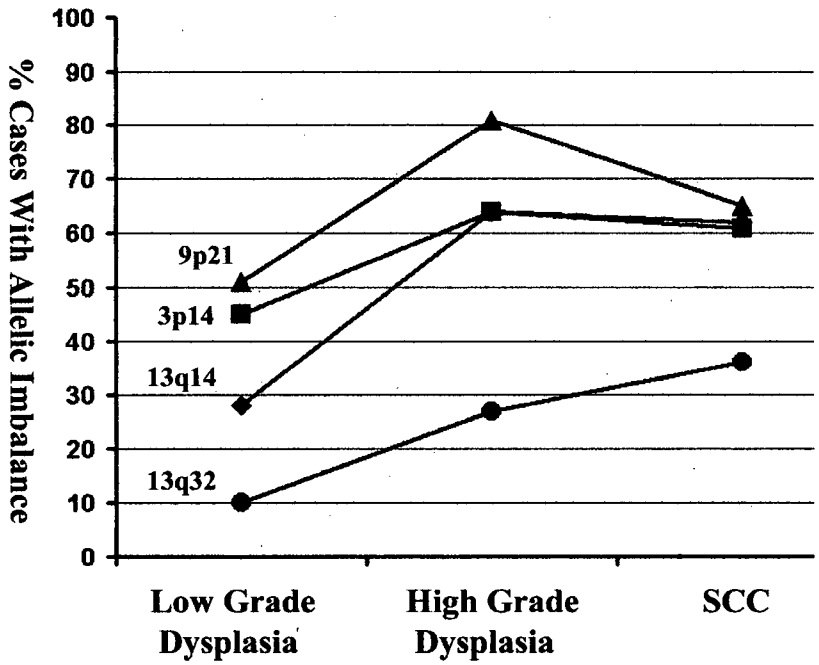

Figure 10. Frequency of AI in Oral Premalignant Lesions and Squamous Cell Carcinomas. 51 dysplasia and 39 SCC cases were analyzed using microsatellite markers in 3p14, 9p21, 13q14.11 and 13q32 shown in Table 1.

before 13q14.11. This is consistent with the fact that AI is observed at 3p14 and/or 9p21 in the absence of 13q14.11.

We also analyzed AI at 13q32 using the marker *D13S170*, 40 Mbp telomeric to *D13S1297*, because this region has also been reported to show AI in oral SCC (Califano et al., 1996). AI occurred in only 10% (3 of 29 cases) of low grade dysplasia, with this frequency increasing to 27% (3 of 11 cases) of high grade dysplasia and 36% (14 of 38) of SCCs (Figure 10). AI occurred in only 1 of the 2 loci (*D13S170* or *D13S1297*) in 19 of 61 cases that are informative for both loci, supporting their occurrence as separate events.

Within the 1.9 Mbp minimal region there are three known genes, *Diacylglycerol Kinase* (*DGKH*), *A-Kinase Anchoring Protein 220* (*AKAP220*), and *Receptor Activator of NK-kappa-B Ligand* (*RANKL*) (also known as *Osteoclast Differentiation Factor* [*ODF*], *Osteoprotegerin ligand* [*OPGL*], or *Tumor Necrosis Factor Ligand Superfamily Member 11* [*TNFSF11*] or *TNF-Related Activation-Induced Cytokine* [*TRANCE*]). We verified the map position of these genes by sequence alignment with BACs as shown in Figure 8. *DGKH* maps to RP11- 4K24, *AKAP220* maps to RP11–215B13, and *RANKL* maps to RP11-86N24.

To determine whether the three candidate genes are expressed in epithelial cells of normal oral mucosa the epithelial layer was microdissected from 11 tissue samples from individuals without cancer or dysplasia. RNA was extracted, cDNA produced, and expression measured using semi-quantitative RT-PCR. Since there are multiple splice forms for these two genes, primers were designed to recognize an exon common to all splice forms. *GAPDH* expression levels were used to normalize between samples. In all

11 of the normal samples we detected expression of both *RANKL* and *AKAP220*. *RANKL* exhibited a generally higher overall expression in normal mucosa than *AKAP220* (Figure 11). *DGKH* expression was not detected in normal oral tissue.

RNA was extracted from 16 microdissected oral SCCs. There was no elevation in *DGKH* or *RANKL* expression in tumors compared to normals (none of the tumors tested for *RANKL* expression produced a signal >1 SD from the normal average) (Figure 12). In contrast, 12 of 16 tumors showed *AKAP220* expression levels that were >1 SD from the normal average. Of these 12, six expressed *AKAP220* levels that were two to five times greater than the normal average (Figure 12).

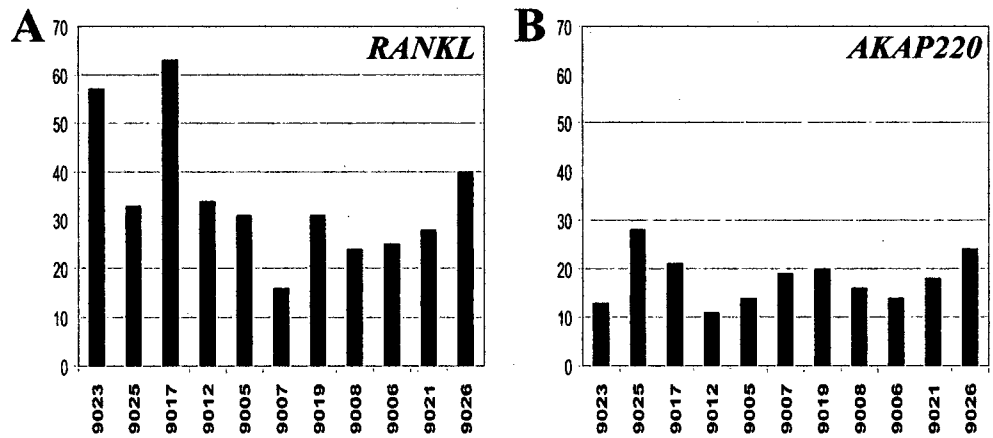

Figure 11. Expression Level of *RANKL* and *AKAP220* in Normal Oral Mucosa as Determined by RT-PCR. Values are normalized against *GAPDH* expression level in each of 11 samples. (A) *RANKL*. (B) *AKAP220*. Numbers on the x axis denote patient number.

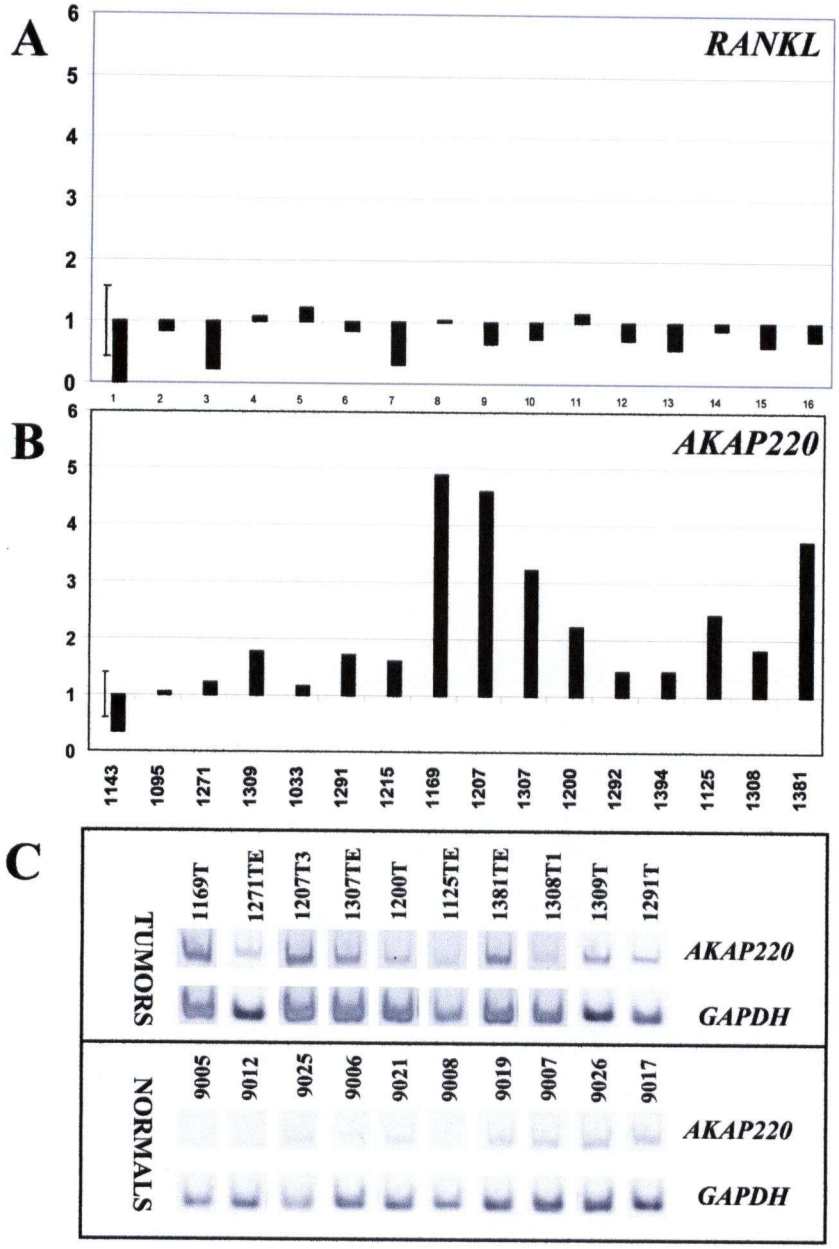

Figure 12. Comparative Expression Levels for *RANKL* and *AKAP220* in Oral Tumors. (A) Fold difference in *RANKL* expression of 16 tumors compared to average of 11 normal tissues shown in Figure 5a. Standard deviation for normal expression levels is indicated at far left of figure. (B) Fold difference for *AKAP220* in tumor compared to average of normals in Figure 5b. (C) Gel images showing RT PCR products for *AKAP220* and corresponding *GAPDH* in 10 example cases. X axes show the patient sample number.

In conclusion, we have identified a novel genetic alteration in oral cancers that lies within a 1.9 Mbp MRA that contained three known genes. One of the genes, *AKAP220* showed altered expression in oral cancers. To our knowledge this is the first report of *AKAP220* alteration in tumorigenesis although the involvement of this AKAP protein has been implicated in the cell cycle.

AKAP220 acts as a competitive inhibitor of type 1 protein phophatase (*PP1*) activity with this inhibition enhanced by the presence of the RII regulatory unit of protein kinase A (*PKA*) (Schillace and Scott, 1999; Schillace et al., 2001). PP1 catalyzes the dephosphorylation of the *RB* protein thus acting as a negative regulator of cell cycle progression (Oliver and Shenolikar, 1998; Rubin et al., 1998). Since AKAP220 inhibits this activity, its overexpression (as described in Figure 12) could lead to hyperphosphorylation of pRb, release of E2F, and the transcription of genes involved in cell cycle and lead to proliferation (Figure 13).

Other members of this pathway have been studied in oral and head and neck cancers. Both *Cyclin D1* and *MTS1/p16/INK4* are frequently dysregulated by multiple mechanisms (Lese et al., 1995; Piboonniyom et al., 2002; Yakushiji et al., 2001). In contrast, RB is seldom mutated (Li et al., 1994; Yoo et al., 1994). The involvement of *AKAP220* may be yet another mechanism of disrupting this critical pathway. It should be noted that, like the *CDKN2A* region (9p21), the *AKAP220* region on 13q14.11 is altered early in development of oral cancer. It is present in low-grade dysplasia and increases significantly with progression to high-grade dysplasia (Figure 10). These data strongly support the need for further studies to assess the impact of *AKAP220* alterations in early cancers.

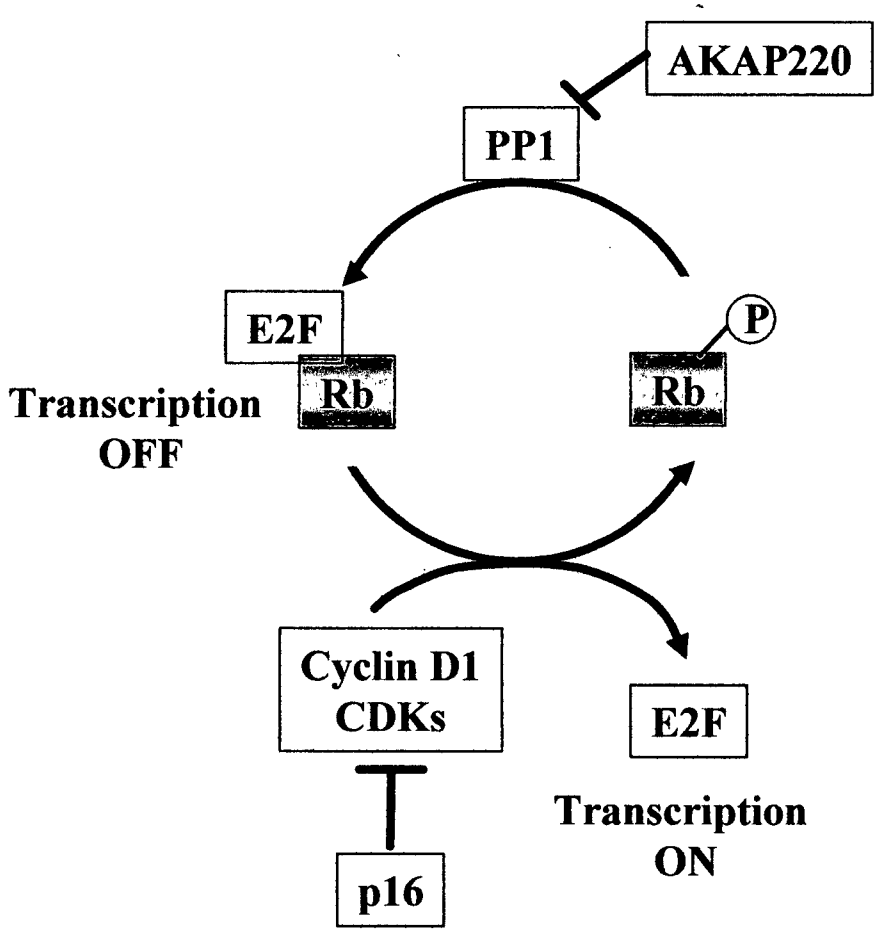

Figure 13. A Schematic Diagram Summarizing the Role of *AKAP220* in Cell Cycle Regulation. *AKAP220* inhibits the activity of *PP1*, the enzyme which dephoshphorylates *Rb*. In its dephosphorylated state *Rb* can bind to transcription factor E2F and prevent the initiation of gene transcription.

3.1.2 Fine mapping 8q22

Conventional CGH identified 8q amplification in a number of cancer types, including cancers of the breast, prostate, pancreas, bladder, vulva, and lung (Allen et al., 2002; Goeze et al., 2002; Hermsen et al., 1998; Mahdy et al., 1999; Schleger et al., 2000; Steiner et al., 2002). The well characterized oncogene *MYC*, located at 8q24, has been reported to be overexpressed in a variety of human cancers, and therefore the amplification observed at 8q has often been associated with this overexpression (Locker, 1991).

Cloning and sequencing of alterations that occurred in multiple dysplasias identified two recurring changes that subsequently mapped to chromosome arm 8q: a 190 bp signal at 8q22, which was present in three of 20 dysplasias, and a 160 bp alteration near the *MYC* gene, which was identified in 2 of 20 samples. The alterations appeared as additional bands in the dysplasia fingerprints that were absent in the patient-matched normal DNA fingerprints. Additional bands, not present in the matched normal samples, occur when the DNA in the dysplasia samples have been altered resulting in two primer sites becoming close enough to form a new product. The positions of all microsatellite markers were verified by BLAST alignment against corresponding BACs.

We employed microsatellite analysis to confirm independently the presence of a novel alteration at 8q22, separate from *MYC*. We assayed for LOH at *D8S1830*, which is within one of the amplified regions at 8q22, and at *D8S1793*, which maps between *D8S1830* and the *MYC* locus (Figure14). For informative cases, LOH was inferred when the signal ratio of the two alleles differed in the normal samples by at least 50%.

The data support a high frequency of alteration at 8q22 separate from 8q24. Ninety-three cases - 39 tumors and 54 dysplasias (13 severe/CIS, 15 moderate, 26 mild) - were

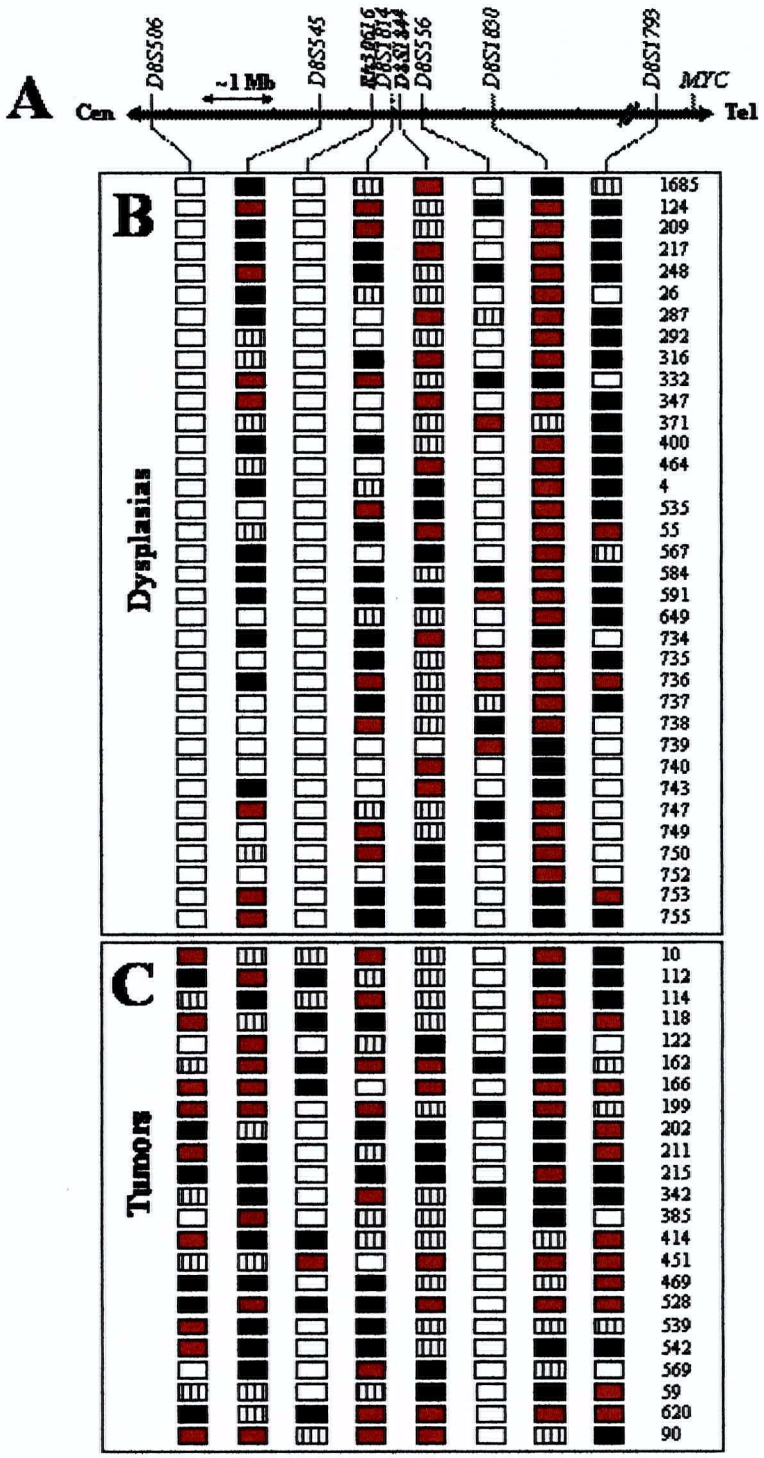

Figure 14. Microsatellite analysis of 8q22. (A) Relative position of markers. (B) Dysplasias with AI. (C) Tumors with AI. Color of boxes: AI (red); retention of heterozygosity (green); non-informative (striped); not determined (white). Cases that showed retention or AI of all markers are not shown.

examined, of which 80 (86%) were informative for *D8S1830*. Of these, 39 (49%) showed LOH. These cases were further analyzed for LOH at *D8S1793*, of which 37 were informative at this locus. Twenty-three of the 37 (62%) informative cases had LOH at *D8S1830* but retention at *D8S1793*. It is noteworthy that the frequency of LOH at D8S1830 was as high for dysplasias as it was for tumors. LOH was observed in 26 of 50 (52%) informative dysplasias and 13 of 30 (43%) informative tumors. Although a previous study suggested that alteration at 8q24 is an early event in oral carcinogenesis (Huang et al., 2002), *MYC* may not be the only critical gene in this region. To our knowledge, this represents the first description of frequent amplification of 8q22 in oral dysplasia, raising the possibility of a novel oncogene at 8q22 that may be relevant to the development of oral premalignant lesions.

Our data suggest the presence of other oncogenes centromeric to *MYC*. The observation of CGH alterations at 8q22 in breast and prostate cancers lends support to this hypothesis (Pollack et al., 2002; Sattler et al., 1999). Whereas previous studies attributed *MYC* overexpression to amplification of 8q21–24, differential expression of genes other than *MYC* has been reported in several types of cancer. *NOV* (nephroblastoma overexpressed gene), located at 8q24, has been reported to be overexpressed in Wilms' tumor (Chevalier et al., 1998). *NOV* is a member of the CCN family of proteins thought to be involved in the control of cell proliferation (Snaith et al., 1996). At 8q23, *EBAG9* (*Estrogen Receptor-binding-site Associated Antigen*), also known as *RCAS1*, has been reported to be overexpressed in breast, lung, thyroid, and pancreatic cancers (Akashi et al., 2003; Ito et al., 2003; Oizumi et al., 2002; Tsuneizumi et al., 2002). *EBAG9* is a human cancer cell surface antigen that contains an estrogen

response element. *Focal Adhesion Kinase* (*FAK*), found at 8q24, has been shown by immunohistochemistry to be overexpressed in several cancer types (Su et al., 2002). Differential expression of *FAK* has also been reported in colorectal cancer and in oral cancer (Lark et al., 2003; Schneider et al., 2002). Other genes at 8q21–24 that have not yet been implicated in cancer development but are functionally related to processes commonly disrupted in tumorigenesis include: *CCNE2*, involved in cell cycle regulation; *MMP16*, a matrix metalloproteinase at 8q21; and *ANGPT1*, involved in development of vascular structures during embryogenesis. It is possible that these genes are affected by the 8q21–24 amplification, and therefore they are candidate genes for further studies in OPLs.

In conclusion, we have demonstrated that there are multiple alterations occurring on chromosome bands 8q21–24 in oral tumors and have used microsatellite analysis to show the existence of at least one novel alteration centromeric to *MYC* that is a frequent occurrence in dysplasia (52%) suggesting a potential role in the development of OPLs.

3.2 Chapter 3 Summary

The work done using the RAPD screening technique coupled with LOH analysis supports a number of the hypotheses presented in this thesis. We have shown that there are in fact fewer changes present in the pre-invasive lesions through the RAPD fingerprints as well as provided support for hypothesis #1, #2, and #5 (see section 1.10.2). Hypothesis #1 states that certain genetic events occur at specific stages in tumorigenesis. This is true with the alteration at 13q14. Figure 10 clearly demonstrates

that this alteration is most prominent in high grade dysplasia whereas the alterations on 3p and 9p occur much earlier in progression. This LOH observed with marker *D8S1830* at 8q22 demonstrates how alterations that occur early in disease development may become masked by later events. This LOH occurs at a high frequency. It is distinct in the dysplasia samples whereas in the tumor samples there are fewer samples that show a distinction between the alteration at 8q22 and the *MYC* loci, thus supporting hypothesis #2. Lastly, the overexpression of *AKAP220* within the altered region on 13q14 supports hypothesis #5 which states that if a pathway is important to the progression of the disease it is likely that more than one component of that pathway will be altered as *AKAP220* is involved in regulating the cell cycle.

4.0 RESULTS: REGIONAL ARRAY

The work presented in this chapter resulted in six manuscripts:

Garnis C, Campbell J, Zhang L, Rosin MP, Lam WL. (2004) OCGR array: an oral cancer genomic regional array for comparative genomic hybridization analysis. *Oral Oncology* 40:511-9.

Garnis C, Baldwin C, Zhang L, Rosin MP, Lam WL. (2003) Use of complete coverage array comparative genomic hybridization to define copy number alterations on chromosome 3p in oral squamous cell carcinomas. *Cancer Research* 63:8582-5.

Garnis C, Coe BP, Zhang L, Rosin MP, Lam WL. (2004) Overexpression of LRP12, a gene contained within an 8q22 amplicon identified by high-resolution array CGH analysis of oral squamous cell carcinomas. *Oncogene* 23:2582-6.

Garnis C, Davies JJ, Buys TPH, Tsao M, Lam S, MacAulay C, Lam WL. Chromosome 5p Aberrations and Glial Cell Line-Derived Neurotrophic Factor Activation Are Early Events In Lung Cancer. *Oncogene*, In Press.

Garnis C, Campbell J, Davies JJ, MacAulay C, Lam S, Lam WL. (2005) Involvement of multiple developmental genes on chromosome 1p in lung tumorigenesis. *Human Molecular Genetics* 14(4):475-82.

Garnis C, MacAulay C, Lam S, Lam WL. (2004) Genetic alteration on 8q distinct from MYC in bronchial carcinoma in situ lesions. *Lung Cancer* 44:403-4.

As lead author the writing of these manuscripts and the majority of the experiments were performed by me. The following people aided in analysis: Jennifer Campbell (*Oral Oncology* 2004), Bradley P. Coe (*Oncogene* 2004), Corisande Baldwin (*Cancer Research* 2003), Jonathan J. Davies (*Oncogene* 2005, *Human Molecular Genetics* 2005). The Immunohistochemistry and Real Time PCR for the *Oncogene* 2005 paper was performed in collaboration with Dr. Ming Sound Tsao at the Ontario Cancer Institute.

RAPD analysis revealed a number of frequently altered regions in both oral and lung cancer. While LOH analysis defined frequency as well as the minimal regions of alteration at both 13q and 8q, the technique is limited by the presence of markers at the region of interest as well as the quantity of DNA for a given sample, as each LOH reaction requires 5 ng of DNA. In order to fine map numerous regions simultaneously with minimal DNA input we designed and constructed a bacterial artificial chromosome array for CGH analysis. This array consisted of 2770 BAC clones providing tiling resolution across 26 regions as well as full coverage of chromosome arms 1p, 5p, and 3p. These regions represent chromosomal loci detected from the RAPD analysis as well as specific regions of interest for lung and oral cancer in the literature.

4.1 Detecting Single Copy Alterations

Before using clinical samples on the regional array we needed to show that the array was sensitive enough to detect single copy alterations. We hybridized female genomic DNA (XX) against male genomic DNA (XY) and compared the BAC clones containing sequences from the X and Y chromosomes. Male genomic DNA was labeled with cyanine 5 and the female genomic DNA was labeled with cyanine 3. The two probes were combined and co-hybridized onto the regional array. The signal intensities were graphed using Microsoft Excel. Figure 15 shows the X loci BACs compared to representative autosomal BAC clones.

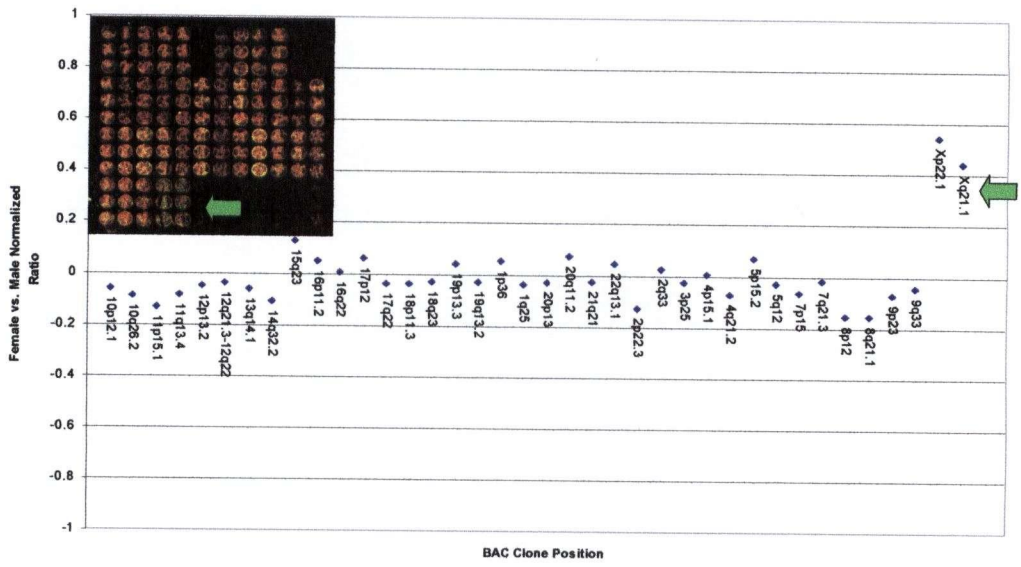

Figure 15. Detection of Single Copy Alteration with ArrayCGH. Female genomic DNA co-hybridized with male genomic DNA. Each black dot represents a single BAC clone. Signal intensity ratios for each clone are plotted. The log2 signal intensity ratios for the autosomal BAC clones are around zero indicating no copy number changes. The log2 signal intensity ratios or the X clone BACs (green arrow) are between 0.4 and 0.6 indicating a gain of the X chromosome.

4.2. Using Archival Material for Array CGH

In order to use the archival material microdissected for this study we had to show that in addition to being able to detect single copy alterations in high molecular weight DNA the regional arrays could also detect single copy alterations with less than optimal DNA, which is often associated with archival material. In a similar manner we compared archival material from a male individual against female genomic DNA. Figure 16 shows the plot of the log2 signal intensity ratios illustrating the detection of 2:1 allelic ratio for BACs on the X chromosome and a higher log2 ratio for the clones on the Y chromosome.

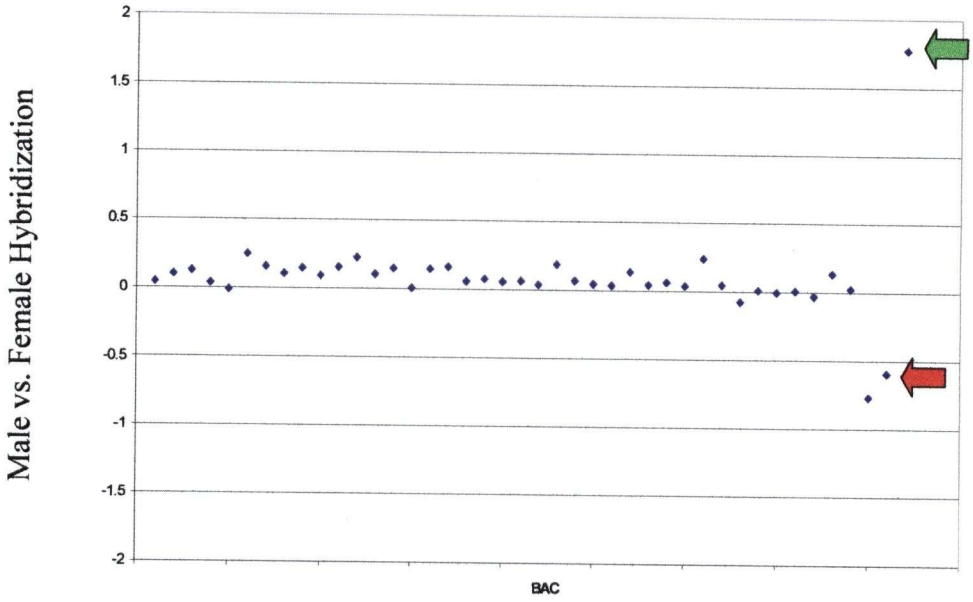

Co-hybridization of a reference male DNA and a formalin fixed female archival DNA

Figure 16. Detection of Single Copy Alteration Using Archival Material with ArrayCGH. Male genomic DNA co-hybridized with female genomic DNA. Each black dot represents a single BAC clone. Log2 signal intensity ratios for each clone are plotted. Clones mapping to autosomal loci are around zero indicating equal copy numbers in both male and female. The Y chromosome clones (green arrow) have a log2 signal intensity ratio >1 indicating a gain (Male XY/ female XX) and the X chromosome clone (red arrow) have a log2 signal intensity ratio <1 indicating a loss.

4.3 Regional Array Profiling of Oral Tumors

With the confidence that our arrays could detect alterations from archival material we profiled 14 microdissected oral tumors with our regional array. Figure 17 shows a graphical representation of the normalized cyanine 5/cyanine 3 log2 signal ratio versus relative tiling path BAC clone position. Figure 17A shows a control hybridization comparing two normal DNA samples. As expected, spots within all regions show log2 signal ratios close to zero indicating similar copy numbers in each normal sample. Figure 17B is an example of one of the 14 oral squamous cell carcinoma (OSCC) samples showing DNA segmental copy number increase at 7p11 and 11q13 with segmental copy number decreases at 3p14, 3p24, 9p22, and 8p23. Figure 17C is another OSCC sample showing segmental deletions at 3p14, 3p24, 9p22, 13q21, and 8p23 and amplification at 7p11. Figure 18 provides a summary of the copy number increases and decreases for each BAC clone in 9 of the regions represented on the array for each of the 14 OSCC samples.

Transition to different phases within the eukaryotic cell cycle is regulated by many cellular proteins. Key regulatory proteins are the cyclin-dependent kinases (CDK), a family of serine/threonine protein kinases which are activated at specific points in the cell cycle (Vermeulen et al., 2003). The *CDKN2A* gene, also known as *p16*, *INK4A*, and *MTS1*, is involved in cell cycle regulation through the retinoblastoma (*RB*) pathway (Serrano et al., 1993).

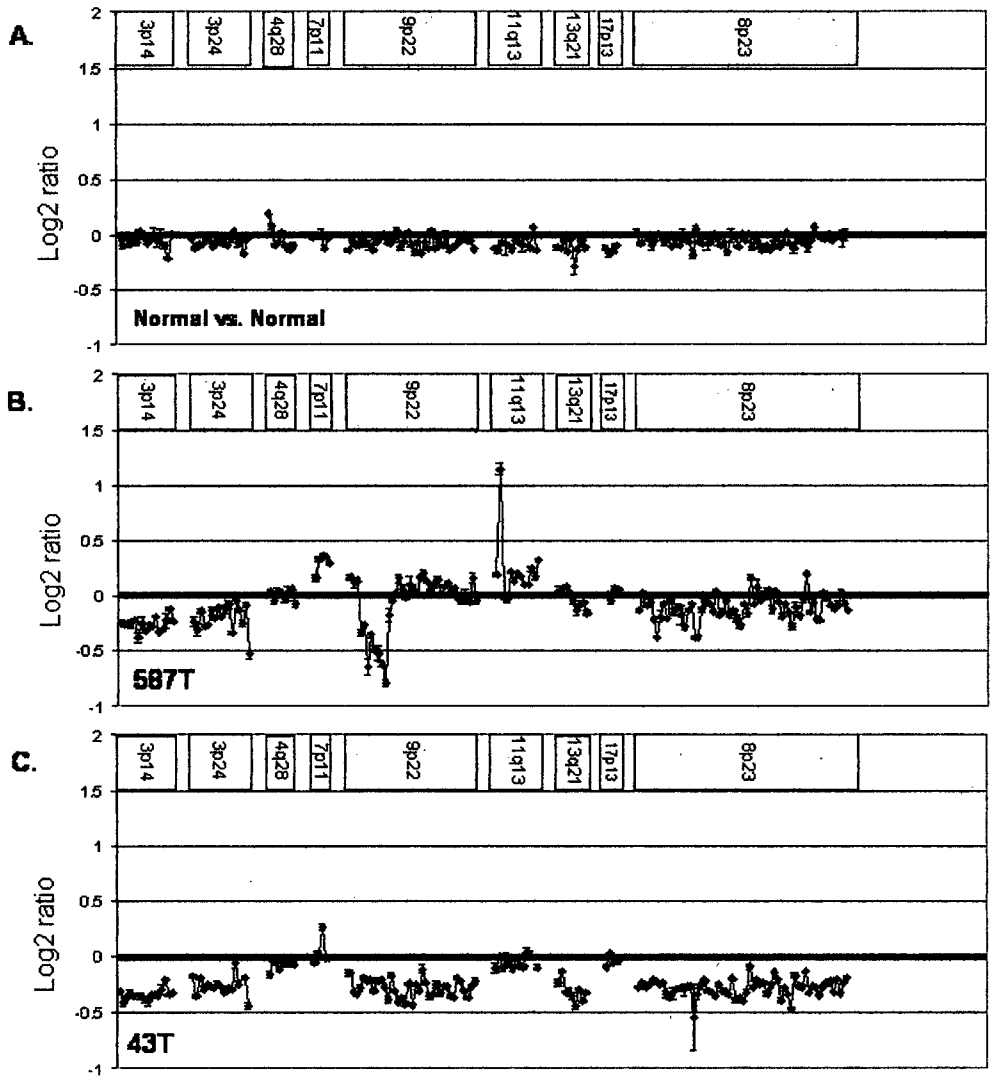

Figure 17. Examples of Array CGH Analysis of Oral Tumors for 9 Regions Represented on the Regional Array. Array CGH plots for normal human genomic DNA and two OSCC samples are displayed to illustrate copy number alterations. Each data point represents the average value derived from triplicate spots for each BAC locus. Standard deviations are indicated. Chromosomal regions represented on the array are outlined at the top of each plot in grey boxes. (A) Analysis of normal human genomic DNA versus normal human genomic DNA showing no significant copy number differences. (B) Tumor 587T showing regions of normal copy number at 4q28, 13q21, 17p13, regions of deletion within 3p14, 3p24, 8p23, 9p22, and regions of increased copy number within 7p11 and 11q13. (C) Tumor 43T shows regions of normal copy number at 4q28, 11q13, and 17p13, regions of decreased copy number within 3p14, 3p24, 9p22, 13q21, and 8p23 and a region of copy number increase within 7p11 (Garnis et al., 2004b).

Allelic loss at 9p21 (the *CDKN2A* locus) is one of the earliest genetic events to occur in the progression of oral cancer, with LOH frequencies up to 72% (Ah-See et al., 1994; Califano et al., 1996; Nawroz et al., 1994; van der Riet et al., 1994). In contrast, copy number reduction at BAC RP11-149I2, which contains *CDKN2A,* was present in only 4 of 14 cases (29%) analyzed in this report (Figure 18). However, this frequency is consistent with observations by Brieger et al. (7 of 22 or 32%) and by Huang et al. (21 of 75 or 28%) using conventional CGH studies in HNSCC (Brieger et al., 2003; Huang et al., 2002). The latter study also reports 9p amplification at a low frequency in pharyngeal, laryngeal, and OSCC. We detected copy number increase at 9p21-22 in 3 of the 14 cases analyzed. These data highlight the need for using complementary methods for detecting allelic loss and copy number changes in identifying regional alterations.

The high resolution of the oral cancer specific array allowed detection of small alterations on 7p11, 8p23, and 11q13. Figure 19 shows the log2 signal intensity ratios for the BAC set spanning a small region at 7p11 for 6 selected cases. Copy number increase was not detected in sample 539T. In contrast, the entire region is amplified in sample 587T. A high level of amplification was observed in sample 453T telomeric to RP11-436F9. Samples 628T, 43T, and 451T revealed amplification of only a single BAC clone: RP11-339F13. In total, this BAC is amplified in 10 of 14 cases analyzed. Superimposition of this BAC onto the draft sequence of the human genome identified amplification of the *EGFR* gene. *EGFR* is a well-characterized tyrosine protein kinase known to be overexpressed in a number of cancers, including head and neck cancer (Bei et al., 2001; Xia et al., 1999).

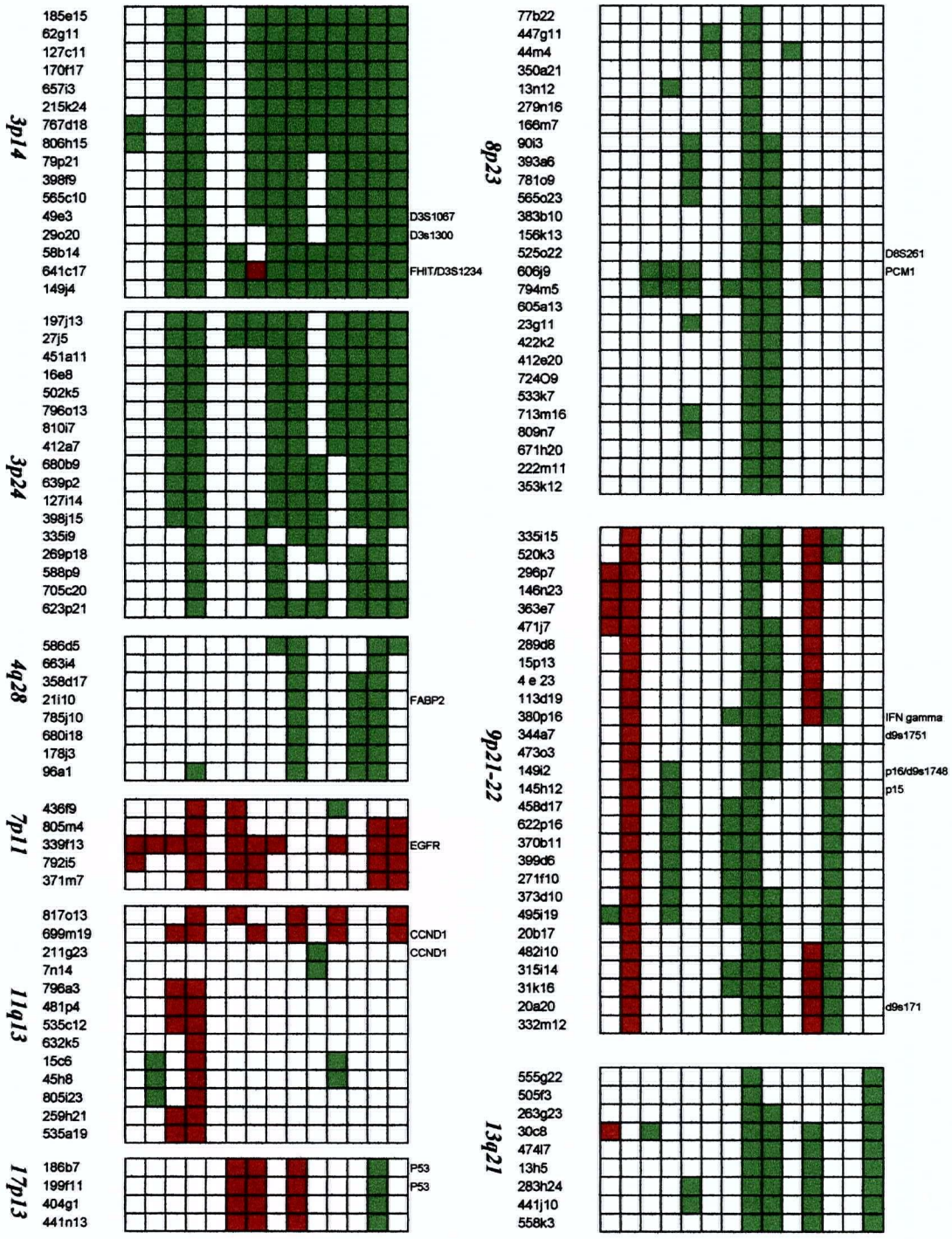

Figure 18. Summary of the 14 OSCC Profiled. Summary of copy number increase and decrease of chromosomal regions known to be involved in oral cancer progression. Tumor names are listed at the top of each column. RP11 BAC identity is listed on the left of each row. Key genes and markers that have been mapped to BACs are shown on the far right. Green boxes represent copy number decrease, red boxes represent copy number increase, and white boxes represent no change in copy number (Garnis et al., 2004b).

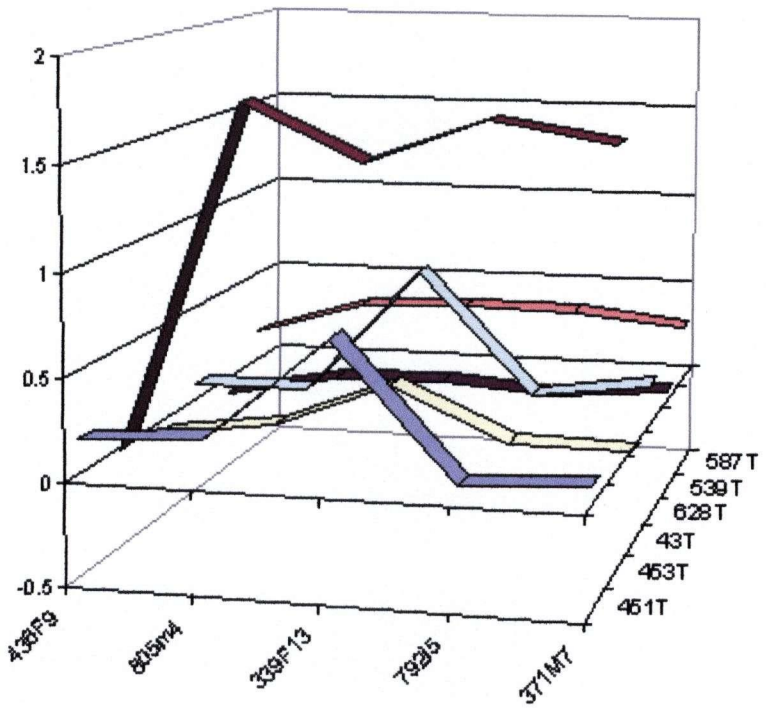

Figure 19. Microamplification at 7p11. Graphical representation of copy number alteration of 6 OSCC samples at the 7p11 region. 539T shows no copy number change while 587T has an increase in copy number for all BACs in the region. 453T has a high level of copy number increase across BACs 805M4, 339F13, 792I5, and 371M7. Samples 451T, 43T, and 628T all show an increase restricted to a single BAC (339F13) which contains the gene *EGFR* (Garnis et al., 2004b).

In addition to the microamplification observed at the *EGFR* locus the regional array copy number changes were also detected at the *Cyclin D1* locus localized to 11q13. Overexpression of *Cyclin D1* is well-documented in OSCC and has been reported to be associated with disease progression and poor prognosis (Kuo et al., 1999; Shintani et al., 2002). Half of the cases analyzed showed copy number increase in this region. Two of these samples (2T and 628T) showed single BAC amplifications. The micro-amplification of BAC clone RP11-699M13 contains three genes: *TAOS1*, *FGF19*, and *Cyclin D1*. Amplification of *Cyclin D1* and *TAOS1* and their corresponding expression have been demonstrated in OSCC cell lines (Huang et al., 2002). Furthermore, amplification of the 11q13 region is a genetic alteration frequently observed in patients with HNSCC's (Bekri et al., 1997; Muller et al., 1997).

Micro-deletions were also observed with the regional array. Several reports of alteration in oral dysplasia at 8p23, using microsatelite marker *D8S261* have been reported (Califano et al., 1996; Rosin et al., 2000). Twenty-seven BAC clones (~5 Mbp) centered at this marker were selected for the regional array. Array CGH analysis showed a number of distinct deletions on chromosome 8p23. Those deletions with the highest frequency occurred at BACs RP11-606J9 and RP11-794M5, which were present in half of the samples (Figure 18). These two BACs contain the *Pericentriolar Material 1* (*PCM1*) gene. Although the role of *PCM1* in oral cancer has not been explored, fusion of *PCM1* with the *RET* oncogene as a result of a translocation event is evident in papillary thyroid carcinoma (Corvi et al., 2000).

Conventional methods for detecting genetic alterations have provided insight into the gross alterations that occur in oral cancer. Array CGH complements these methods

by improving the detection of segmental copy number alterations to single BAC clone resolution. This is significant since, as we have demonstrated, many alterations are small in size and would have escaped detection with conventional approaches.

This array facilitated the detection of multiple segmental copy number changes as well as single BAC clone alterations. The data support the use of high resolution coverage of specific chromosomal regions to facilitate fine mapping of alterations and ultimately aid in the discovery of novel oncogenes and tumor suppressors.

4.4 Fine Mapping Chromosome 8q22

The 8q22-24 region was first noticed as a region of interest with the RAPD-PCR results (Table 3) in both oral and lung cancer and two separate regions of alteration at this loci were identified in OPLs and tumors by LOH analysis. To further investigate this region we built a contiguous set of 169 BAC clones spanning a ~52 Mbp region over 8q21-24 selected from the RPCI-11 library.

Array CGH experiments verify that amplification is occurring within 8q21-24 in oral cancer as well as CIS of the lung. We observed at least two separate regions of amplification centromeric to the amplification at 8q24, that contains *MYC*. Figure 20 illustrates 3 patterns of alteration in oral cancer samples: no amplification (Figure 20B); amplification of the entire tiling set (Figure 20C); multiple amplifications at 8q22, separate from 8q24 (Figure 20D and 20E). Figure 21 shows the similar pattern of amplification in the pre-invasive lung samples.

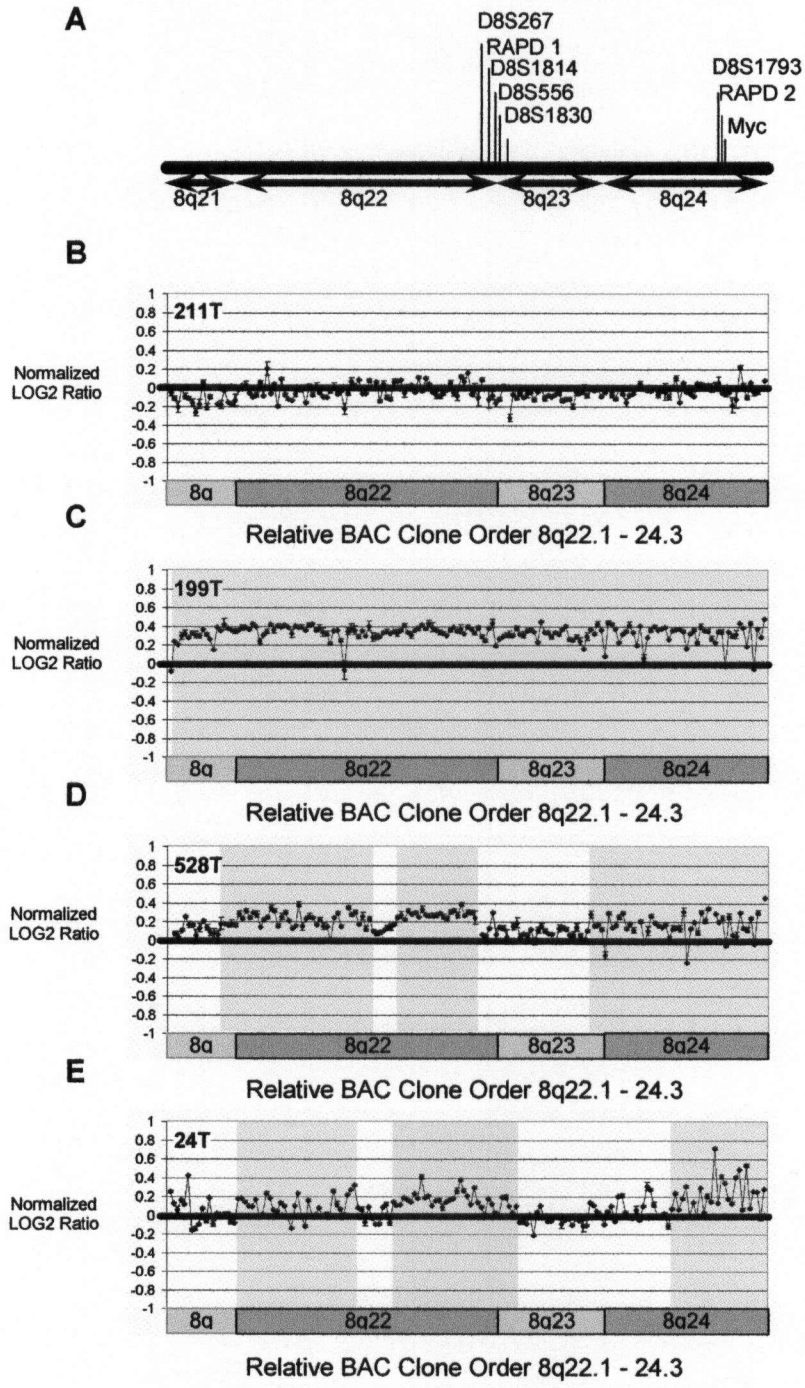

Figure 20. Array CGH Analysis of Oral Tumors at 8q21-24. The 169 BAC clones spanning a ~52 Mbp region are listed in Table 1. (A) shows a map of 8q21-24 with microsatellite markers and the location of RAPD alterations. B-E are CGH plots of 4 oral tumors. Shaded areas highlight regions of amplification. (B) Tumor 211T shows no copy number change within 8q21-24. (C) Tumor 199T shows amplification of the entire tiling set. (D) and (E) Tumor 528T and 24T show multiple amplifications at 8q22, in addition to that at 8q24.

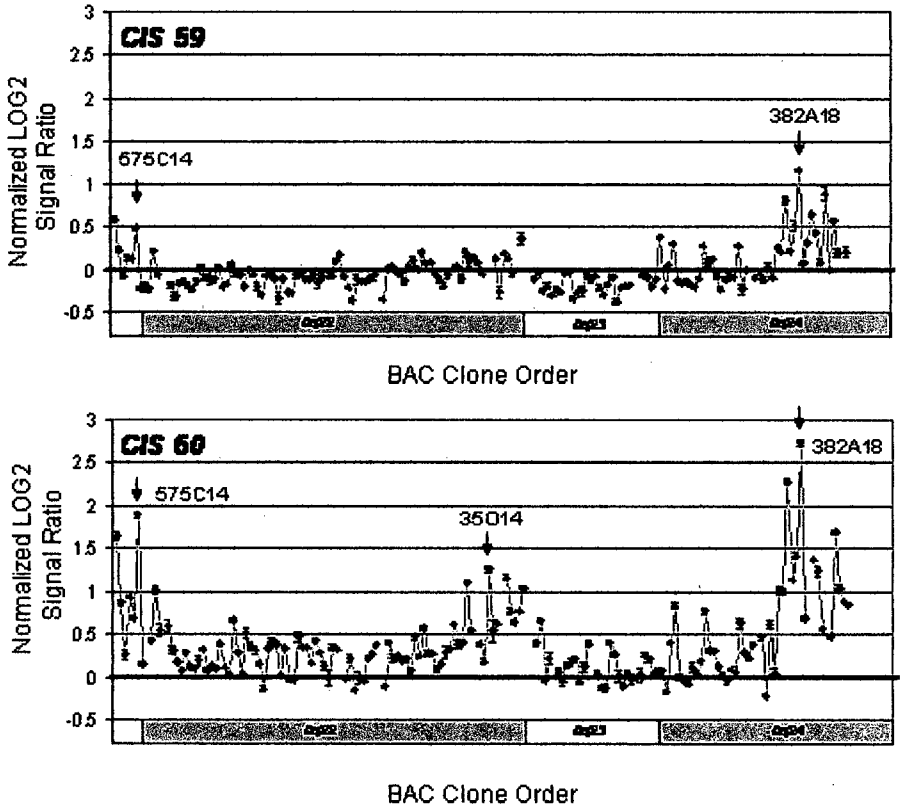

Figure 21. Array CGH Analysis of Lung CIS Samples at 8q21-24. The set of 169 BAC clones spanning an ~52 megabase pair region over 8q21-24 is available at (http://www.bccrc.ca/cg/OralCancer.html). Both example profiles show amplification at the *MYC* containing region at 8q24 as well as additional regions of amplification. Arrows indicate the RP11 BAC clone at the center of the amplified region. Data for each dye was normalized by applying a scale factor to each channel, which placed the median signal intensity of the reference human male genomic DNA spots at 1. The average signal ratios and standard deviations for each triplicate spot set were calculated and the data was displayed as a plot of cyanine 5/cyanine 3 log2 ratio versus relative tiling path position (Garnis et al., 2004e).

In this study I focused on one of the genes at 8q22: *LRP12* which encodes a low density lipoprotein receptor-like protein that is associated with several cancer related pathways and has been localized to BAC clone RP11-437B2 by sequence alignment. LRP12 was previously called *ST7* but recently renamed by Battle et al.(Battle et al., 2003). This gene should not be confused with the well-studied *ST7* gene on 7q31 (Dong and Sidransky, 2002).

Differential expression of *LRP12* and its two neighboring genes, *Dihydropyrimidinase* (*DPYS*) (immediately centromeric to *LRP12*) and *Friend of GATA2* (*FOG2*) (immediately telomeric to *LRP12*) were assayed (Figure 22). RNA was extracted from the epithelium of 15 microdissected frozen OSCCs and from 16 oral epithelial specimens from individuals without cancer. The normal samples were relatively uniform in expression levels of *LRP12* with minor fluctuations observed between samples. In contrast to the normal samples, five of the 15 tumor samples showed overexpression of *LRP12* to levels >2 SDs of the average normal value (Figure 22A). The two neighboring genes to *LRP12*, *DPYS* and *FOG2*, did not show significant altered expression in the tumor samples.

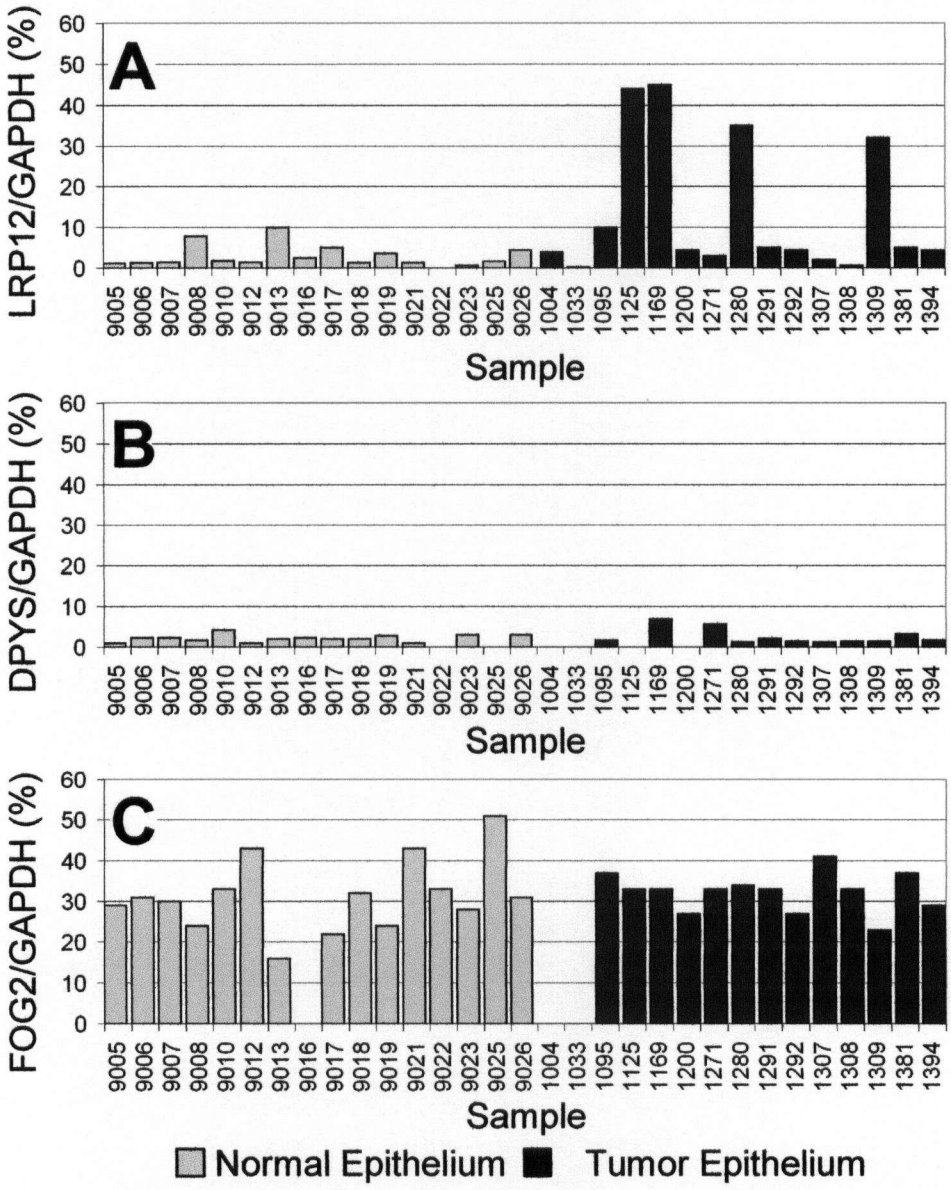

Figure 22. Expression Analysis of *LRP12* and its Neighboring Genes. (A) Histogram of expression levels of *LRP12* relative to that of *GAPDH* (B) Levels of *DPYS* relative to that of *GAPDH* (C) Levels of *FOG2* relative to that of *GAPDH* (Garnis et al., 2004d).

Our observations that *LRP12* is overexpressed in oral tumors is inconsistent with the work by Qing *et al.* in the fibrosarcoma cell line model which report a decrease in expression of *LRP12* associated with the transformation of a fibroblast cell line to a tumorigenic derivative (Qing et al., 1999). *LRP12* is not expressed in fibrosarcoma cells or is greatly down regulated at the mRNA and protein levels when compared with the parental fibroblasts or other normal human fibroblasts. This difference could be associated with the usage of a transformed cell line (MSU-1.1) for determining the normal expression baseline of *LRP12*. Our observations indicate that *LRP12* does not behave as a tumor suppressor gene and is likely a proto-oncogene in the context of oral cancer. However, the overexpression of *LRP12* does not rule out the possibility of other overexpressed genes in this amplified region.

Archival material from formalin-fixed paraffin blocks was available for a subset of the cases used in the expression analysis above. This allowed us to test whether the overexpression of *LRP12* is accompanied by genetic alteration. Although the amount of DNA recovered from the microdissected cancer cells was insufficient for array CGH analysis, we were able to examine these samples for LOH/AI at *D8S1459*, a microsatelite marker mapping near *LRP12* on BAC RP11-171O13 (Figure 23A). Although microsatellite analysis does not distinguish between amplification and deletions, the data is consistent with a correlation between genetic alteration and *LRP12* overexpression. Four tumors and three normal samples were polymorphic at *D8S1459*. Three of the four cases overexpressing *LRP12* showed LOH/AI while three cases with normal *LRP12* expression exhibited retention of both alleles (Figure 23B).

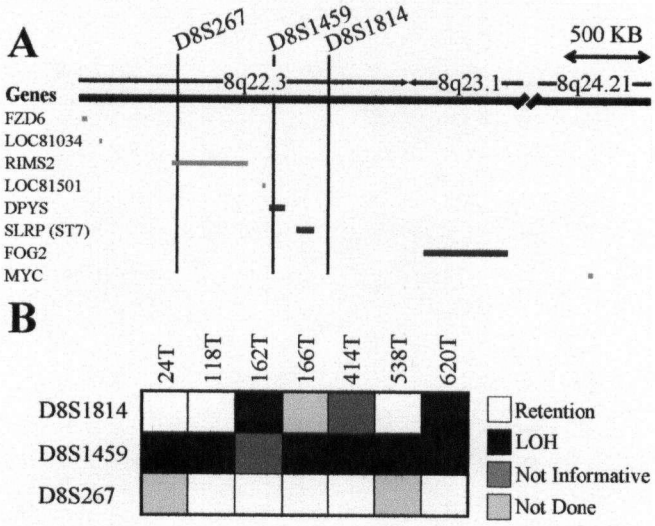

Figure 23. Microsatelite Analysis of Samples Showing Overexpression of LRP12. (A) Map of the 8q22-8q24 region. Genes within the region are located on the left and their coverage is depicted by a horizontal line. (B) Microsatelite analysis of seven samples that overexpressed *LRP12*. Markers listed on the left and sample names are on top.

In contrast to these results, expression levels of the two genes flanking *LRP12-DPYS* and *FOG2* (Figure 22 B-C)- were similar in both tumor and normal samples, suggesting that the overexpression is specific to *LRP12* and not a consequence of regional upregulation. However, our study, which focuses on *LRP12,* does not rule out the possibility of the presence of other differentially expressed genes in the 5.3 Mbp region.

LRP12 belongs to the LDLR superfamily and may play a role in signal transduction (Qing et al., 1999). Battle et al. showed that the cytoplasmic C terminus of LRP12 could interact with several proteins, including the receptor for activated protein C kinase 1 (RACK1), a protein that interacts with a myriad of cellular proteins, muscle integrin binding protein (MIBP) which plays a role in myogenesis, and SMAD anchor receptor activation (SARA), which interacts with the TGFβ pathway (Battle et al., 2003).

In summary, through the use of high resolution array CGH we have identified a recurrent 5.3 Mbp amplified region at 8q22 that is present in oral tumors. The *LRP12* gene found in the 8q22 region showed an increase in gene expression in oral tumors, while the adjacent genes *FOG2* and *DPYS* exhibited normal expression levels. The frequent amplification of the 8q22 genomic region in combination with the over-expression of *LRP12* and the association of the *LRP12* protein to pathways implicated in carcinogenesis suggests its involvement in head and neck epithelial carcinogenesis. Alteration at *D8S1459* in oral dysplastic lesions suggests that the role of *LRP12* in early oral cancer development should be further explored.

4.5 Regional Array: Chromosome Arms

4.5.1 Chromosome Arm 3p

Deletion on 3p is a frequent event that is likely to play a significant role in the pathogenesis of many cancer types, including OSCC (Rowley et al., 1996; Roz et al., 1996). The current literature suggests that there are multiple regions of chromosomal loss on this arm. However, these regions are poorly defined and their prognostic significance are unknown with the exception of one region (3p14) where allelic loss has been associated with risk of progression of oral premaligant lesions to cancer (Califano et al., 1996; Mao et al., 1996; Partridge et al., 1999; Rosin et al., 2000). The recent development of array CGH technology and its application to microdissected archival tissue support the feasibility of high resolution profiling of copy number changes on an entire chromosome arm in a single experiment (Pinkel et al., 1998). However, the only report of array CGH analysis of an entire chromosome arm involves the use of a full coverage array of chromosome 22 (~450 BAC clones) (Buckley et al., 2002). The present study represents the first use of this approach to demarcate regions of copy number alterations in OSCC.

Part of the regional array consists of 535 overlapping BACs, providing nearly complete coverage of chromosome 3p from telomere (3p26.3) to centromere (3p12.3).

Twenty oral tumors were microdissected and the DNA was analyzed for segmental copy number change. Nineteen of these 20 tumors had profiles where the internal control DNA spots gave consistent signal ratios. Of these 19, two had no

apparent copy number alteration, three showed a whole arm deletion, and the remaining 14 showed multiple segmental copy number alterations (Figure 24). As shown in Figure 24, the pattern of alteration in these tumors was complex, showing discontinuous copy number change with either several regions of deletion or combinations of decreases and increases in copy number.

A large region of copy number decrease (~27 Mbp) occurred at 3p14 (Figure 24, Region 1). This alteration is present in 7 of the 15 tumors with segmental alterations. This region contains the fragile histidine triad gene, or *FHIT*, which has been shown to be altered in many tumor types as well as in oral premalignant lesions. Loss of *FHIT* expression is a predictor of poor outcome in oral cancer (Lee et al., 2001). The wide extent of alteration in Region 1 supports the possibility of other tumor suppressor genes in addition to *FHIT*.

Although there were numerous regions of copy number change in the 14 cases with segmental alterations, three regions (Figure 24, Regions 3–5) were present at frequencies equal to or greater than that of the *FHIT* containing Region 1. These regions were small (<2 Mbp each, Table 4), and together contain only two known genes, *RBMS3* and *GRM7*, neither of which have been previously linked to oral cancer. *GRM7*, in Region 5, is a metabotropic glutamate receptor and *RBMS3*, in region 4, is a *MYC* gene single strand-binding protein (MSSP). MSSPs are thought to cooperate with *MYC* to regulate DNA replication, gene transcription, apoptosis, and cell cycle progression (Penkov et al., 2000).

To date, only deletions have been associated with 3p in oral cancer. The final region identified at 3p21.31 (Region 2) is unique in that it contains an increase in copy number. This alteration is present in six of 14 cases, with five cases defining a ~0.7 Mbp

Table 4. Description Of Regions Of Copy Number Alteration On 3p.

Region	Location	Centromeric BAC[a]	Telomeric BAC[a]	Extent (Mbp)	Known Genes
1	3p12.2-3p21.1	603J22 (AC107030)	122D19 (AC018354)	27	750
2	3p21.3	447D11 (AC104447)	509I21 (AC104304)	0.7	8
3	3p22	56P22 (AC093557)	598J13 (AC073353)	0.7	0
4	3p24.1	35C18 (AC018359)	539L2 (AC092503)	2	1
5	3p26.1	77I5 (AC011327)	7M24 (AC012136)	0.8	1

[a]GenBank accession number is given in parenthesis.

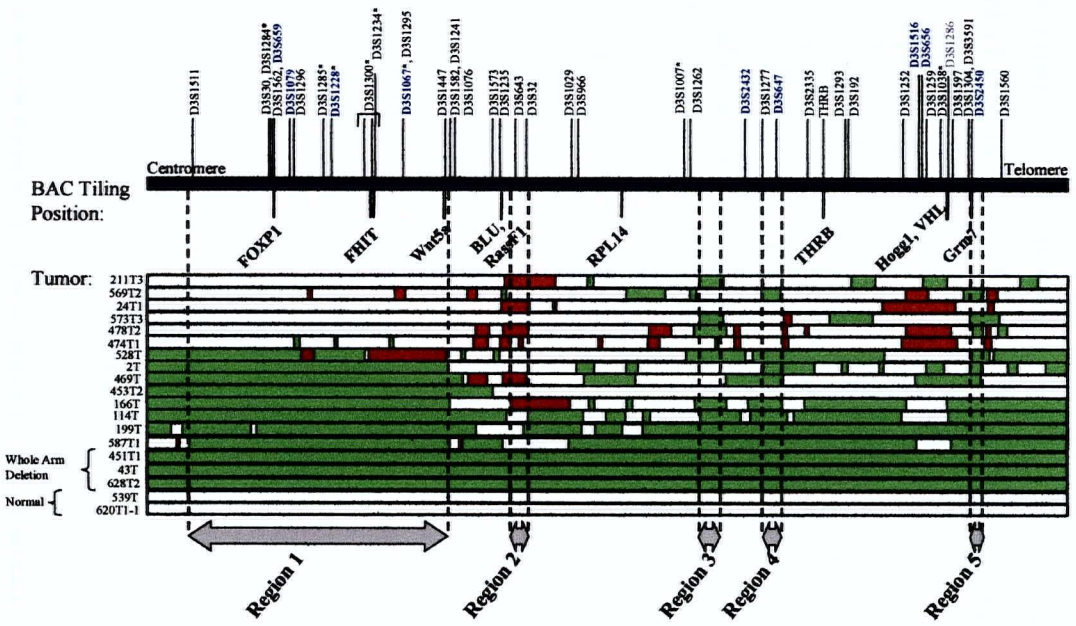

Figure 24. Alignment of 19 OSCC Array CGH Profiles for Chromosome Arm 3p. Five common regions of copy number change are marked by grey arrows. Red bars denote regions of copy number increase, while green bars represent regions of copy number decrease. Tumor specimens are listed on the left. Microsatellite markers historically used in fine-mapping studies have been mapped to the tiling set and are shown on top of the figure. Markers in blue have been reported in previous studies to have LOH frequencies greater than 60% (Garnis et al., 2003).

segmental copy number increase. For the sixth case (474T), the region covers only 0.2 Mbp. Based on the UCSC Human Genome Browser (April 2003 version) there are eight known genes within the 0.7 Mbp region. Although none have been implicated in oral cancer, two are putative oncogenes. *Testes Specific Protease 50* (*TSP50*) has been shown to be overexpressed in breast cancer (Yuan et al., 1999) and *Teratocarcinoma-Derived Growth Factor 1* (*TDGF-1*) is overexpressed in a number of cancer cell lines (Baldassarre et al., 2001).

Interestingly, genetic alterations near or within Region 2 have been described previously. Immediately centromeric to Region 2 is *RASSF1A*, which is frequently silenced by methylation in many cancers, although infrequently in head and neck cancers (Burbee et al., 2001; Hogg et al., 2002).

We compared the known and novel regions of copy number alterations with previously published regions defined by fine mapping efforts using microsatellite markers and CGH analysis (Beder et al., 2003; Huang et al., 2002; Kayahara et al., 2001; Partridge et al., 1999; Rowley et al., 1996; Roz et al., 1996). Historically, fine mapping by LOH in tumors is difficult due to the paucity of microsatellite markers as well as the constant revision of the human genome map. We have positioned the microsatelite markers used in the OSCC 3p fine mapping studies (Kayahara et al., 2001 ; Partridge et al., 1999; Rowley et al., 1996; Roz et al., 1996) and highlighted those that showed allelic loss in >66% of cases in Figure 24. Interestingly, these markers fall within Region 1 (containing *FHIT*) at 3p14, Region 4 at 3p24 and Region 5 at 3p26.1 as defined by array CGH.

In summary, this is the first report of complete profiles of copy number changes on 3p in OSCC. The data show the complex type of alterations which occur on this arm, many of which are small in size, requiring high resolution assays to define critical regions of change relevant to oral cancer. Using this approach, we detected a large region containing the extensively studied *FHIT* gene. We also detected three novel regions of deletions (3p22, 3p24.1, and 3p26.1) that were small and occurred at high frequency. We also report the first observation of a region showing copy number increase on 3p in OSCCs.

4.5.2 Chromosome Arm 5p

Molecular cytogenetic studies have shown that chromosomal aberrations occur on the short arm of chromosome 5 (5p) in all major lung tumor types (Balsara et al., 1997; Luk et al., 2001; Ried et al., 1994; Ullmann et al., 1998). The 5p subset of the regional array comprehensively covers chromosome 5p in 491 overlapping segments, allowing for high resolution detection of copy number alterations (Coe et al., 2004). We analyzed bronchial CIS and SCC tumors through the use of a unique 5p-specific BAC array. Alignment of array CGH profiles revealed multiple distinct regions of amplification and deletion in CIS that would otherwise appear to be masked in the later stage tumor samples. The identification of these recurrent alterations not only led to the discovery of candidate genes but also highlights the importance of studying the genomics of early stage lung cancer.

We compared eight microdissected bronchial CIS lesions and nine SCC tumor samples for genetic alterations. Signal intensity ratios for each triplicate-spotted BAC clone (giving a total of >25,000 data points across all 17 samples) were calculated and displayed as a log2 plots using SeeGH software (Chi et al., 2004). Figure 25A gives examples of 5p SeeGH karyograms illustrating a profile with minimal copy number changes (T5850), a profile with whole arm amplification (T11773), and profiles with multiple segmental gains and losses (T10999, T8611). Alterations were detected in nearly all of the samples analyzed: in seven of the eight CIS samples and all of the tumors. Figure 25B shows the alignment of all 17 profiles, displayed in Java TreeView with colorimetric representation. Four tumors and one CIS (T11278, T3010, T8611, T11773, C125) showed amplifications spanning nearly the entire chromosome arm. Notably, smaller and more distinct regions of gain and loss were apparent in the CIS profiles, for example the amplified Regions A3 and A4 within 5p15.2. Furthermore, recurrent deletions were prominent in CIS but undetected in tumors, suggesting the possibility that deletions could be masked in tumors by later genetic events.

Our data revealed broader alterations in tumors relative to those seen in CIS samples. Array CGH profile alignment enabled identification of six recurrent regions of amplification amongst the tumor and CIS samples (A1-A6) and three recurring regions of deletion within the CIS samples (D1-D3) (Figure 25, Table 5). Due to the comprehensive nature of the 5p array, we observed submegabase changes which account for seven of the nine recurrent regions of alteration. These small alterations would likely have escaped detection through the use of traditional marker-based techniques.

Table 5. Recurrent Minimal Regions Of Genetic Alterations On 5p

Region *	Cytoband #	Estimated size (Mbp)	Base pair position#	Boundary BAC clones§	Known genes in region#
A1	p15.33	4.1	97,762-4,260,073	348B13 to 328F21	*hTERT*, 13 others
A2	p15.31-32	0.90	6,010,119-6,905,520	107F17 to 203A14	*SRD5A1*
A3	p15.2	0.15	11,062,828-11,209,193	471G19 to 293P3	*CTNND2*
A4	p15.2	0.27	14,196,287-14,471,241	20B15 to 611H4	*TRIO*
D1	p14.3	1.1	21,113,936-22,241,939	627F13 to 402L24	*CDH12*
D2	p13.3	0.38	29,217,035-29,592,188	784O7 to 258I24	none
A5	p13.3	0.22	31,243,308-31,464,867	705N10 to 784O19	*CDH6, RNASE3L*
D3	p13.2	0.075	34,098,642-34,173,623	110H4 to 15A6	none
A6	p13.2	0.34	37,711,349-38,049,921	285H4 to 695L19	*GDNF*

*A recurrent region is present in over 50% of the CIS array CGH profiles; regions correspond to those indicated on Figure 25 ("A" denotes amplification, "D" denotes deletion).

#Base pair, cytoband and known (reviewed) genes are based on the Human April 2003 Assembly at the UCSC Genome Browser, version hg15.

§BAC clones derive from the RP11 library.

Figure 25. 5p Segmental Copy Number Alterations. Normalized log2 signal intensity ratios were plotted using SeeGH software, version 1.7(Chi et al., 2004). A log2 signal ratio of zero represents equivalent copy number between the sample and the reference DNA. Clones with standard deviations among the triplicate spots >0.075 or a signal to noise ratio >20 were disqualified from further analysis. (A) 5p array CGH profiles showing normal copy number (T5850), whole arm amplification (T11773), and multiple segmental copy number changes (T10999, T8611). 5p cytoband pattern is to the left. Vertical lines denote log2 signal ratios from -1 to 1 with copy number increases to the right (red lines) and decreases to the left (green lines) of zero (purple line). Each black dot represents a single BAC clone. (B) Colorimetric representation of 5p array CGH data viewed by Java TreeView. To compare multiple profiles, we used Java TreeView version 1.0.3 to generate a colored gene copy number matrix (http://jtreeview.sourceforge.net). Intensities of red and green coloration indicate an increased or decreased log2 signal ratio for each clone respectively. Gray coloration indicates clones discarded due to high standard deviations (>0.075) or signal to noise ratios. Each column represents a separate array CGH profile. Each row corresponds to a BAC clone and each column represents a CIS or tumor sample (sample ID at top). 5p cytoband pattern is to the left. Recurrent amplifications are denoted by vertical blue lines to the right and deletions to the left. The close up views of regions A4 and A6 are shown to the right with the genes of interest represented by black lines. (C) Magnification of the A4 region containing the *TRIO* gene. (D) Magnification of the A6 region containing the *GDNF* gene.

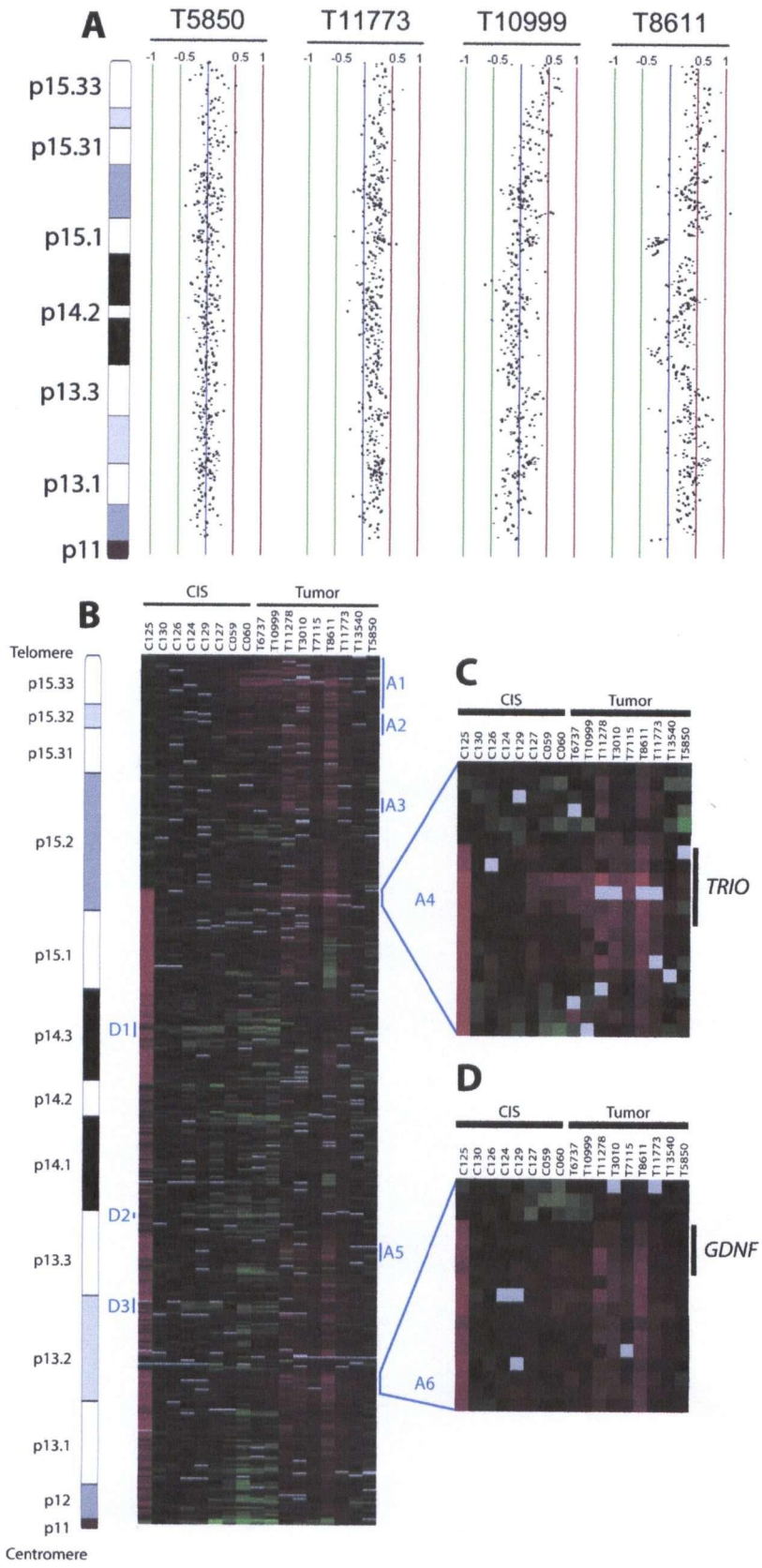
A
T5850
T11773
T10999
T8611
-1
-0.5
0.5
1
p15.33
p15.31
p15.1
p14.2
p13.3
p13.1
p11
B
CIS
Tumor
C125
C130
C126
C124
C129
C127
C059
C060
T6737
T10999
T11278
T3010
T7115
T8611
T11773
T13540
T5850
Telomere
p15.33
p15.32
p15.31
p15.2
p15.1
p14.3
p14.2
p14.1
p13.3
p13.2
p13.1
p12
p11
Centromere
A1
A2
A3
A4
A5
A6
D1
D2
D3
C
CIS
Tumor
TRIO
D
CIS
Tumor
GDNF

To establish a threshold, normal male DNA versus normal male DNA hybridizations were used to determine the background experimental noise at three SDs (Garnis et al., 2003). This placed our threshold at a ±0.13 log2 raw ratio which was used to define regions of genetic alteration. In addition, for a region to be defined as altered, it had to involve at least two consecutive overlapping BAC clones. To increase the likelihood of identifying causal genetic events we applied stringent selection criteria requiring the presence of alterations in at least half of the CIS samples to define a recurrent region. Strikingly, of the six recurrent amplified regions defined, five (Regions A2-A6) have not been previously reported in lung SCC. The previously reported amplification at 5p15 (Bryce et al., 2000; Saretzki et al., 2002), which contains the well characterized *Human Telomerase Reverse Transcriptase* gene (*hTERT*), falls within Region A1. However, the other locus known to be amplified in tumors (5p13.2), containing *S-Phase Kinase-Associated Protein 2* (*Skp2*), although detected in the array CGH tumor profiles, did not qualify as a region of interest in our study due to the absence of amplification in the CIS samples at this loci (Zhu et al., 2004). Remarkably, with the exception of Region A1, all other amplifications were <1 Mbp in size (Table 5). Regions A2, A3, A4, and A6 contain only a single annotated gene, while A5 contains only two known genes. The boundaries of these narrow regions are listed in Table 5. Of the four genes in single gene regions, *Catenin Delta-2* (*CTNND2*) has been shown to be overexpressed in prostate cancer (Burger et al., 2002) and *Steroid 5-Alpha-Reductase* (*SRD5A1*), which catalyzes the conversion of testosterone into the more potent androgen dihydrotestosterone (Harris et al., 1992), has been shown to be overexpressed in breast cancer (Wiebe and Lewis, 2003). The *Triple Functional Domain* gene (*TRIO*) in Region

A4 (Figure 25C) and the *Glial Cell Line-Derived Neurotrophic Factor* gene (*GDNF*) in Region A6 (Figure 25D), however, have not been directly implicated in cancer and were further investigated in this study (see below).

Previous chromosomal CGH studies have identified 5p amplification as a common event in NSCLC, however copy number reduction is rarely described. Studies using microsatellite markers have revealed LOH at the centromeric end of 5p (Wieland and Bohm, 1994; Wieland et al., 1996). Our analysis of the tumor profiles is consistent with previous reports in that we did not detect recurrent regions of deletion in tumor samples. To our knowledge, specific recurrent regions of deletion have not been defined within 5p in NSCLC. However, when we aligned the eight CIS profiles, three distinct recurrent regions of deletion emerged (Figure 25B). Recurrent deletions were defined by their presence in at least four of the eight samples. Two of the three regions were <1 Mbp in size (Table 5). The 1.1 Mbp Region D1 contains only one known gene - *Cadherin 12* (*CDH12*) - while no genes have been annotated within Regions D2 and D3. These observations reinforce the value in analyzing pre-invasive disease as it has led to the identification of a small deletion that contains a single gene candidate.

We have identified seven candidate genes that fall within small regions containing only one or two genes (Table 5). Since a detailed analysis of all the candidate genes is beyond the scope of this study, we focused on two genes: *TRIO* and *GDNF*.

Figure 26A shows a close-up image of SeeGH karyograms for the four CIS profiles that are amplified at the *TRIO* locus. CIS samples (C59, C127, and C60) show discrete amplification at this region whereas C125 shows a larger amplification that extends from BAC RP11-20B15 to the centromere. Amplification of the *TRIO* region is maintained in

tumors (Figure 25C). Next, we investigated *TRIO* for differential expression by real-time-PCR in eight paired normal and SCC samples. We observed overexpression of *TRIO* in six of the eight pairs ($P < 0.05$) (Figure 26B). This expression pattern is confirmed in an additional panel of 13 paired normal and tumor SCC samples by semi-quantitative reverse transcriptase-PCR, where nine of 13 tumors showed significant overexpression ($P = 0.002$) (Figure 26C and D). The concordance of copy number increase with overexpression in tumor samples implicates a role for *TRIO* in lung SCC, while its frequent amplification in pre-invasive lesions suggests its early involvement in tumorigenesis. The TRIO protein contains three functional domains: a serine/threonine kinase domain and two guanine nucleotide exchange factor domains for the family of Rho-like GTPases, specific for Rac1 and RhoA respectively. These functional domains suggest that this enzyme may play a key role in several signaling pathways that control cell proliferation (Debant et al., 1996; Zheng et al., 2004).

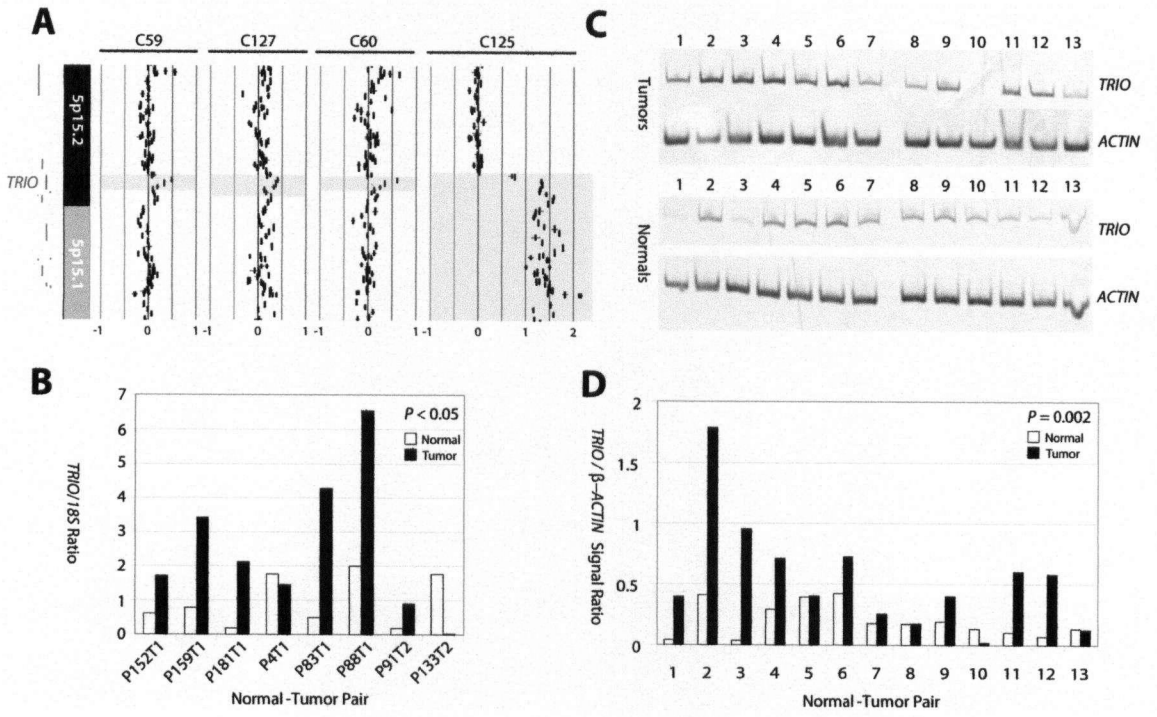

Figure 26. Genomic and gene expression analysis of *TRIO*. (A) SeeGH karyogram of the *TRIO* region for four CIS samples. Cytobands are indicated on the left of the profiles. Vertical lines denote log2 signal ratios with copy number increases to the right and reduction to the left of zero. Each black segment represents a single BAC clone. Amplified regions containing *TRIO* are highlighted. (B) Real-time PCR expression analysis of *TRIO* in eight matched normal (grey) and tumor (black) samples. (C) Reverse transcription PCR analysis of *TRIO* and *Beta-Actin* in an additional panel of 13 matched normal and tumor samples. PCR products were resolved by polyacrylamide gel electrophoresis, stained with SYBR green, quantified using the Storm Phosphoimager, and summarized in (D).

Similar to *TRIO*, the *GDNF* region is amplified in CIS samples as well as in tumor samples (Figure 25D). In Figure 27A the amplified region containing *GDNF* is highlighted in five CIS profiles. Real-time-PCR analysis showed striking overexpression of *GDNF* in five of the eight paired normal and tumor RNA samples ($P < 0.05$) (Figure 27B). The absence of *GDNF* expression in normal adult lung tissue agrees with the previous observation that *GDNF* is expressed in fetal but absent in post-natal lung tissue (Fromont-Hankard et al., 2002). Our data suggest reactivation of *GDNF* expression in tumors.

To further evaluate the tumor-specific expression of *GDNF* at the protein level immunohistochemical analysis was performed. A monoclonal antibody specific for GDNF showed conspicuous membrane staining with less intense cytoplasmic staining (Figure 27). Staining was not detected in normal bronchial epithelium. We further analyzed a panel of samples which included hyperplasia, CIS, and tumor samples. Immunostaining was not evident in hyperplasia but was detected in CIS samples and invasive tumors. This data suggests expression of *GDNF* in early histological lung cancer stages. This is further supported by the fact GDNF is the ligand for the RET proto-oncogene, which is known to transduce signals for cell growth and differentiation (Figure 27E) (Takahashi, 2001).

Figure 27. Genomic, Gene expression, and Immunochemical Analysis of GDNF. (A) SeeGH karyogram of the GDNF region for five CIS samples. Cytobands are indicated on the left of the profiles. Vertical lines denote log2 signal ratios with copy number increases to the right (red lines) and reduction to the left (green lines) of zero (purple line). Each black segment represents a single BAC clone. Amplified region containing GDNF is highlighted. (B) Real-time PCR expression analysis of GDNF in eight matched normal (grey) and tumor (black) samples. For real-time PCR analysis, mRNA expression levels were quantitatively assessed by reverse transcription-PCR using the ABI PRISM 7700 Sequence Detection System, as previously described (Wang et al., 2002). To avoid amplification of contaminating genomic DNA sequences, primers were designed to span two adjacent exons. All assays were done using duplicate samples of each RT product. The sample-to-sample variation of RNA/cDNA quantity was normalized using the 18S ribosomal RNA as the reference gene (Wang et al., 2002). (C) Immuno-staining of squamous cell lung tumor tissue sections with anti-GDNF monoclonal antibody (SantaCruz Biotech). (D) Immunohistochemistry analysis of GDNF expression in a bronchial biopsy. This specimen contains multiple cell populations of various histopathological stages. GDNF expression is evident in hyperplasia, moderate dysplasia, as well as carcinoma. (E) Schematic of RET signaling pathway. Unregulated extracellular GDNF binds to the RET receptor resulting in pro-oncogenic intracellular signals.

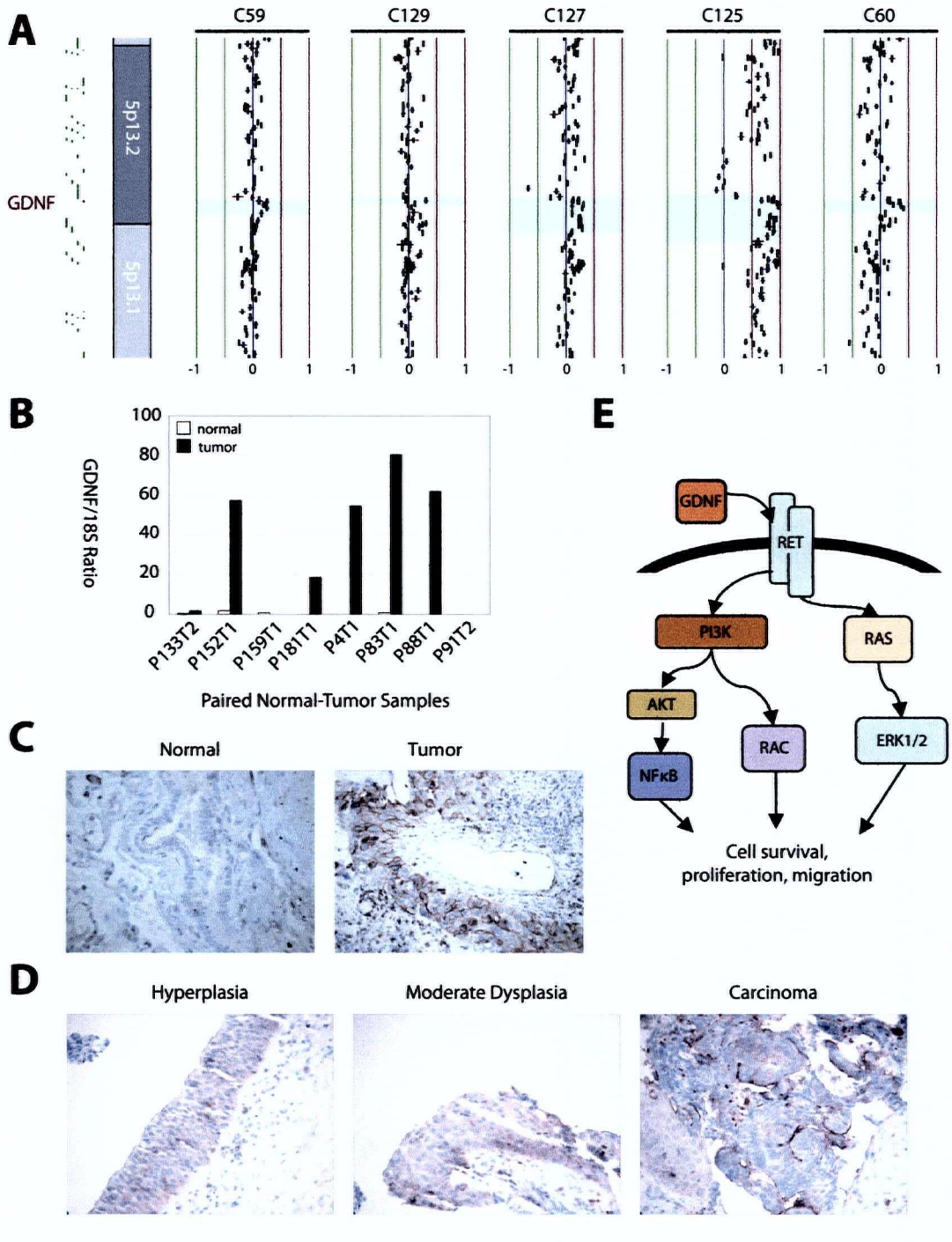
A
C59
C129
C127
C125
C60
GDNF
5p13.2
5p13.1
-1
0
1
B
normal
tumor
GDNF/18S Ratio
100
80
60
40
20
0
P133T2
P152T1
P159T1
P181T1
P4T1
P83T1
P88T1
P91T2
Paired Normal-Tumor Samples
C
Normal
Tumor
D
Hyperplasia
Moderate Dysplasia
Carcinoma
E
GDNF
RET
PI3K
RAS
AKT
RAC
ERK1/2
NFκB
Cell survival,
proliferation, migration

In summary, the identification of early stage genetic events that drive the progression of squamous cell lung cancer requires the study of pre-invasive lesions. Our data suggest the possibility that early causal events in tumorigenesis may be masked by later stage genomic instability. The ability of the CIS profiles to narrow our focus within the tumor profiles demonstrates the importance of studying early stage disease. In the past, such studies have been limited by the rarity and minute size of early stage specimens. The development of the 5p genomic array has facilitated comprehensive analysis of the 5p chromosome arm for these precious samples. Consequently, we have identified nine distinct regions of alteration across 5p, of which eight are novel and seven are submegabase in size. These small alterations would likely have escaped detection through the use of limited resolution conventional marker-based techniques. This study has shown that the analysis of CIS samples with a comprehensive tiling path array is arguably one of the most effective ways to focus attention on those regions of the chromosome arm that contain genes potentially critical to disease progression.

We have assayed the expression levels of two of the candidate genes that fall within amplified regions, *TRIO* and *GDNF*, and found that both are significantly overexpressed in a panel of tumors compared with their matched normal RNA samples. More significantly, immunohistochemical analysis of GDNF, a ligand for RET, not only showed tumor-specific staining but was also present in pre-invasive stage specimens. Interestingly, *GDNF* expression is normally restricted to the fetal lung and is involved in lung development (Fromont-Hankard et al., 2002). Our findings suggest that reactivation of this developmental gene may contribute to lung tumorigenesis at an early stage.

4.5.3 Chromosome Arm 1p

Aberration of the short arm of chromosome 1 (1p) is a common event in lung and many types of cancer (e.g. colorectal, gastric, neuroblastoma, liver, pancreatic, and breast cancer)(Han et al., 1999; Testa et al., 1994). Cytogenetic studies have shown that 1p harbors structural rearrangements in NSCLC (Nomoto et al., 2000), while microsatellite analysis demonstrates frequent LOH at 1p36 in all major lung cancer subtypes (Testa et al., 1994). Moreover, alignment of LOH data revealed multiple regions of alteration on 1p (Girard et al., 2000; Han et al., 1999; Ragnarsson et al., 1999; Testa et al., 1994). Although there appears to be a high frequency of LOH across the entire chromosome arm, three large but distinct regions (1p36, 1p32, and 1p12) have been reported, suggesting the presence of more than one oncogene/tumor suppressor gene on the short arm of chromosome 1. Notably, there are several genes associated with the Wnt and Notch developmental pathways mapping to chromosome 1p.

Pathways involved in development may play a role in tumorigenesis. Recent focus on the Wnt pathway in colorectal cancer has prompted gene expression analysis of pathway components in other cancer types including breast, prostate, and lung (Gasparian et al., 1998; Taketo, 2004). WNT ligands bind to their target membrane receptors, Frizzled (FZD) and Low Density Lipoprotein Receptor-related Proteins (LRPs), and interfere with the multi-protein APC/β-catenin destruction complex, resulting in the downstream activation of gene transcription by β-catenin. While the complex role of β-catenin in cell proliferation and cell adhesion has been the main focus of many mechanistic studies, it is becoming increasingly evident that upstream components such

as *WNT*, *FZD*, *SFRP*, *LRP*, and *DVL* genes are also involved in cancer (Brennan et al., 2004; Garnis et al., 2004d; Lee et al., 2004; Lu et al., 2004; Taketo, 2004; Tamai et al., 2000; Uthoff et al., 2001; Wissmann et al., 2003). Recent reports of *DVL3* and *WNT2* overexpression in NSCLC suggest a potential role of this pathway in cell proliferation (Lu et al., 2004; Suzuki et al., 2004). However, *WNT7a* silencing, which leads to β-catenin-mediated loss of *E-Cadherin* expression and subsequently impacts cell migration, suggests that the Wnt pathway plays a role in the later stages of lung cancer (including metastasis) (Caldwell et al., 2004). Additionally, the Notch developmental pathway, which interacts with Wnt components, has also been implicated in cancer. For example, *NOTCH3* translocation and overexpression has been observed in lung cancer (Uematsu et al., 2003a). Interestingly, aberrant Wnt pathway signaling is an early event found in ~90% of colorectal cancers (Uematsu et al., 2003b). This possibility has not been explored in lung cancer.

We investigated 1p alterations in early stage development of lung cancer. Hitherto, genomic analysis of early stage lesions has been limited presumably due to the difficulty in obtaining pre-invasive lesions and the minute size of such material, which yield limited DNA sufficient only to support locus-specific analysis but far too impractical for large scale gene discovery. In this work, we combine the use of fluorescent bronchoscopy to capture pre-invasive lesions and BAC genomic array to comprehensively analyze the 1p arm in microdissected pre-invasive bronchial CIS and invasive SCC specimens. The BAC clones of the 1p specific array span the chromosome arm in a tiling fashion, allowing focused characterization of genetic alterations in order to identify candidate genes that may be causal to the development of lung cancer.

As mentioned above, the role of developmental pathways has become increasingly appreciated in cancer etiology. Remarkably, candidate genes within three of the five novel regions of genetic alteration defined in this study are associated with the Notch and Wnt developmental pathways.

Figure 28 shows the 1p profiles from two lung SCC samples. Multiple segmental copy number changes were evident across the chromosome arm. Due to the redundancy and the high degree of overlap of clones, small regions of genetic alterations were readily detected. While such small alterations may have gone undetected by marker-based techniques and conventional chromosomal CGH, the tiling nature of the array enables the definition of breakpoints flanking an altered region. In our example, we magnified three regions to illustrate simultaneous localization of multiple breakpoints (Figure 28).

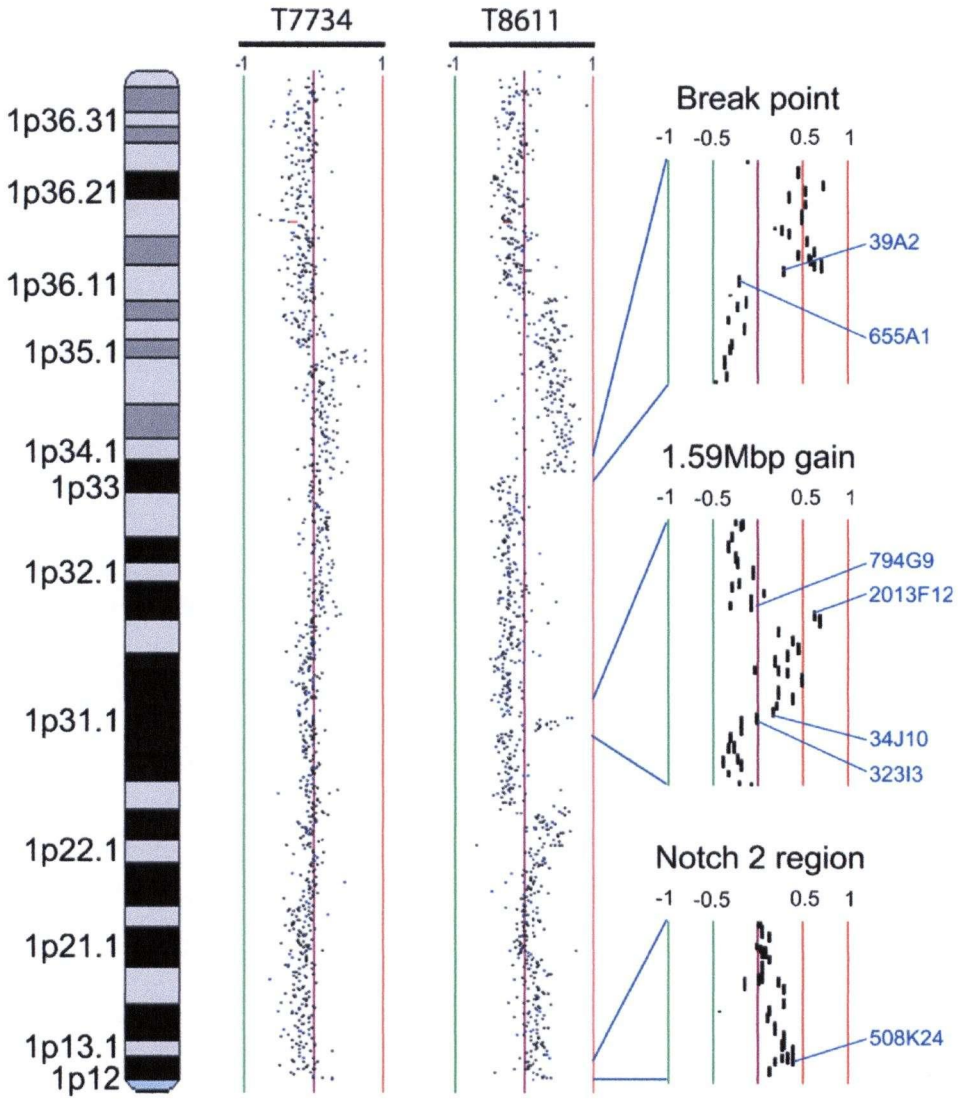

Figure. 28. Detection of Copy Number Gains and Losses on Chromosome 1p. Profiles of two lung tumor samples (T7734 and T8611) as viewed by SeeGH software. Each black dot represents a single BAC clone. Purple line represents log2 signal intensity ratio of 0, green line is log2 signal intensity ratio of -1, and red line represents +1. Far right is a magnified picture showing a breakpoint (top), a 1.59 Mbp amplification (middle), and the amplified region containing *NOTCH2*.

Genetic alterations critical to lung cancer are likely to be present in multiple patients. Twenty lung squamous cell carcinomas (8 CIS samples and 12 tumors) were microdissected and the DNA analyzed. Although there are sporadic alterations on 1p in the CIS samples, only one region was deemed to be recurrent under our stringent criteria (half of the CIS samples had to contain the amplification). This recurrent alteration was identified by alignment of 1p profiles, generated from a two clone moving average across the entire chromosome arm (Figure 29). Amplification at 1p36.12 was observed in 6 of 8 CIS samples defining the ~0.2 Mbp minimal region of alteration between BAC clones RP11-489K12 and RP11-415K20. This region contains two known genes, interestingly, one of which is *WNT4*, a member of the wingless-type MMTV integration site family (Region A1, Table 6). *WNT4* has been shown to be abnormally expressed in human breast cancer cell lines (Nau et al., 1985). The involvement of the Wnt pathway in cancer is best known through *Adenomatous Polyposis Coli* (*APC*) mutations in colorectal cancer (Korinek et al., 1997). In the context of lung cancer, this pathway has been implicated in NSCLC, due to overexpression of *Dishevelled Homolog 3* (*DVL3*) (Lu et al., 2004). Although the amplification was observed in six of the eight samples, the small sample size precludes generalization of frequency in squamous cell lung cancer. However, to our knowledge this study is the first to suggest early involvement of the Wnt pathway in pre-invasive lung lesions.

Table 6. Summary Of Regions Of Recurrent Amplification On 1p.

Region	Cytoband	Size	Genes	Boundary clones	Occurrence in tumors	Occurrence in CIS
A	1p36.12-p36.33	21 Mb	184	158F2-277F18	5/12	
A1*	1p36.12 (CIS only)	0.2 Mb	2*	489K12-415K20		6/8
B**	1p33-p35.1	15 Mb	165**	777F21-655A1	5/12	3/8
C	1p32.3	0.13 Mb	1#	351E14-809G7	7/12	1/8
D	1p32.1	0.32 Mb	0	206P1-592P11	8/12	1/8
E	1p11.2	0.05 Mb	1#	641F2-754O9	9/12	2/8

*A1 is within Region A and contains the *WNT4* gene.

** A 0.79 Mb alteration containing *L-MYC* was observed in one additional tumor.

#*LRP8* is the only gene in region C and *NOTCH2* is the only gene in region E.

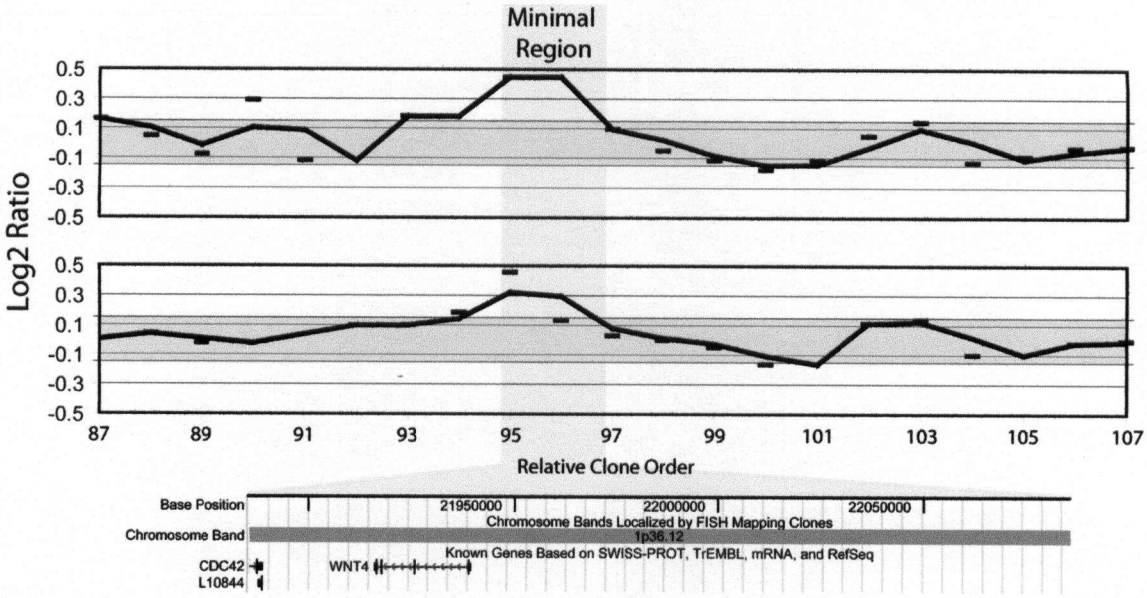

Figure 29. Amplification of *WNT4* Region in *Carcinoma in situ* Specimens. Representative CIS copy number profiles. Each BAC clone is represented by a black line segment. The moving average for a two clone window is plotted. Shading indicates the ±0.15 threshold range. *WNT4*, resides within this minimal region (bottom panel)

In contrast to the CIS samples, all of the tumors analyzed contained both segmental amplifications and deletions. Figure 30 is a summary of the segmental copy number changes in the tumor samples by colorimetric representation. Examination of 1p at a continuous resolution of overlapping BAC DNA segments has allowed for the identification of novel small recurrent alterations. Recurrent regions of alteration were observed in cytobands 1p36, 1p33-35, 1p32, and 1p11 (regions A-E in Figure 30). Regions A and B are wide (>20Mbp), while Regions C, D, and E are localized to 0.13, 0.32, and 0.05 Mbp, respectively, as revealed by alignment of array CGH profiles (Table 6). Regions B-E were detected at very low frequencies in the CIS samples (Table 6).

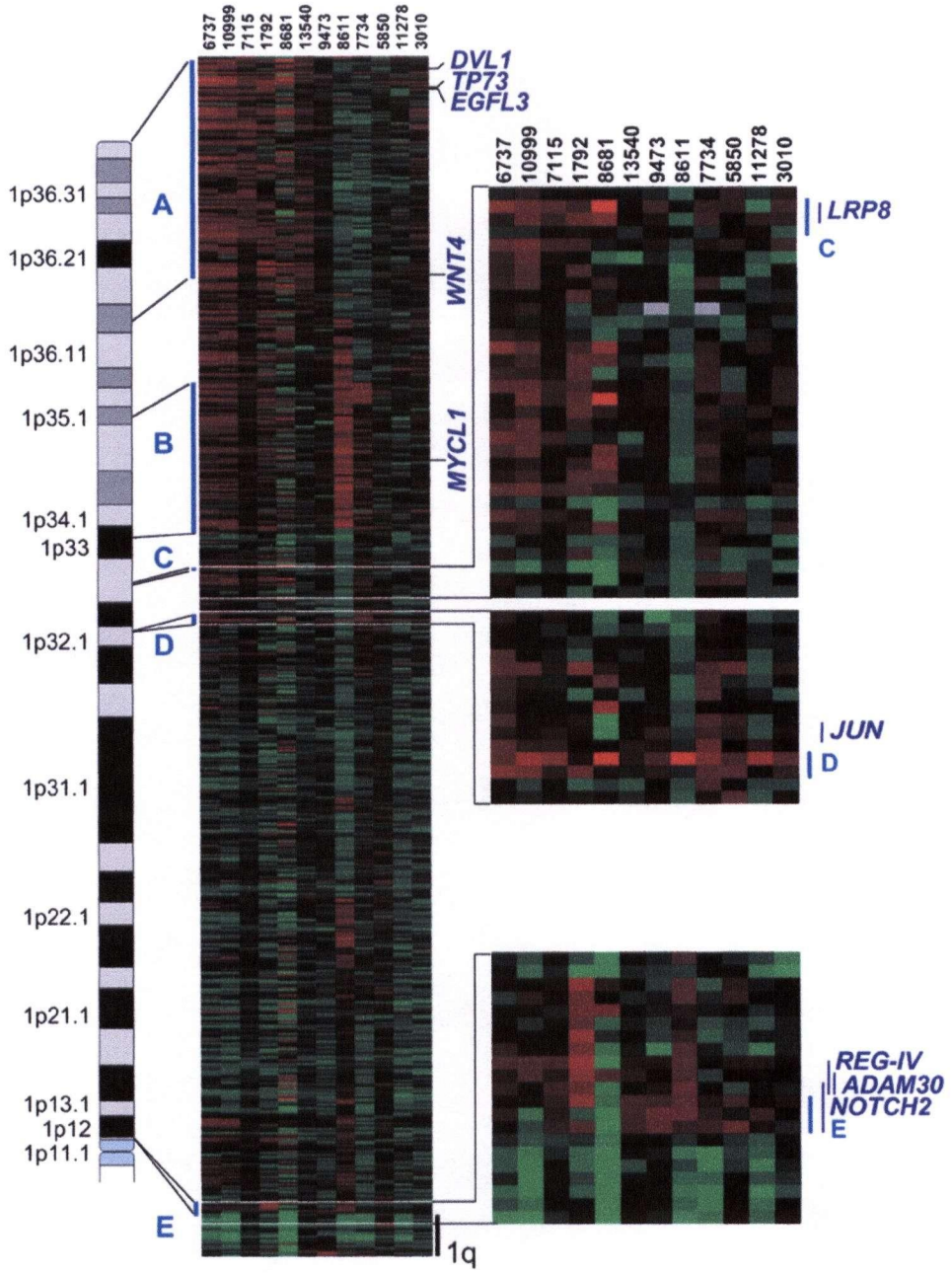

Figure 30. Colorimetric Representation of 1p Array Tumor Data.
Visualization of the 1p arm as viewed by Java TreeView. Each row corresponds to a BAC clone and each column represents a tumor sample. Red indicates a gain in copy number, whereas green, black, and grey indicates a loss in copy number, no change in copy number, or uninformative data respectively. Regions of frequent alteration (A-E) are denoted by a vertical light blue line. Genes of interest have been mapped to the 1p heat map on the left. The close up view of regions C and D is shown to the right with the genes of interest represented by dark blue lines. Note: The lines simply indicate which BACs the genes reside in, and do not imply that the genes overlap.

Region A at 1p36, observed in five of the 12 samples, is the largest and most prominent region of alteration, from BAC clone RP11-158F2 to RP11-277F18. This 21 Mbp region encompasses the 0.4 Mbp A1 region observed in the CIS samples. Previous searches for tumor suppressor genes on chromosome 1p in NSCLC have largely focused in this frequently altered region. However, definitions of the minimal region based on LOH studies have yielded conflicting results, raising the possibility of more than one candidate gene at 1p36 (Kaye et al., 1988). Many of the genes in Region A could potentially be related to tumor development. *TP73*, located at 1p36.33, has been implicated as a possible tumor suppressor gene due to its homology to *TP53*. However, *TP73* mutations are infrequently detected in lung cancer. In addition to *TP73,* there are over 250 other known and predicted genes in this region, of which several could potentially be linked to cancer. They include *WNT4*, whose amplification was observed in most of the CIS samples (see above); *EGFL3*, which resembles Epidermal Growth Factor Receptor (EGFR) in structure; and *DVL1,* which shares sequence identity with *DVL3*, whose overexpression is critical to Wnt signaling activation and cell growth in NSCLC (Lu et al., 2004). The expression profiling of these three genes in NSCLC is described below. Region B at 1p33-1p35.1 is observed in five of the 12 tumors (Table 6). This large 15 Mbp region is also gene rich. Interestingly, in a sixth tumor a much smaller (0.79 Mbp) amplification within the 15 megabases was observed containing the *L-MYC* gene. *L-MYC* is thought to be activated late in lung cancer although the mechanism by which MYC regulates tumorigenecity is not yet established (Johnson et al., 1996; Zajac-Kaye, 2001). This is consistent with our observation that the *L-MYC* region is amplified in only one of the eight CIS samples. The 0.13 Mbp Region C at

1p32.3 is present in seven of the 12 tumors (Table 6; Figure 30). *LRP8* is the only gene mapping within this region. Intriguingly, LRP8 belongs to the same low density lipoprotein receptor-related protein family as LRP5 and LRP6, which are known co-receptors for WNT ligands (Schneider and Nimpf, 2003). The 0.32 Mbp Region D is at 1p32.1. Amplification is observed in eight of the 12 tumor samples but contains no known genes. Interestingly, Region D is only 90 kb centromeric to the *JUN* oncogene, but RT-PCR assay of paired normal and tumor samples did not detect elevated *JUN* expression levels (see below). However, five ORFs are located in the amplified region according to the Genescan track at UCSC (http://genome.ucsc.edu/) and its recurrence suggests an importance in lung cancer development. Region E is the smallest of the recurrent alterations, spanning only 0.05 Mbp between BACs RP11-641F2 and RP11-754O9 at 1p11 (Table 6; Figure 30). This region near the centromere is amplified in nine of the 12 tumors and contains a single Refseq gene *NOTCH2* (Drosophila Notch homologue 2). Amplification of this region has been recently reported in small cell lung cancer cell lines (Dang et al., 2000).

Interestingly, nearly all of the altered regions identified on chromosome 1p harbored genes belonging to gene families known to be involved in cancer development through either the Wnt or Notch developmental pathways. Coupling our early observation of an amplified region containing *WNT4* in CIS and the identification of amplified regions containing additional genes related to these developmental pathways in the tumors prompted further evaluation of these genes at the expression level.

We investigated the expression pattern of *WNT4*, *DVL1*, and *EGFL3* (Region A), *LRP8* (Region C), *JUN* (Region D), and *NOTCH2* (Region E). As a control, *NOTCH2*

expression levels were compared to those of the neighboring *ADAM30* and *REGIV*. We examined the expression levels of these genes in 13 microdissected matched normal and tumor SCC cases by RT-PCR (Figure 31). The expression analysis revealed significant overexpression in tumors of Notch and Wnt pathway gene family members *DVL1* (P = 0.003), *LRP8* (P = 0.008), and *NOTCH2* (P = 0.029). *EGFL3*, *JUN*, *ADAM30*, and *REGIV* showed no significant expression changes. *WNT4* levels were too low to allow for detection of differential expression. However, though expression levels of *WNT4* are not high in tumors, this does not preclude the importance of *WNT4* in early development as the genetic evidence suggested. Further investigation of the role of *WNT4* at the expression level in pre-invasive lesions – albeit challenging to obtain – will be necessary for validation.

Pair-wise comparison of *DVL1* expression data showed a large difference between five of the eleven (Tumor 1, 3, 5, 10, 11) matched tumor and normal samples (Figure 31A). This is in contrast to Uematsu et al., who report only the overexpression of *DVL3* and not *DVL1* or *DVL2* in NSCLC; however, their sample set was small, comprising of only 4 squamous and 4 adenocarcinomas (Uematsu et al., 2003a). The Drosophila *Dishevelled* gene (*Dsh*) encodes a cytoplasmic phosphoprotein that regulates cell proliferation, acting as a transducer protein for developmental processes that include segmentation and neuroblast specification (Henderson et al., 2004). It has been reported that Dsh is required for the function of the Wingless gene product, Wg, a segment polarity gene homologous to the mammalian proto-oncogene *WNT1* (Dickinson and McMahon, 1992; Klingensmith and Nusse, 1994; Rijsewijk et al., 1987). Human DVL1

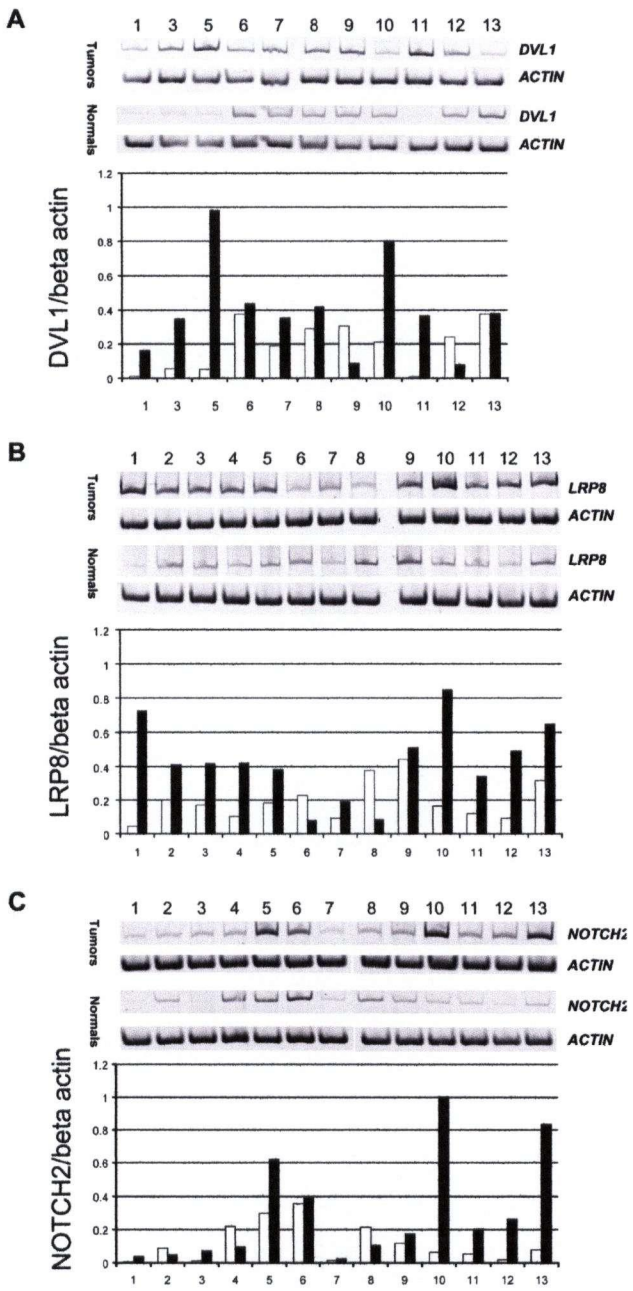

Figure 31. Expression Analysis of 1p Candidate Genes. The expression levels of *DVL1*, *LRP8*, and *NOTCH2* were assessed by RT-PCR analysis of paired microdissected normal and tumor frozen samples. (A) *DVL1* reverse transcription product amplified from cDNA of the matched pairs resolved by polyacrylamide gel electrophoresis and stained with SYBR green. Below is a bar graph of expression levels of *DVL1* relative to that of *β-actin.* White bars are normal samples and black bars are tumor samples. (B) *LRP8* reverse transcription product. Below is a bar graph of expression levels of *LRP8* relative to that of *β-actin.* (C) *NOTCH2* reverse transcription product. Below is a bar graph of expression levels of *NOTCH2* relative to that of *β-actin.*

shares approximately 64% amino acid identity with DVL3 and therefore may serve similar functions (Nusse and Varmus, 1992).

Expression analysis of *LRP8* was striking, with overexpression observed in 11 of the 13 samples (Figure 31B). The LRP family encodes membrane proteins involved in receptor-mediated endocytosis of many ligands and signal transduction pathways (Schneider and Nimpf, 2003). Although LRPs appear to have multiple functions (Herz and Strickland, 2001) *LRP5*, *6*, and *12* have been linked to carcinogenesis (Brennan et al., 2004; Hoang et al., 2004; Qing et al., 1999). LRP5 and LRP6 are known to be co-receptors for WNT ligands in Drosophila, Xenopus, and mice (Schneider and Nimpf, 2003). The role of LRP5 and 6 in Wnt signaling in humans is observed, but the mechanism remains unclear (Rodriguez et al., 2003). It has been suggested that *LRP5* is a possible marker for progression in high grade osteosarcoma (Hoang et al., 2004). In addition, *LRP12* has recently been shown to be amplified and overexpressed in oral squamous cell carcinoma (Brennan et al., 2004; Garnis et al., 2004d). LRP8, or ApoER, is a lipophilic protein that mediates high-affinity binding of APOE-containing lipoproteins, one of which is Reelin, to the Very Low-Density Lipoprotein (VLDL) receptor. Binding of Reelin to the receptor results in phosphorylation of Dab1; this activates an unknown chain of events that ultimately suppresses the activity of glycogen synthase kinase (GSK) 3β. Interestingly, the Wnt signaling pathway also functions through the regulation of GSK3β (He et al., 2004; Herz and Bock, 2002). The amplification and overexpression of *LRP8* in squamous cell lung carcinoma reported here combined with previous functional reports of other LRP family members suggests that LRP8 may play an oncogenic role in lung cancer.

In addition to alterations affecting the Wnt developmental pathway, we also observe alterations in the Notch developmental pathway. Not only is *NOTCH2* frequently amplified in lung tumors (see above), its expression is also higher in the tumor samples assayed (Figure 31C). The Notch signaling pathway affects a wide variety of cellular processes, including the maintenance of stem cells, specification of cell fate, differentiation, proliferation, and apoptosis (Ohkubo et al., 2003). Although little is known about the role of *NOTCH2* in cancer, its involvement is not surprising as *NOTCH1* has been repeatedly implicated in disease (Ohkubo et al., 2003). Furthermore, a *NOTCH3* translocation has been previously observed in NSCLC (Uematsu et al., 2003a). The Notch and Wnt developmental pathways interact through a number of mechanisms. Depending on the mechanism of action these pathways can either act synergistically or antagonistically (Ohkubo et al., 2003; Radtke and Raj, 2003).

In summary, this study provided evidence for the genetic basis of Wnt and Notch involvement in both the early and late stages of tumorigenesis. Furthermore, previous description of WNT7a involvement in cell adhesion suggests a role in lung cancer metastasis (Caldwell et al., 2004). Through the comparison of pre-invasive and invasive lung carcinomas we have identified novel genetic alterations which contain overexpressed genes related to both developmental pathways (Figure 32). These pathways are important for normal lung development (Axelrod et al., 1996; Soriano et al., 2001; Wesley, 1999); however the ectopic expression of genes within these pathways reported here may lead to abnormal cellular activity. Importantly, our implication of developmental pathways in lung cancer supports the proposed model of lung cancer ontology whereby tumors arise from dysregulated pluripotent stem cells (Saura et al.,

2000). Also, by identifying five novel regions on chromosome 1p in tumors as well as a recurrent alteration in CIS samples, this study demonstrates the value of genetically profiling early pre-invasive lesions and the use of a comprehensive tiling set approach to array CGH. Extension of this approach to the analysis of entire tumor genomes, for example using the newly developed whole genome submegabase resolution tiling set array, will provide more complete understanding of lung cancer progression (Ishkanian et al., 2004).

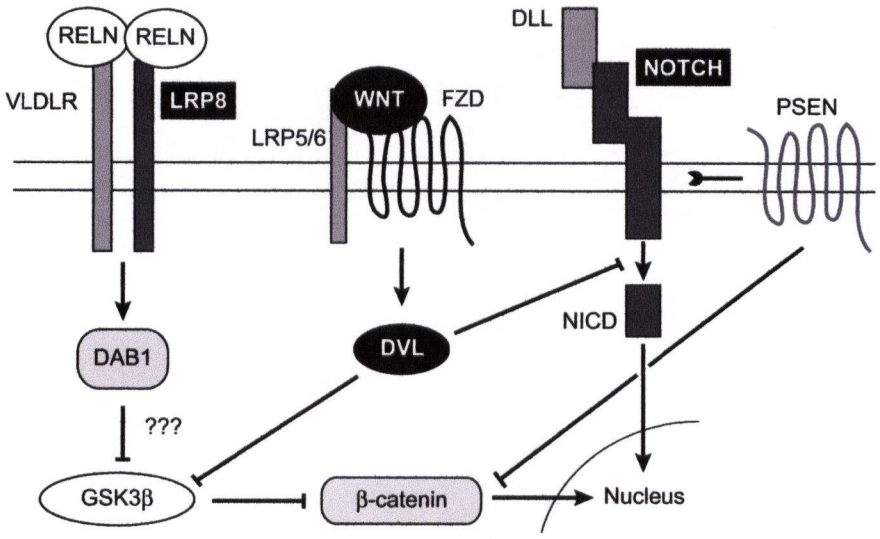

Figure 32. Schematic Diagram Highlighting the Interaction of the Wnt, Notch, and Reelin Pathways. Frizzled (FZD) and its co-receptor Low Density Lipoprotein Receptor-related Protein (LRP) bind to the extra cellular Wingless (WNT) ligand, thereby phosphorylating the intracellular Disheveled (DVL) homologue which inhibits GSK-3β leading to the stabilization of free β-catenin. Stable β-catenin translocates to the nucleus and acts as a transcription factor. Activation of NOTCH by an extra cellular ligand such as Delta (DLL) results in processing via Presenilin (PSEN) and subsequent cleavage of the NOTCH intracellular domain (NICD) which translocates to the nucleus and acts as a transcription factor.

4.6 Chapter 4 Summary

The regional array allowed us, for the first time, to look at alterations within pre-invasive lesions with unprecedented resolution. We have been able to define boundaries of suspected alterations in one experiment, saving both time and sample. The combination of both the array and the precious pre-invasive samples has resulted in the ability to address the hypotheses put forward in this thesis. We have shown with the *WNT4* alteration that certain genetic events occur at specific stages in tumorigenesis (Hypothesis #1), as this alteration is specific to CIS. Additionally, we observed multiple regions of deletion across the 5p arm specific to the CIS lesions as they appear to become masked in the invasive tumors (Hypothesis #2). We have also shown that the pre-invasive lesions generally have fewer genetic alterations than tumors which makes fine mapping candidate gene selection more effective (Hypothesis #3). Coupling this with the many genes that we were able to find overexpressed supports the hypothesis that the genetic alterations that are important to progression appear in the CIS stage of progression (Hypothesis #4). Lastly, the numerous Wnt and Notch related genes along the 1p chromosome arm that were found to be amplified and overexpressed show that if a pathway is important to disease progression more than one component of that pathway is likely to be altered (Hypothesis #5).

5.0 RESULTS: WHOLE GENOME ANALYSIS OF PRE-INVASIVE AND INVASIVE ORAL AND LUNG CANCER

5.1 Whole Genome Analysis

Although the conclusions drawn from the data obtained using the DNA fingerprint approach (Chapter 3) and the region-specific array (Chapter 4) have addressed all the hypotheses put forth in this thesis, expanding this work to profile the entire genome is now possible and will further our ability to identify novel genetic alterations and the basic understanding of cancer progression (Ishkanian et al., 2004). As we have seen with the regional arrays, especially with the pre-invasive lesions, some of the most frequent changes detected are submegabase in size and therefore the only way to detect these changes is using a tiling path array. The SMRT array is the first tiling resolution BAC array providing complete coverage of the entire human genome (Ishkanian et al., 2004). This whole genome tiling path array consists of 32,433 fingerprint verified individually amplified BAC clones, spotted in triplicate across two glass slides.

Figure 33 shows an example of a whole genome profile of a well established lung SCC cell line, HCC2450. This cell line contains numerous amplifications and deletions, in fact most chromosomes in this profile contain multiple segmental copy number changes. Whole arm deletions are observed with chromosomes 9p, 15q, and 21q. While whole arm amplifications are observed at 5p, 8q, 6p, 7p, and 20q. The majority of changes in this profile are complex changes such as those on chromosome 16 where multiple regions of both deletion and amplification are observed. At this resolution we

can also detect small changes, that were previously undetectable with lower resolution techniques, such as the ~1.5 Mbp amplification on chromosome 10q22.3.

In a few instances the same tumor samples were profiled with both the regional array as well as the whole genome array. Comparison of the two types of profiles revealed identical segmental gains and losses. However, the whole genome approach to copy number profiling allows us to detect alterations without prior knowledge of a specific region and therefore will not only serve to fine map regions currently known to be frequently altered but will also facilitate the discovery of novel changes.

5.2 Oral and Lung Cancer Progression Profiles

To show the value of the whole genome array and the role it can play in analyzing premalignant lesions of both lung and oral cancer various histopathological stages were profiled. The vast amount of data obtained from using such a comprehensive array, especially when comparison among samples is required, can be challenging. Data alignment and visualization is an important step in the discovery of novel regions recurrently altered in cancers; however, to date there is no one method that can adequately handle the large-scale genomic data sets generated in this study. In order to summarize the copy number changes and highlight the recurrent events in the data sets we used a frequency plot diagram. This method first relies on alteration calls based on smoothed data, which is generated by a computer algorithm (Jong et al., 2004b). Then the frequency of change is calculated across the sample set to provide the actual frequency diagram. This procedure summarizes regions of frequent gains and losses but

may miss or "smooth over" small alterations. A second pass analysis by careful visual inspection is then performed focusing on identifying small alterations. Section 5.2.1 and 5.2.2 describes the application of this whole genome approach in analyzing the samples from various histopathological progression stages in oral and lung cancer respectively.

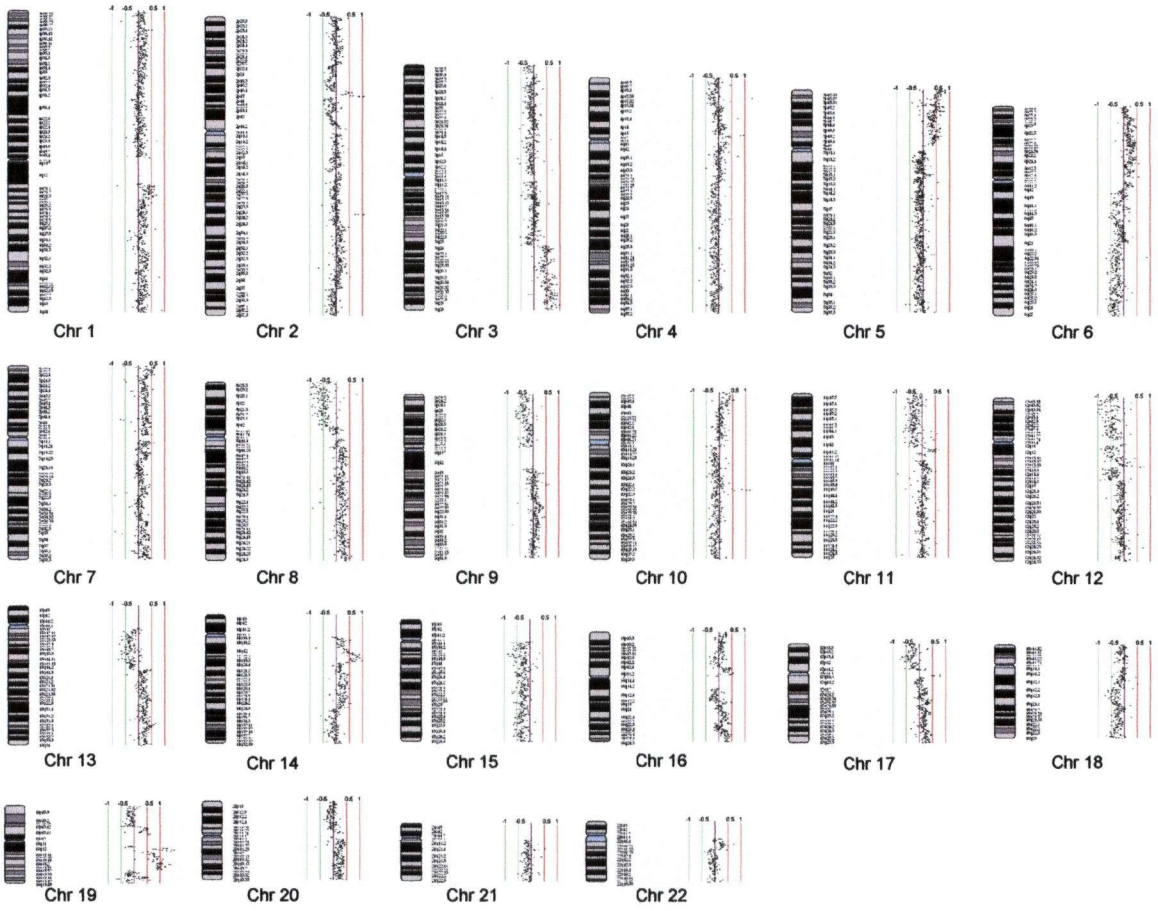

Figure 33. SeeGH Plot of Squamous Cell Lung Cancer Cell Line HCC2450. SeeGH translates spot signal ratio data from array CGH experiments to give high resolution chromosome profiles. Signal ratios are plotted as a log2 scale. This figure shows a whole genome profile of a squamous cell lung cancer cell line. Vertical green and red lines are scale bars indicating log2 ratios. Copy number losses are indicated by a shift in ratio to the left of zero, while gains are reflected by a shift to the right.

5.2.1 Oral Cancer Progression

Oral lesions are readily observable in the mouth for example as leukoplakia. The challenge in disease management is with predicting progression risk. Very few of the early dysplastic lesions progress and often the lesion will eventually disappear. Therefore, surgical treatment of these lesions, that may cause discomfort for the patient, is only deemed necessary when it becomes clear that the lesion has increased in severity. Predicting progression in the early dysplastic lesions would increase the rate of survival as treatment could be provided earlier. By comparing the profiles of mild/moderate dysplasia, severe dysplasia/CIS, and invasive tumors we can identify alterations specific for the various histopathological grades and use these as potential biomarkers for disease progression and/or treatment. Figure 34 shows a typical whole genome profile of an oral CIS sample. The typical oral CIS sample contains a number of whole arm changes. For example this case has a whole arm deletion of 3p, chromosome 5, 9, 10 13, 14, and 15 and a whole arm amplification of 3q, 4q, 6p, chromosome 7, 8, and 20. In addition to these large changes some of the CIS samples have smaller microamplifictions such as the ones observed on chromosome 2p16.2 and 11q13.1.

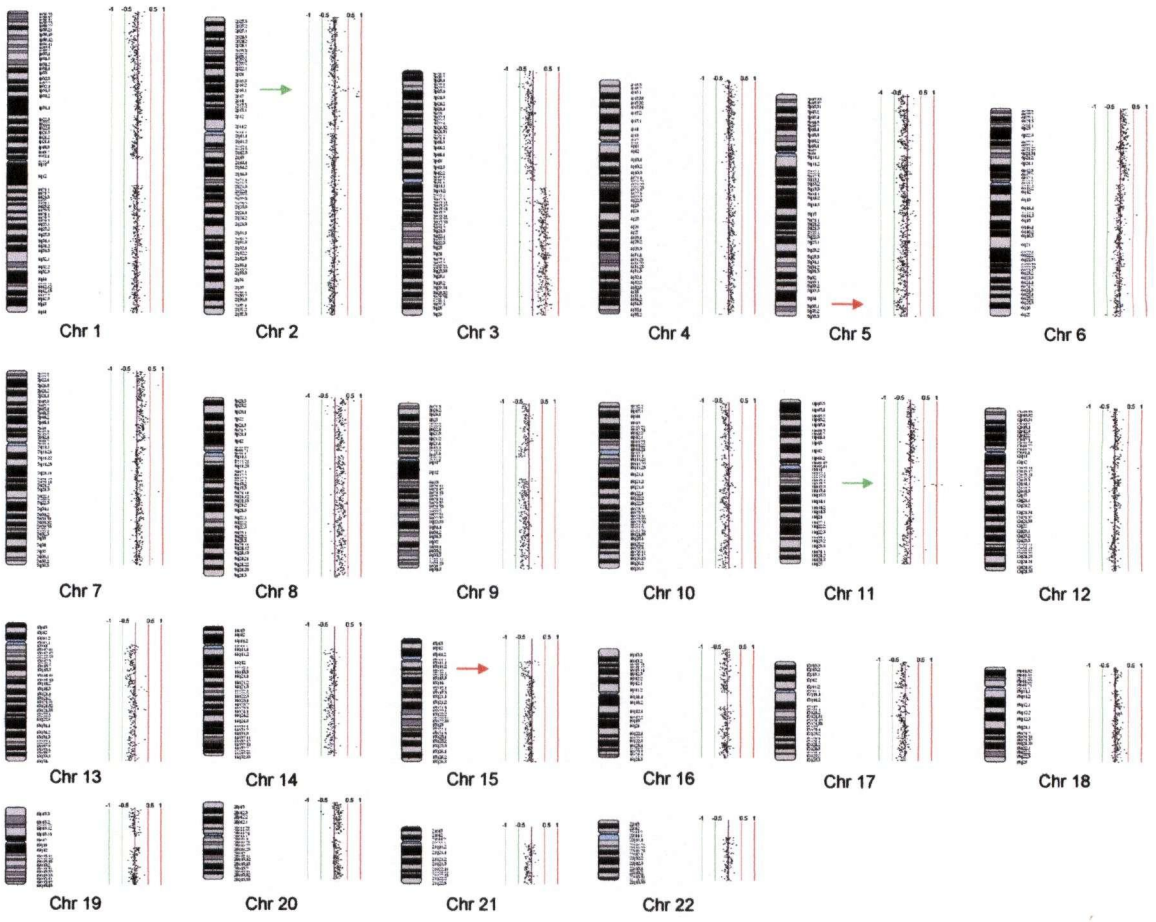

Figure 34. Oral CIS SeeGH Plot. SeeGH translates spot signal ratio data from array CGH experiments to give high resolution chromosome profiles. Signal ratios are plotted as a log2 scale. This figure shows a whole genome profile of an oral CIS lesion. Vertical green and red lines are scale bars indicating log2 ratios. Copy number losses are indicated by a shift in ratio to the left of zero, while gains are reflected by a shift to the right. Red and green arrows highlight examples of copy number deletions or gains respectively. Microamplifications were observed at 2p16.2 and 11q13.1.

Ten samples from each group (mild/moderate dysplasia, severe dysplasia/CIS, and invasive tumor) were compared through frequency plot analysis. As expected in these profiles we generally observe an increased number of alterations with lesion severity. Figures 35-37 show the frequency analysis for each histopathological group. As expected the mild/moderate group showed very few changes. Since the majority of the mild/moderate lesions will not progress the changes observed are considered the base-line for alterations. At the other extreme, the tumors exhibit numerous frequent changes, mostly large deletions. Due to the vast number of alterations in the late stage tumors it is difficult to decipher which are important to disease progression and which are due to genomic instability. In comparison, the severe dysplasia/CIS samples showed fewer alterations than the tumors while still progressing in 90% of the cases thus indicating that the additional alterations observed in the invasive tumors may not be important for progression of disease or may only be required for metastasis.

In the CIS cases the most frequent changes occurred on chromosome 1q (although there was more than the average amount of background change observed on 1q in the mild dysplasias), chromosome 3, 5p, 8q, 11q13, and chromosome 20. Most of these changes are large spanning the entire chromosome arm. The only recurrent distinct alteration in this sample set occurred at 11q13. This is the only high level amplification observed in the oral CIS samples and is seen in two cases (Figure 38). The minimal region of alteration spans ~2.5 Mbp and contains Cyclin D1, which has already been implicated in oral cancer.

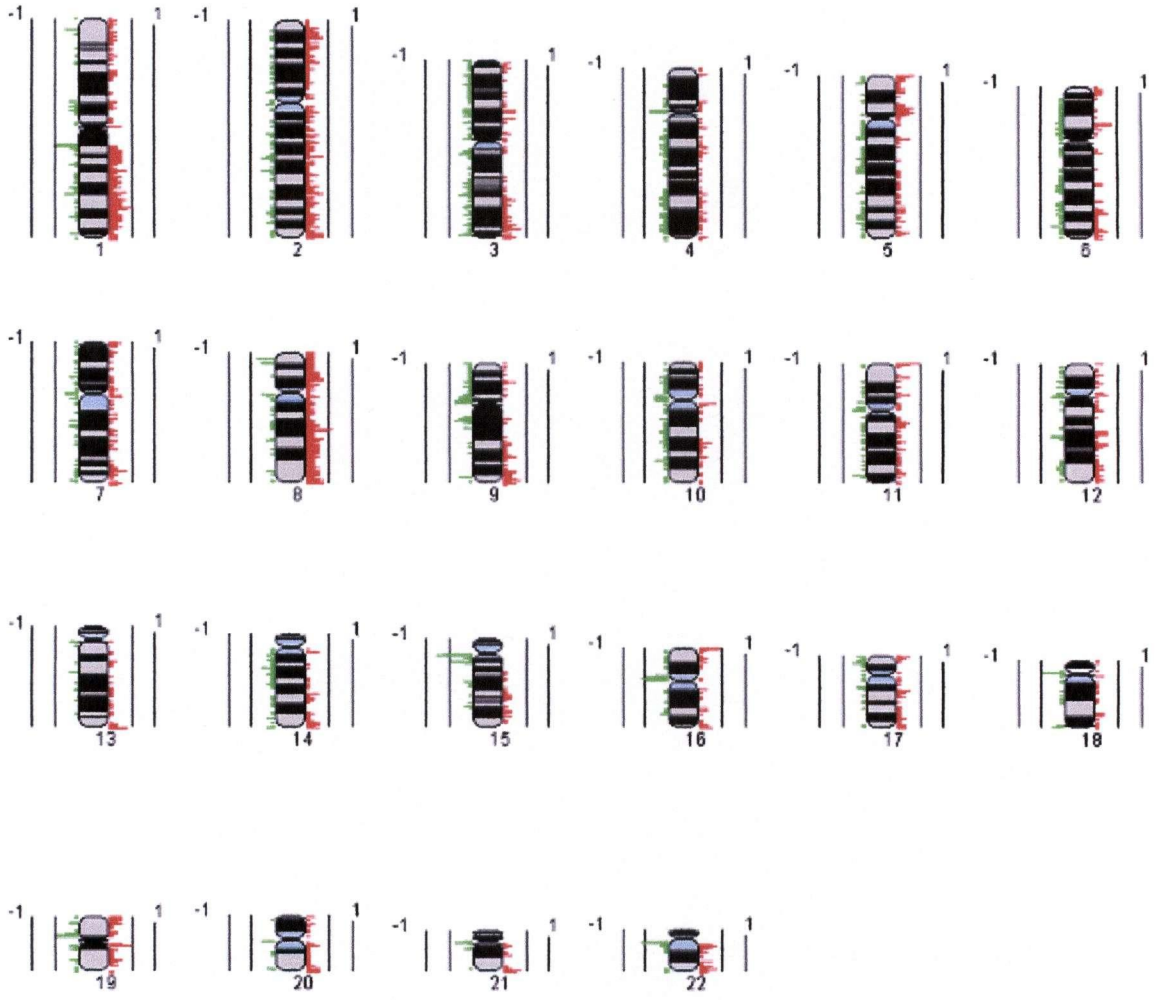

Figure 35. Oral Progression Frequency Analysis: Mild/Moderate Dysplasia. The frequency of change is represented for each chromosome. Red are regions of amplification and green are regions of deletion. Black horizontal bars denote frequency of change observed where 1 is 100% of cases.

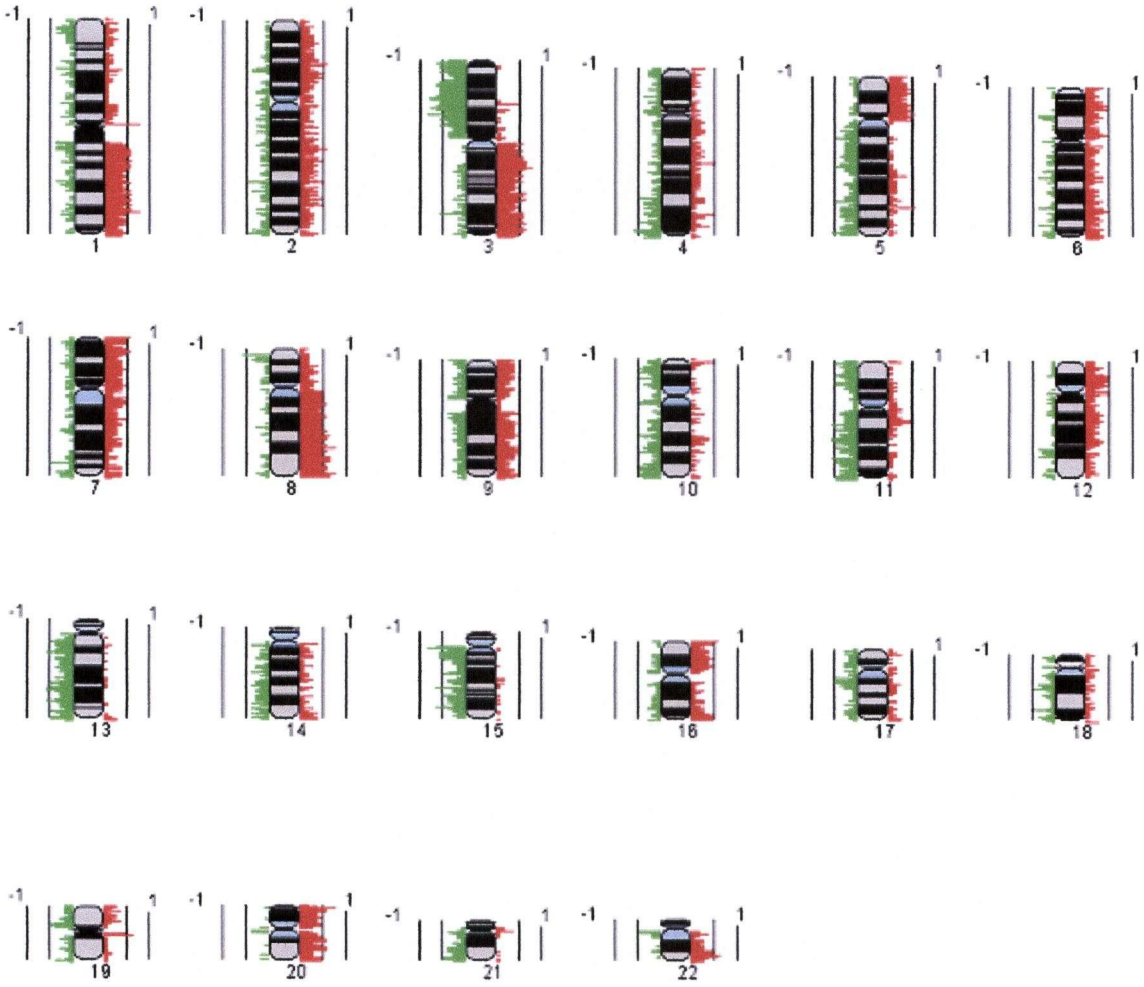

Figure 36. Oral Progression Frequency Analysis: CIS. The frequency of change is represented for each chromosome. Red are regions of amplification and green are regions of deletion. Black horizontal bars denote frequency of change observed where 1 is 100% of cases.

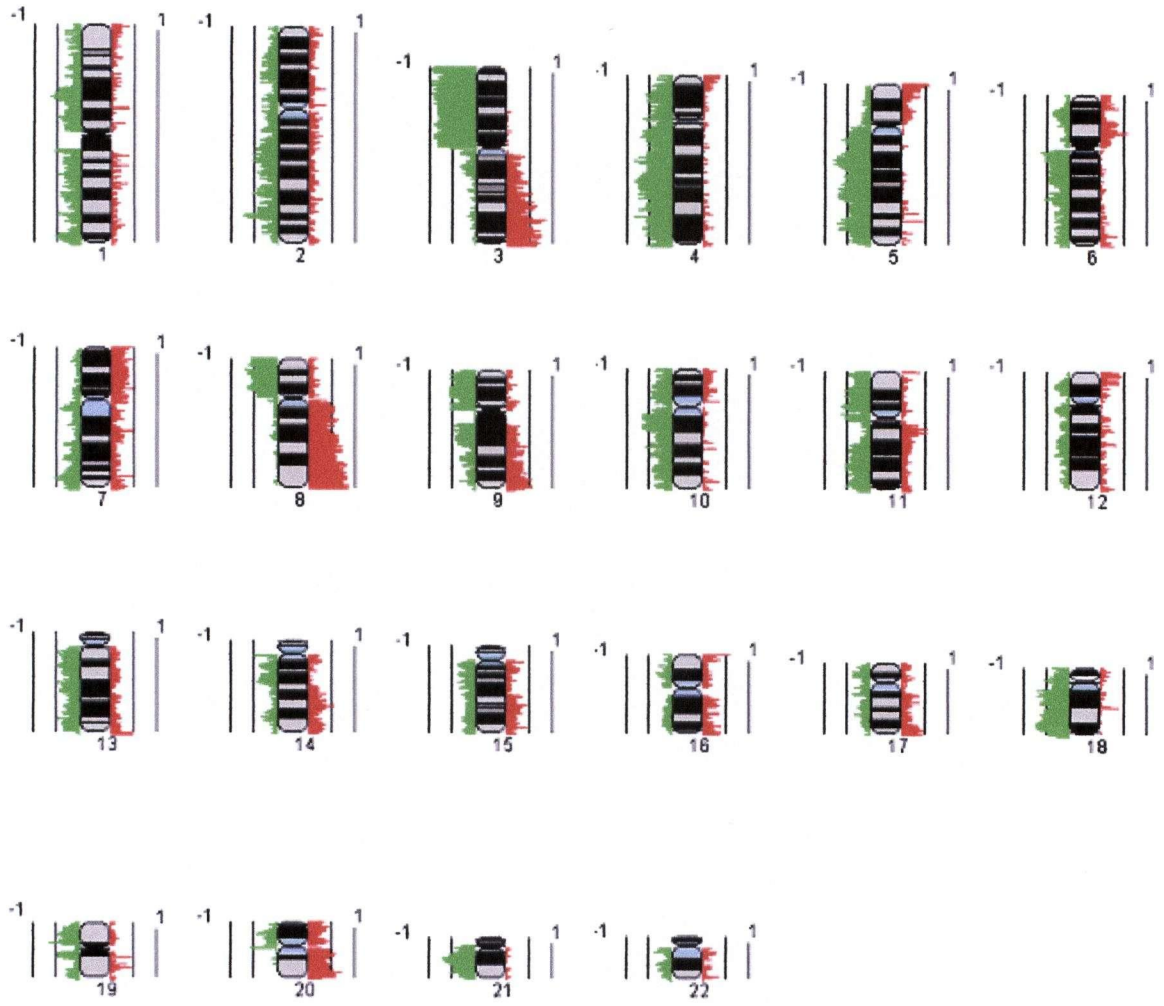

Figure 37. Oral Progression Frequency Analysis: Invasive Tumors. The frequency of change is represented for each chromosome. Red are regions of amplification and green are regions of deletion. Black horizontal bars denote frequency of change observed where 1 is 100% of cases.

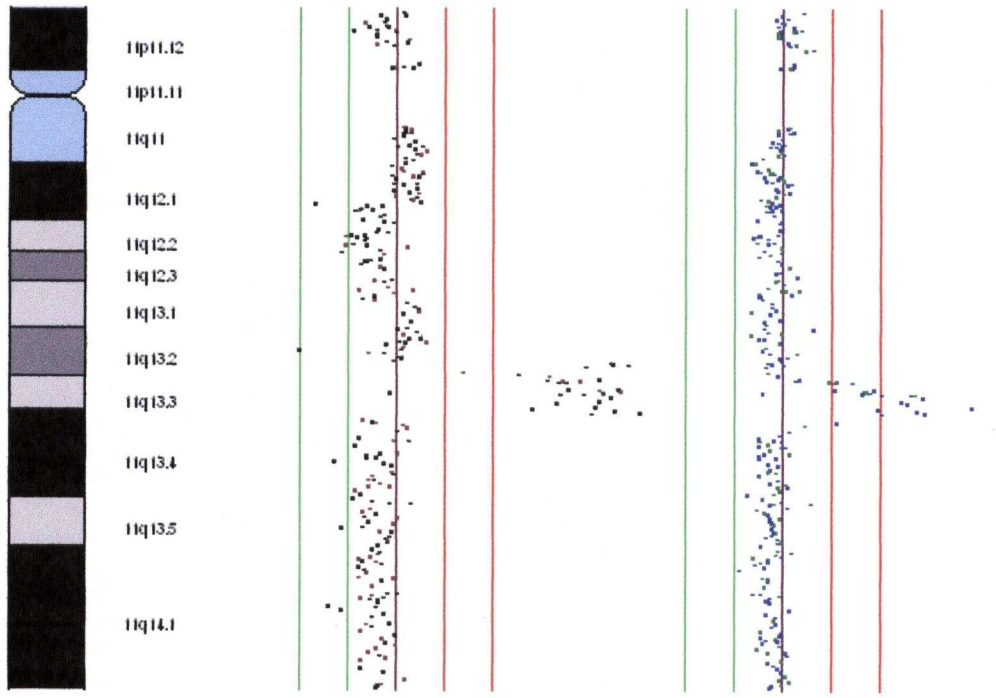

Figure 38. High Level Amplification. Two oral CIS profiles showing high level amplification at 11q13.2-13.3. Each dot represents a single BAC clone. Purple line represents log2 signal intensity ratio of 0, green line is log2 signal intensity ratio of -1, and red line represents +1.

5.2.2 Lung Cancer Progression

Lung cancer differs from oral cancer in that dysplasia and CIS lesions are rarely detected mainly due to the late stage of diagnosis. A pulmonologist or thoracic surgeon in the United States or Canada who is not involved in early detection studies is unlikely to see more than one case every ten years or so (Dr. Stephen Lam, personal communication). Screening the lung CIS lesions is extremely valuable as the amount of genomic instability in these lesions is considerably less than what is observed in late stage invasive tumors and ~90% of lung CIS lesions progress and therefore the alterations observed at this stage can be considered important for progression. Figure 39 shows an example of a squamous cell lung CIS genome profile.

Ten CIS lesions and 12 invasive squamous cell lung tumors were profiled. Figures 40 and 41 show the frequency analysis for the CIS and invasive lung samples. The most frequently altered regions in the CIS samples occur at chromosome 3, 5, 8p23, 8p11, 9p, 13q, and 17p. One of the interesting differences between the CIS and tumor sample sets is chromosome 3. From the frequency analysis it appears as though the p arm is more frequently deleted and the q arm is more frequently amplified in the CIS lesion than the invasive tumors and that the invasive tumors contain multiple segmental regions of alteration (Figure 42A). Inspection of the raw data confirms that the tumor samples possess numerous distinct alterations that are not seen in the earlier lesions (Figure 42B). This suggests that in the late stage tumors complex breakage and rearrangement events are occurring. Interestingly, this pattern is generally not observed in the oral samples.

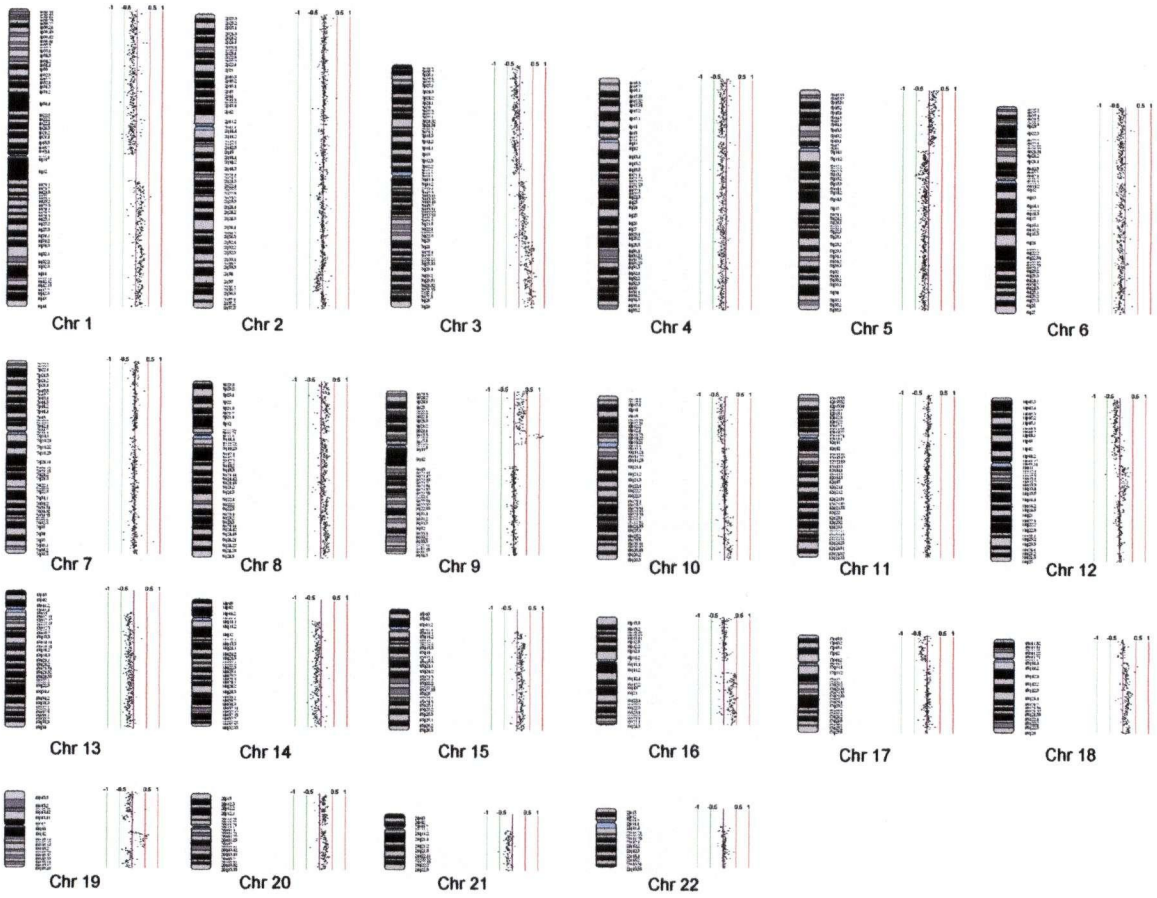

Figure 39. Lung CIS SeeGH Plot. SeeGH translates spot signal ratio data from array CGH experiments to give high resolution chromosome profiles. Signal ratios are plotted as a log2 scale. This figure shows a whole genome profile of a squamous cell lung CIS lesion. Vertical green and red lines are scale bars indicating $\log_2$ ratios. Copy number losses are indicated by a shift in ratio to the left of zero, while gains are reflected by a shift to the right. Red and green arrows highlight examples of copy number deletions or gains respectively.

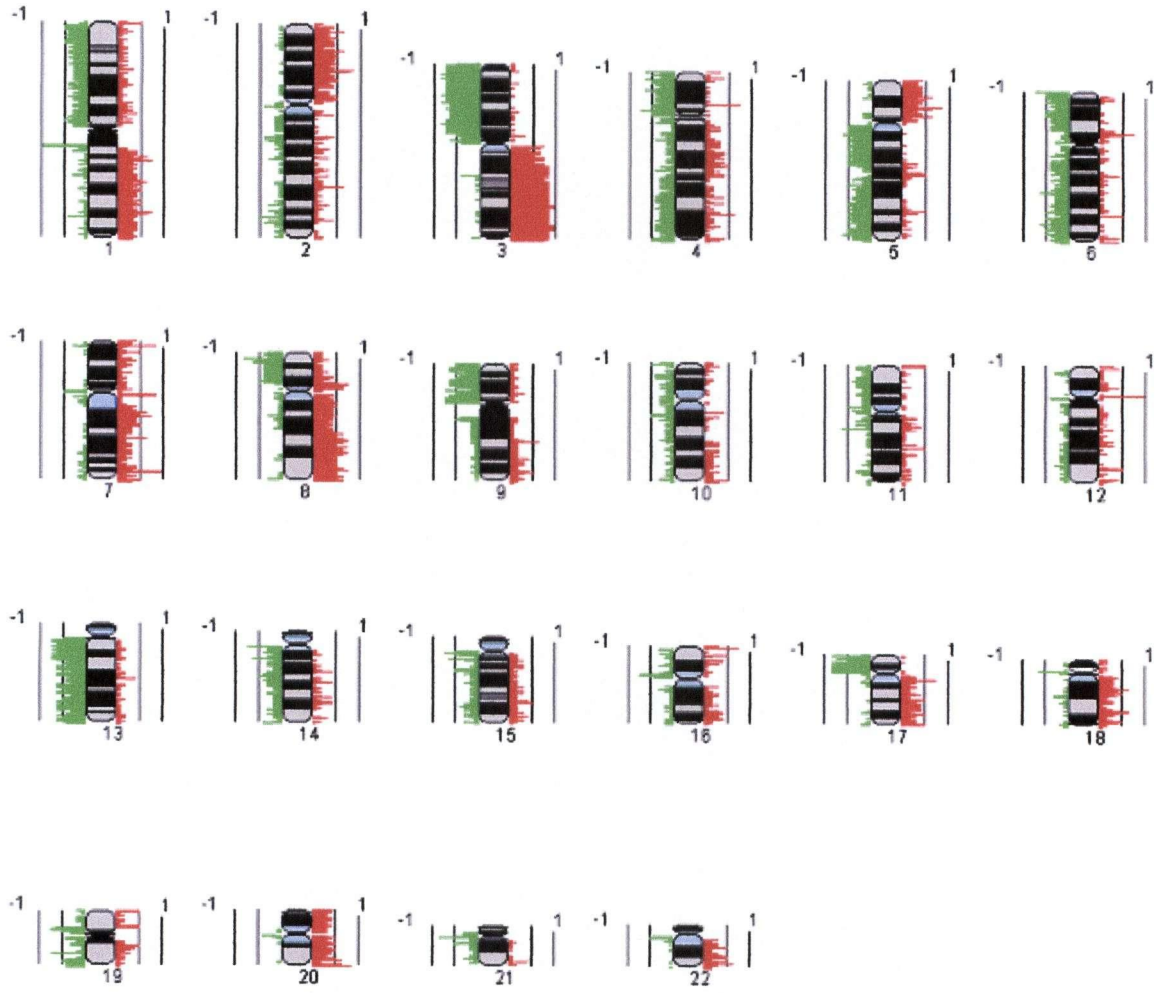

Figure 40. Frequency Analysis For Lung CIS. The frequency of change is represented for each chromosome. Red are regions of amplification and green are regions of deletion. Black horizontal bars denote frequency of change observed where 1 is 100% of cases.

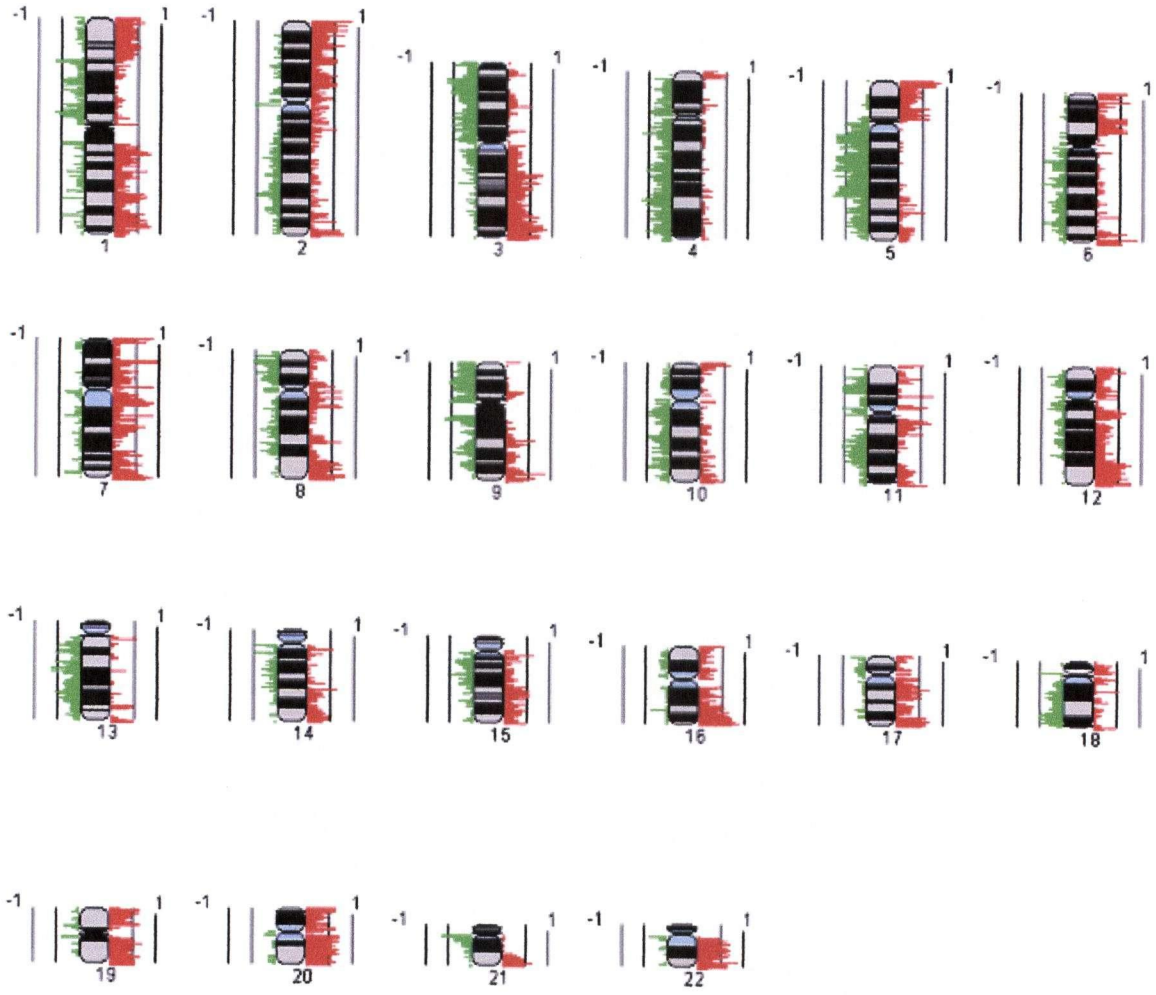

Figure 41. Frequency Analysis For Lung SCC. The frequency of change is represented for each chromosome. Red are regions of amplification and green are regions of deletion. Black horizontal bars denote frequency of change observed where 1 is 100% of cases.

Figure 42. (A) The frequency diagram for chromosome 3q (top is lung CIS and bottom is lung SCC). (B) 3q profile alignments for lung CIS (top) and tumors (bottom). Each dot represents a single BAC clone. Purple line represents log2 signal intensity ratio of 0, green line is log2 signal intensity ratio of -1, and red line represents +1.

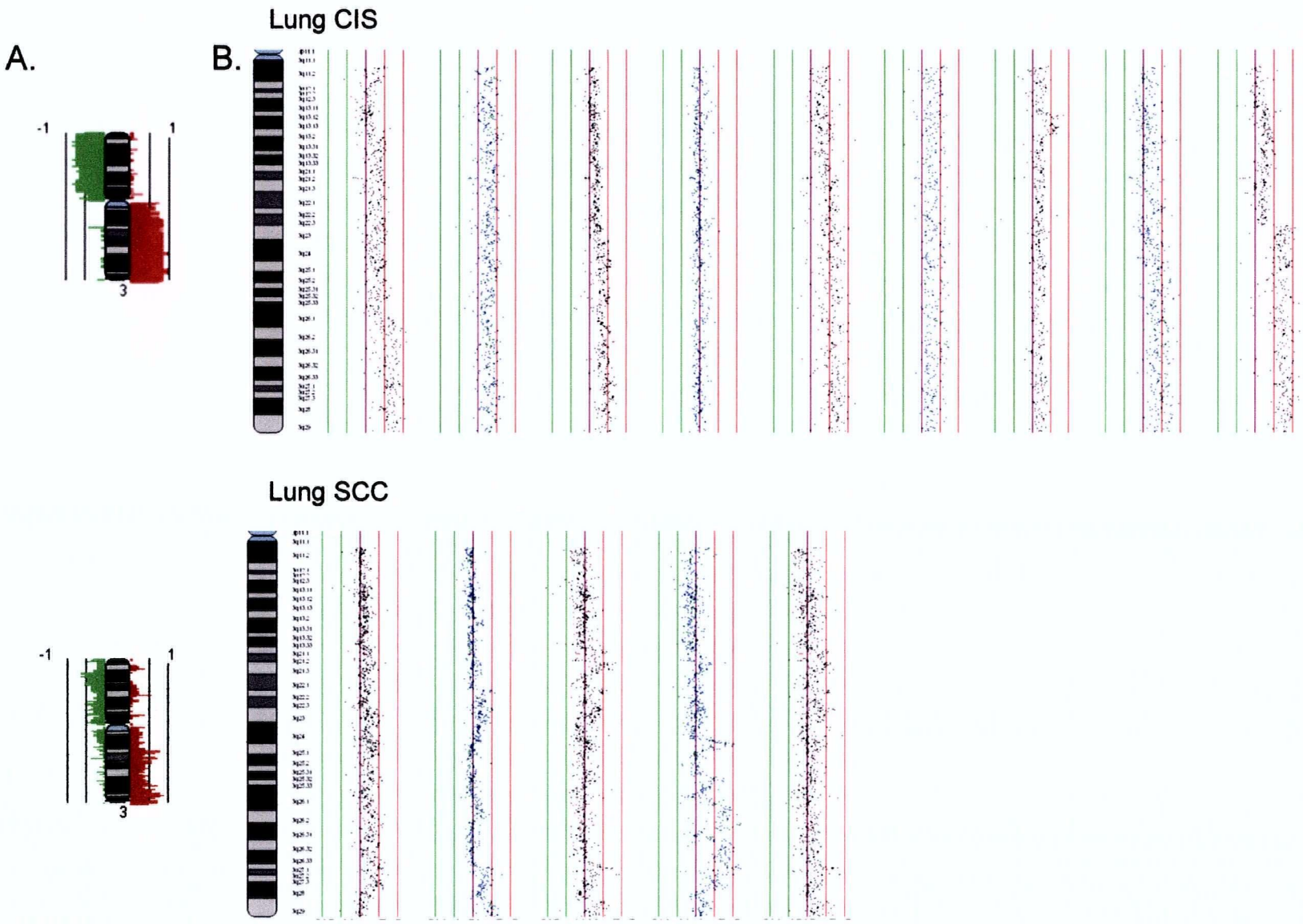
Lung CIS
A.
B.
-1
1
3
Lung SCC
-1
1
3

Two of the most striking alterations in the CIS lesions occur on chromosome 8p. On this chromosome we observe both a recurrent deletion at 8p23.1 and also a recurrent high level amplification at 8p12. The deletion spans ~1 Mbp and contains the gene *sperm-associated antigen 11* (*SPAG11*) as well as a cluster of defensin genes (Figure 43). Alignment of the CIS profiles at 8p11 revealed an ~1 Mbp minimal region of amplification (Figure 43). This region contains a small cluster of genes including *ASH2L*, *BAG4*, and *FGFR1* none of which have been previously implicated in lung cancer.

ASH2L has never been implicated in the development of cancer. However, this gene, like those of the Wnt and Notch pathways, plays a role in development and therefore inappropriate expression of this gene could lead to tumorigenesis. The *ASH2L* product positively regulates expression of homeotic selector genes and is implicated in early development and formation of various disc patterns in the fruit fly. *ASH2L* was ubiquitously expressed, but it was predominantly expressed in adult heart and testis and fetal lung and liver, with barely detectable expression in adult lung, liver, kidney, prostate, and peripheral leukocytes. Ikegawa et al. (1999) suggested that *ASH2L* functions as a transcriptional regulator (Ikegawa et al., 1999).

Fibroblast growth factors (*FGF*) also play a role in development. Pirvola et al. (2002) detected *FGFR1* expression at several stages during inner ear development in the mouse (Pirvola et al., 2002). They observed a reduction in the number of auditory hair cells in *FGFR1* mutants and hypothesized that *FGFR1* is required for proliferation of

Figure 43. Amplification and Deletion on Chromosome 8p. SeeGH chromosome alignments of chromosme 8p for lung CIS (top) and lung SCC (bottom). Each dot represents a single BAC clone. Purple line represents log2 signal intensity ratio of 0, green line is log2 signal intensity ratio of -1, and red line represents +1. Green arrow indicates the region of deletion observed in the CIS samples and red arrow indicates region of amplification observed in the CIS samples.

Chromosome 8p Squamous Cell Lung CIS Samples

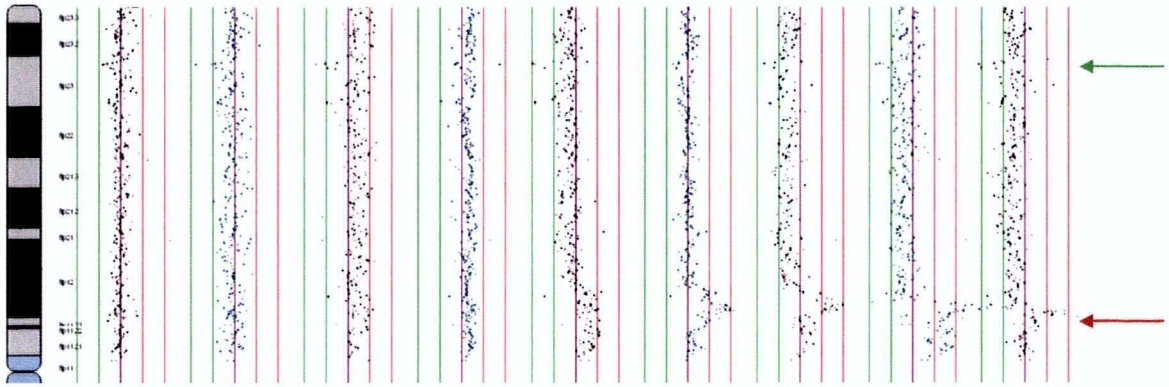

Chromosome 8p Squamous Cell Lung Carcinoma

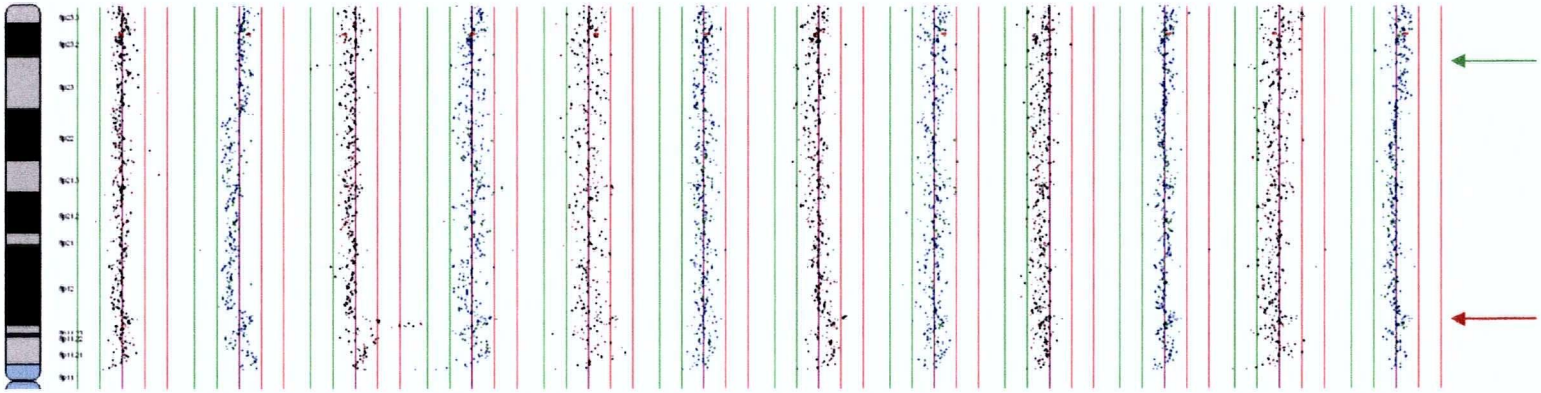

precursor cells that give rise to the auditory sensory epithelium. *FGFR1* has also been implicated in the development of mammalian liver (Jung et al., 1999). In addition many components of the FGF signaling system are found to be aberrantly expressed in prostate tumors (Dorkin et al., 1999; Giri et al., 1999).

Silencer of Death Domain (*SODD*), has been shown to block signaling pathways downstream of *Tumor Necrosis Factor Receptor 1* (*TNFR-1*) and *DR3* (Jiang et al., 1999). Members of the TNF family have been shown to induce apoptosis in susceptible cells (Ashkenazi and Dixit, 1998). The overexpression of *SODD* has been shown to block the activation of apoptosis promoting mechanisms (Jiang et al., 1999; Ozawa et al., 2000).

Interestingly when this same region is analyzed in the invasive tumors the amplification is still detected but at a lower level amplification indicating that this alteration is being masked by later stage events (Figure 43). Additionally, these alterations on 8p appear to be specific to lung cancer as they are not detected in any of the oral samples profiled.

5.3 Oral Cancer and Lung Cancer Comparison

The oral cavity and the lungs share many similarities in terms of the development of squamous cell carcinoma. Both of these cancer types are derived from the epithelial layer and progress through a series of histopathological stages. The major etiological factor for both diseases is tobacco smoke and both cancer types suffer from poor prognosis and high rate of recurrence.

Many oncogenes and tumor suppressor genes, such as *RAS*, *MYC*, *CCND1*, *EGFR*, *TP53*, *CDKN2A*, and *FHIT*, have been implicated in both cancer types and the earliest genetic events to occur in both cancers is alteration of 3p and 9p. However, when we compare the profiles of these two cancer types, they appear to be less common than the current literature would suggest. While they do share common genetic alterations, changes in the oral tumors are usually large whole arm changes whereas lung tumors typically exhibit multiple segmental changes across a chromosome arm. This suggests that there is a separate mechanism driving the progression of the diseases. This is consistent with the fact that we observe multiple chromosome breakage in the late stage lung samples but not in the oral cases.

There were generally more alterations observed in the lung CIS samples compared to the oral severe dysplasia/CIS samples, albeit the histopathological staging of these two cancers may not be identical. The oral samples were likely earlier lesions given that the CIS and severe dysplasia samples were treated as one group. From the whole genome profiles of the oral and lung premalignant lesions it is apparent that these two diseases share some common traits but also seem to possess alterations specific to the disease type. For example both cancers show a highly frequent loss of 3p and gain of 3q. Interestingly, although loss of 9p is reported to be an early event in both cancer types it appears to be much more frequent in the lung samples than the oral samples. In fact gain of 9p is a more frequent event than loss of 9p in the oral CIS lesions. Similarly, chromosome 17p loss, which has also been reported as an early event in both cancers, is seen in all but one lung CIS and only two of the oral CIS samples. As previously

mentioned (Section 5.2.2) the microamplification and microdeletion observed on chromosome 8p in the pre-invasive lung samples was not detected in the oral samples.

The observation that these two cancer types contain different patterns of change coupled with the different common regions of alteration indicate that molecular markers for early diagnosis and or risk assessment would be different for these two disease. On the other hand new therapeutic targets would be more affected by the different pathways involved in the progression of the disease and therefore although these two cancer types may possess different frequently altered regions the biological impact of these changes may be directed towards the same pathway. Further analysis is required to determine the pathways involved in these diseases.

5.4 Chapter 5 Summary

Whole genome tiling resolution profiling using the SMRT array allows for the most comprehensive genomic copy number analysis. This new tool is ideal for novel gene discovery as no prior knowledge of regions is required. It is especially useful when profiling pre-invasive material as the whole genome is analyzed in one experiment using limited quantities of DNA. Whole genome profiling of the different histopathological stages of both oral and lung cancer gives us some insight into the genetic alterations associated with these diseases. While oral and lung cancer share some similarities (such as the early loss of 3p and 9p) there are also some drastic differences. One example is the high level amplification on chromosome 8p observed specifically in the lung CIS samples that is absent in the oral samples.

6. CONCLUSION

6.1 Summary of Results

The aim of this thesis is to identify the genetic alterations associated with oral and lung cancer progression and to fine-map these alterations in order to identify candidate genes that may be useful as potential biomarkers and/or therapeutic targets. Initially, RAPD-PCR analysis was used to scan the genomes of both pre-invasive lung and oral lesions as well as late stage oral tumors. At the time, RAPD-PCR was the only genome-wide scanning technique that could support the low DNA input requirements of the pre-invasive lesions. A total of 15 recurrent alterations were identified. Two of these regions, one at 13q14 and the other at 8q22, were fine-mapped to reveal two candidate genes: *AKAP220* and *LRP12*. Both of these regions were associated with pre-invasive as well as late stage tumors. To fine-map the remaining regions and to identify additional novel alterations associated with these diseases a regional BAC array for CGH analysis was constructed. Profiling pre-invasive as well as late stage lung and oral tumors with the regional array identified alterations that have already been associated with these diseases as well as numerous novel submegabase alterations such as the alterations on chromosome 5p and 1p (Section 4.5.2 and 4.5.3). Overexpression of candidate genes, such as *TRIO*, *GDNF*, *DVL*, *NOTCH*, and *LRP8* within these small regions of alteration support the biological impact of these amplifications. We also discovered that many small alterations in the pre-invasive lesions, such as the amplification of the *WNT4* gene on chromosome 1p and the numerous regions of alteration on chromosome 5p, were

masked by the genomic instability associated with the late stage disease. Analysis of the various histopathological stages was expanded to include the whole genome with a tiling set resolution whole genome BAC array.

6.2 Importance of Studying the Pre-invasive Lesion

Cell lines and late stage tumors are typically used for screening for genomic alterations. While these studies have provided us with great insight into the disease there remains numerous recurring changes that have yet to be associated with genes. Additionally, the changes that drive cancer progression are largely unknown. This is presumably due to the difficulty in obtaining pre-invasive oral and lung material. By studying pre-invasive lesions in both lung and oral cancer we have shown that certain genetic events occur at specific times during the progression of the disease. Through LOH analysis, alteration at 13q14 was shown to be specific to high grade dysplasia. Similarly, *WNT4* amplification was shown to be specific to lung CIS. An additional benefit to studying pre-invasive lesions is that early genetic alterations observed may be masked in late stage tumors due to the increased genomic instability in the later stages. This was evident in the 5p analysis of lung CIS and invasive tumors where we observed numerous deletions in the CIS samples that were later masked by the near whole arm amplification of this arm in the tumors. Another example is the high level microamplification of 8p11 in the CIS lesions that were barely detected in the tumors. Pre-invasive lesions also facilitate fine-mapping of candidate genes as genetic alterations in these lesions are often much smaller than those observed in late stage tumors.

6.3 The Involvement of Developmental Pathways in Cancer Progression

Cancer progression and organ development are similar processes. Both involve rapid bursts of proliferation, angiogenesis, tissue remodeling, and cell migration. Therefore it should not be surprising that the same signaling pathways are involved in both processes. Recent studies have suggested that cancer is a disease triggered by the erroneous re-activation of signaling pathways that are typically down regulated after embryonic development (Kolligs et al., 2002; Miyamoto et al., 2003; Thayer et al., 2003). The embryonically expressed *GDNF* is a case in point where the expression is absent in the adult lung but has been re-activated in cancer. Furthermore, our finding of a 0.4 Mbp amplified region at 1p36.12 containing *WNT4* in pre-invasive lung cancer, coupled with the identification of three additional alterations in invasive tumors that also contain genes related to the Notch and Wnt pathways, strongly suggest a key role of these developmetal pathways in early and late stages of lung tumorigenesis. Furthermore, ectopic expression of *DVL1*, *LRP8*, and *NOTCH2* in malignant lung tissue validates the biological impact of these genetic alterations. Importantly, this implication of pathways known only to be activated in fetal lung development lends support to the proposed model of lung cancer ontology whereby tumors arise from dysregulated pluripotent stem cells.

6.4 What Makes a Good Biomarker/Therapeutic Target?

While this thesis does not address biomarker or therapeutic target validation, the discovery of novel genetic alterations and candidate genes discussed herein could be useful in the future as biomarkers or therapeutic targets.

In the case of oral cancer, where the lesion is easily accessible, it is important to determine whether the lesion will progress or regress. In order to do this the marker being used must be able to predict progression. The only way to determine the efficacy in predicting outcome is to test the marker in a panel of samples that are known to progress versus those that do not. Lung cancer is different from oral cancer in that the lesion is not easily accessible without hospitalization. Since the majority of CIS lesions would progress to cancer, the best markers are those facilitating the detection of the CIS lesion or the presence of an early stage tumor without the need for surgery. For example, increasing the sensitivity of detecting cancer cells in sputum samples which are usually heavily populated with normal cells.

Selection of a diagnostic marker or therapeutic target involves multiple considerations. The first is whether or not the candidate gene is expressed in critical tissues. If it is expressed and the expression of the gene is required for healthy function of the organ to which it associates, there will most likely be complications when trying to manipulate expression and therefore this candidate gene would not be the best choice for potential therapies, however, these genes can still be used as diagnostic markers. Under such circumstances, it is vital to determine if the candidate is expressed in the normal cells. To reduce the risk of false positives the candidate should not be expressed at all in the normal cells so as to be specific only to the tumor cells. Another consideration when selecting a biomarker is the means of detection. If a specific gene is being used,

immunohistochemical staining using a monoclonal antibody against the candidate gene product could be used. If an alteration at a specific chromosomal region is being used, FISH could be used to detect copy number changes.

6.5 Future Directions

This thesis has identified numerous genetic alterations associated with the hisopathological progression of both lung and oral cancer. However, one of the main issues in the progression of the disease is deciphering which lesions will actual progress. Oral mild dysplasia cases with known outcome are rare but obtainable (Rosin et al., 2000). Profiling of these lesions will shed light on what is necessary for progression at the earliest stages. These early genetic alterations could prove useful as potential diagnostic markers and/or therapeutic targets and must be tested. Testing the significance of these changes on a large panel of cases with known clinical outcomes would be useful in determining a diagnostic/risk-associated marker. Additionally, a number of the candidate genes identified have not been previously implicated in cancer and therefore functional analysis of these genes is required to fully understand their biological importance. Cell models would be useful in determining functionality.

6.6 Significance of Work

The objective of this work was to identify genetic alterations associated with the progression of lung and oral cancer and to identify suitable candidates for potential use as diagnostic markers and/or therapeutic targets. Combining high resolution CGH tiling arrays with the precious pre-invasive material, we have for the first time produced a comprehensive genomic view of oral and lung pre-invasive lesions. In doing so we have identified numerous recurrent novel genetic alterations and have shown the biological relevance of these alterations through expression analysis. This has led to the discovery that multiple genes within the Wnt and Notch developmental pathways are altered in lung tumorigenesis. In addition to the Wnt and Notch pathways, we also implicate the RET oncogenic pathway in lung cancer through the overexpression of *GDNF*, which is a ligand for the *RET* oncogene product and is normally expressed during lung development (but absent in adult lung tissue). Not only has this work provided novel targets to be used as potential diagnostic markers and identified pathways to be investigated for therapeutic use, it has also shown that much of the genetic alterations observed in the late stage tumor is not involved in the early stages of disease progression but is most likely due to high degree of genomic instability found in the invasive stages of the disease. This is important because very few studies analyze pre-invasive lesions, most likely due to the difficulty in obtaining these specimens, however, these samples are the most informative with respect to understanding cancer development. While reports of genetic alteration in early stage disease are limited analysis of pre-invasive lesions offers the best prospect for identifying early causal genetic alterations.

Appendix 1. Patient Information

LUNG Sample	Sex	Age	Smoking History	Pack Years	Grade
C3986	M	65	CURRENT SMOKER	35	CIS
C2950	M	57	FORMER SMOKER	107	CIS
C2951	M	65	CURRENT SMOKER	71	CIS
C3988	M	77	FORMER SMOKER	32	CIS
C3678	F	59	FORMER SMOKER	50	CIS
C59	M	78	FORMER SMOKER	47	CIS
C3989	M	52	FORMER SMOKER	30	CIS
C127	F	67	CURRENT SMOKER	96	CIS
C60	F	45	NA		CIS
C125	F	77	CURRENT-SMOKER	42	CIS
C130	M	95	FORMER SMOKER	10	CIS
C126	F	75	CURRENT-SMOKER	96	CIS
C124	M	59	FORMER SMOKER	72	CIS
C129	M	73	FORMER SMOKER	33	CIS
T1792	M	56	NA	40	SCC
T5850	M	48	NA	66	SCC
T3010	M	72	NA	122.5	SCC
T10999	M	67	NA	15	SCC
T8611	F	62	NA	100	SCC
T6737	M	63	NA	60	SCC
T7115	M	60	NA	70	SCC
T7734	M	53	NA	82.5	SCC
T9473	F	70	NA	0	SCC
T11773	M	66	NA	45	SCC
T8681	M	72	NA	55	SCC
T11278	M	76	NA	74	SCC
T13540	M	73	NA	34.5	SCC
T12308	M	68	NA	0	SCC

ORAL Sample	Sex	Age	Smoking History	Pack Years	Grade
10T5A	F	43	NON SMOKER	NA	SCC
112T	M	84	SMOKER	NA	SCC
114T	F	75	SMOKER	NA	SCC
115T	M	72	SMOKER	NA	SCC
116T	M	66	SMOKER	NA	SCC
117T2	M	34	NON-SMOKER	NA	SCC
118T	M	67	SMOKER	NA	SCC
122T5	F	59	NON-SMOKER	NA	SCC
123T1	M	63	SMOKER	NA	SCC
125T	F	85	NON SMOKER	NA	SCC
161T	M	46	NA	NA	SCC
162T	F	55	SMOKER	NA	SCC
166T	F	82	NON-SMOKER	NA	SCC
196T	F	54	SMOKER	NA	SCC
199T	F	89	NA	NA	SCC
790T1-1	M	53	NA	NA	SCC
792T1-1	M	42	NA	NA	SCC
793T1-1	M	64	NA	NA	SCC
794T1-1	M	59	NA	NA	SCC
795T1-1	M	72	NA	NA	SCC
797T1-1	F	38	NA	NA	SCC
800T1-1	F	78	NA	NA	SCC
801T1-1	M	27	NA	NA	SCC
200T1	F	47	NONSMOKER	NA	SCC
202T1	M	70	SMOKER	NA	SCC
211T3	M	72	SMOKER	NA	SCC
215T	M	52	SMOKER	NA	SCC
237T1-1	F	48	NON-SMOKER	NA	SCC
24T1	F	63	NON SMOKER	NA	SCC
2T	F	58	SMOKER	NA	SCC
386T	M	78	NON SMOKER	NA	SCC
414T2	M	72	SMOKER	NA	SCC
43T	M	67	SMOKER	NA	SCC
451T1	M	67	SMOKER	NA	SCC
342T	M	59	NON-SMOKER	NA	SCC
527T1		NA	NONSMOKER	NA	SCC
538T	F	68	NONSMOKER	NA	SCC
539T	F	64	NONSMOKER	NA	SCC
542T	M	47	SMOKER	NA	SCC
569T2	F	76	NON SMOKER	NA	SCC
59T1	M	63	SMOKER	NA	SCC
620T1-1	M	55	SMOKER	NA	SCC
65T1	F	60	HEAVY SMOKER	NA	SCC
709T1-1	F	66	NA	NA	SCC
803T1-1	F	52	NA	NA	SCC
807T1-1	F	68	NA	NA	SCC
809T1-1	M	80	NA	NA	SCC

90T	M	75	SMOKER	NA	SCC
80T	M	79	NA	NA	SCC
528T	M	74	NONSMOKER	NA	SCC
385T1-1	F	86	SMOKER	NA	SCC
469T	M	75	SMOKER	NA	SCC
373D	M	64	SMOKER	NA	CIS
543T	M	74	SMOKER	NA	CIS
577T1	M	50	FORMER SMOKER	NA	CIS
57D3	F	NA	SMOKER	NA	CIS
586D1	M	NA	NA	NA	CIS
753D1-1	F	53	NA	NA	CIS
751D1-1	F	67	NA	NA	CIS
802T1-1	F	52	NONSMOKER	NA	CIS
83D1-1	M	66	NON SMOKER	NA	CIS
4D	F	65	NA	NA	severe dysplasia
210D1-1	F	37	NONSMOKER	NA	severe dysplasia
287D1	F	69	SMOKER	NA	severe dysplasia
380D	F	67	SMOKER	NA	severe dysplasia
589D1	F	NA	NA	NA	severe dysplasia
45D	F	71	NA	NA	severe dysplasia
649D1	F	44	NA	NA	severe dysplasia
6D	F	68	SMOKER	NA	severe dysplasia
755D1-1	M	48	FORMER SMOKER	NA	severe dysplasia
76D	M	64	SMOKER	NA	moderate dysplasia
274D	F	58	NON-SMOKER	NA	moderate dysplasia
371D	M	64	SMOKER	NA	moderate dysplasia
612D1-1	M		NA	NA	moderate dysplasia
612D1-2	M		NA	NA	moderate dysplasia
737D1-1	F	73	SMOKER	NA	moderate dysplasia
738D1-1	M	58	SMOKER	NA	moderate dysplasia
739D1-1	M	57	SMOKER	NA	moderate dysplasia
735D1-1	F	40	SMOKER	NA	moderate dysplasia
747D1-1	M	87	NA	NA	moderate dysplasia
200D1-1	F	47	NONSMOKER	NA	moderate dysplasia
71D	M	53	NA	NA	moderate dysplasia
204D1-2	M	47	NONSMOKER	NA	moderate dysplasia
749D1-1		75	NA	NA	moderate dysplasia
207D	F	66	NA	NA	mild dysplasia
209D	M	44	NON-SMOKER	NA	mild dysplasia
217D2-1	M	43	SMOKER	NA	mild dysplasia
248D	M	55	NA	NA	mild dysplasia
26D1-2	M	66	SMOKER	NA	mild dysplasia
289D	M	39	SMOKER	NA	mild dysplasia
292D	N/A	72	NONSMOKER	NA	mild dysplasia
316D	M	46	SMOKER	NA	mild dysplasia
325D2-1	M	52	SMOKER	NA	mild dysplasia
332D1-3	M	60	NA	NA	mild dysplasia
347D2-1	F	73	NA	NA	mild dysplasia
400D1	M	44	SMOKER	NA	mild dysplasia
454D2	F	56	SMOKER	NA	mild dysplasia
464D1	F	71	NA	NA	mild dysplasia

51D	M	67	NA	NA	mild dysplasia
535D3	M	49	NONSMOKER	NA	mild dysplasia
55D	F	81	SMOKER	NA	mild dysplasia
567D2-1	F	60	NON SMOKER	NA	mild dysplasia
584D1	M	NA	NA	NA	mild dysplasia
585D1	F	NA	NA	NA	mild dysplasia
591D1-1	F	NA	NON SMOKER	NA	mild dysplasia
64D	M	52	SMOKER	NA	mild dysplasia
734D1-1	M	58	NA	NA	mild dysplasia
736D1-1	F	38	SMOKER	NA	mild dysplasia
740D1-1	M	58	SMOKER	NA	mild dysplasia
742D1-1	F	49	NA	NA	mild dysplasia
743D1-1	M	30	SMOKER	NA	mild dysplasia
750D1-1	M	72	NA	NA	mild dysplasia
752D1-1	M	66	NA	NA	mild dysplasia
200D1-2	F	47	NONSMOKER	NA	mild dysplasia
124D2-2	M	52	SMOKER	NA	mild dysplasia

REFERENCES

Ahsan, H. and Thomas, D.C., 2004. Lung cancer etiology: independent and joint effects of genetics, tobacco, and arsenic. Jama, 292(24): 3026-9.

Ah-See, K.W., Cooke, T.G., Pickford, I.R., Soutar, D. and Balmain, A., 1994. An allelotype of squamous carcinoma of the head and neck using microsatellite markers. Cancer Res, 54(7): 1617-21.

Akashi, T. et al., 2003. Expression and diagnostic evaluation of the human tumor-associated antigen RCAS1 in pancreatic cancer. Pancreas, 26(1): 49-55.

Akervall, J.A. et al., 1997. Amplification of cyclin D1 in squamous cell carcinoma of the head and neck and the prognostic value of chromosomal abnormalities and cyclin D1 overexpression. Cancer, 79(2): 380-9.

Albertson, D.G., 2003. Profiling breast cancer by array CGH. Br Cancer Res & Treat, 78(3): 289-98.

Albertson, D.G. and Pinkel, D., 2003. Genomic microarrays in human genetic disease and cancer. Hum Mol Genet, 12 Spec No 2: R145-52.

Alers, J.C. et al., 2001. Molecular cytogenetic analysis of prostatic adenocarcinomas from screening studies : early cancers may contain aggressive genetic features. Am J Pathol, 158(2): 399-406.

Allen, J.E. et al., 2002. Identification of novel regions of amplification and deletion within mantle cell lymphoma DNA by comparative genomic hybridization. Br J Haematol, 116(2): 291-8.

Arribas, R. et al., 1997. Assessment of genomic damage in colorectal cancer by DNA fingerprinting: prognostic applications. J Clin Oncol, 15(10): 3230-40.

Ashkenazi, A. and Dixit, V.M., 1998. Death receptors: signaling and modulation. Science, 281(5381): 1305-8.

Axelrod, J.D., Matsuno, K., Artavanis-Tsakonas, S. and Perrimon, N., 1996. Interaction between Wingless and Notch signaling pathways mediated by dishevelled. Science, 271(5257): 1826-32.

Baak, J.P. et al., 2003. Genomics and proteomics in cancer. Eur J Cancer, 39(9): 1199-215.

Baldassarre, G. et al., 2001. A truncated form of teratocarcinoma-derived growth factor-1 (cripto-1) mRNA expressed in human colon carcinoma cell lines and tumors. Tumour Biology, 22(5): 286-93.

Balsara, B.R. et al., 1997. Comparative genomic hybridization analysis detects frequent, often high-level, overrepresentation of DNA sequences at 3q, 5p, 7p, and 8q in human non-small cell lung carcinomas. Cancer Res, 57(11): 2116-20.

Battle, M.A., Maher, V.M. and McCormick, J.J., 2003. ST7 is a novel low-density lipoprotein receptor-related protein (LRP) with a cytoplasmic tail that interacts with proteins related to signal transduction pathways. Biochemistry, 42(24): 7270-82.

Bayani, J. and Squire, J.A., 2002a. Spectral karyotyping. Methods Mol Biol, 204: 85-104.

Bayani, J.M. and Squire, J.A., 2002b. Applications of SKY in cancer cytogenetics. Cancer Invest, 20(3): 373-86.

Beder, L.B. et al., 2003. Genome-wide analyses on loss of heterozygosity in head and neck squamous cell carcinomas. Laboratory Investigation., 83(1): 99-105.

Bei, R. et al., 2001. Co-localization of multiple ErbB receptors in stratified epithelium of oral squamous cell carcinoma. Journal of Pathology, 195(3): 343-8.

Bekri, S. et al., 1997. Detailed map of a region commonly amplified at 11q13-->q14 in human breast carcinoma. Cytogenetics & Cell Genetics, 79(1-2): 125-31.

Bocking, A., Biesterfeld, S., Chatelain, R., Gien-Gerlach, G. and Esser, E., 1992. Diagnosis of bronchial carcinoma on sections of paraffin-embedded sputum. Sensitivity and specificity of an alternative to routine cytology. Acta Cytol, 36(1): 37-47.

Bockmuhl, U. et al., 1998. Genomic alterations associated with malignancy in head and neck cancer. Head & Neck., 20(2): 145-51.

Boyle, J.O. et al., 1993. The incidence of p53 mutations increases with progression of head and neck cancer. Cancer Res, 53(19): 4477-80.

Brennan, K., Gonzalez-Sancho, J.M., Castelo-Soccio, L.A., Howe, L.R. and Brown, A.M., 2004. Truncated mutants of the putative Wnt receptor LRP6/Arrow can stabilize beta-catenin independently of Frizzled proteins. Oncogene, 23(28): 4873-84.

Brieger, J. et al., 2003. Chromosomal aberrations in premalignant and malignant squamous epithelium. Cancer Genet Cytogenet, 144(2): 148-55.

Bruder, C.E. et al., 2001. High resolution deletion analysis of constitutional DNA from neurofibromatosis type 2 (NF2) patients using microarray-CGH. Hum Mol Genet, 10(3): 271-82.

Brunin, F. et al., 1999. Cancer of the base of the tongue: past and future. Head Neck, 21(8): 751-9.

Bryce, L.A., Morrison, N., Hoare, S.F., Muir, S. and Keith, W.N., 2000. Mapping of the gene for the human telomerase reverse transcriptase, hTERT, to chromosome 5p15.33 by fluorescence in situ hybridization. Neoplasia, 2(3): 197-201.

Buckley, P.G. et al., 2002. A full-coverage, high-resolution human chromosome 22 genomic microarray for clinical and research applications. Hum Mol Genet, 11(25): 3221-9.

Bullrich, F. et al., 2001. Characterization of the 13q14 tumor suppressor locus in CLL: identification of ALT1, an alternative splice variant of the LEU2 gene. Cancer Res, 61(18): 6640-8.

Burbee, D.G. et al., 2001. Epigenetic inactivation of RASSF1A in lung and breast cancers and malignant phenotype suppression. J Natl Cancer Inst, 93(9): 691-9.

Burger, M.J. et al., 2002. Expression analysis of delta-catenin and prostate-specific membrane antigen: their potential as diagnostic markers for prostate cancer. Int J Cancer, 100(2): 228-37.

Burkitt, H.G., Young, B. and Heath, J.W., 1993. Wheater's Functional Histology - A Text and Colour Atlas. Churchill Livingstone, Edinburgh.

Caldwell, G.M. et al., 2004. The Wnt antagonist sFRP1 in colorectal tumorigenesis. Cancer Res, 64(3): 883-8.

Califano, J. et al., 1996. Genetic progression model for head and neck cancer: implications for field cancerization. Cancer Res, 56(11): 2488-92.

Casey, G. et al., 1996. DNA sequence analysis of exons 2 through 11 and immunohistochemical staining are required to detect all known p53 alterations in human malignancies. Oncogene, 13(9): 1971-81.

Chevalier, G. et al., 1998. novH: differential expression in developing kidney and Wilm's tumors. Am J Pathol, 152(6): 1563-75.

Chi, B., DeLeeuw, R.J., Coe, B.P., MacAulay, C. and Lam, W.L., 2004. SeeGH - A software tool for visualization of whole genome array comparative genomic hybridization data. BMC Bioinformatics, 5(1): 13.

Chung, K.Y. et al., 1993. Discordant p53 gene mutations in primary head and neck cancers and corresponding second primary cancers of the upper aerodigestive tract. Cancer Res, 53(7): 1676-83.

Chung, Y.J. et al., 2004. A whole-genome mouse BAC microarray with 1-Mb resolution for analysis of DNA copy number changes by array comparative genomic hybridization. Genome Res, 14(1): 188-96.

Coe, B.P., Chi, B., MacAulay, C. and Lam, L.W., Weighted Frequency Analysis of Array CGH Data Identifies Novel Regions of Alteration in Mantle Cell Lymphoma. BMC Bioinformatics, Submitted.

Coe, B.P. et al., 2004. High resolution Chromosome 5p array CGH analysis of Small Cell Lung Carcinoma Cell Lines. Genes Chromosomes Cancer, in press.

Corvi, R., Berger, N., Balczon, R. and Romeo, G., 2000. RET/PCM-1: a novel fusion gene in papillary thyroid carcinoma. Oncogene., 19(37): 4236-42.

Dang, T.P. et al., 2000. Chromosome 19 translocation, overexpression of Notch3, and human lung cancer. J Natl Cancer Inst, 92(16): 1355-7.

de Juan, C. et al., 1998. Prognostic value of genomic damage in non-small-cell lung cancer. Br J Cancer, 77(11): 1971-7.

Debant, A. et al., 1996. The multidomain protein Trio binds the LAR transmembrane tyrosine phosphatase, contains a protein kinase domain, and has separate rac-specific and rho-specific guanine nucleotide exchange factor domains. Proc Natl Acad Sci U S A, 93(11): 5466-71.

Dickinson, M.E. and McMahon, A.P., 1992. The role of Wnt genes in vertebrate development. Curr Opin Genet Dev, 2(4): 562-6.

Doll, R., 1981. The smoking-induced epidemic. Can J Public Health, 72(6): 372-81.

Dong, J.T., 2001. Chromosomal deletions and tumor suppressor genes in prostate cancer. Cancer Metastasis Rev, 20(3-4): 173-93.

Dong, S.M. and Sidransky, D., 2002. Absence of ST7 gene alterations in human cancer. Clin Cancer Res, 8(9): 2939-41.

Dorkin, T.J. et al., 1999. FGF8 over-expression in prostate cancer is associated with decreased patient survival and persists in androgen independent disease. Oncogene, 18(17): 2755-61.

Eroschenko, V.P., 2000. di Fiore's Atlas of Histology (with functional correlations). Lippincott Williams & Wilkins, Philadelphia.

Farber, E., 1984. The multistep nature of cancer development. Cancer Res, 44(10): 4217-23.

Fearon, E.R. and Vogelstein, B., 1990. A genetic model for colorectal tumorigenesis. Cell, 61(5): 759-67.

Fontana, R.S. et al., 1986. Lung cancer screening: the Mayo program. J Occup Med, 28(8): 746-50.

Forgacs, E., Zochbauer-Muller, S., Olah, E. and Minna, J.D., 2001. Molecular genetic abnormalities in the pathogenesis of human lung cancer. Pathol Oncol Res, 7(1): 6-13.

Fracchiolla, N.S. et al., 1995. Multiple genetic lesions in laryngeal squamous cell carcinomas. Cancer, 75(6): 1292-301.

Franklin, W.A., Veve, R., Hirsch, F.R., Helfrich, B.A. and Bunn, P.A., Jr., 2002. Epidermal growth factor receptor family in lung cancer and premalignancy. Semin Oncol, 29(1 Suppl 4): 3-14.

Fromont-Hankard, G. et al., 2002. Glial cell-derived neurotrophic factor expression in normal human lung and congenital cystic adenomatoid malformation. Arch Pathol Lab Med, 126(4): 432-6.

Garnis, C., Baldwin, C., Zhang, L., Rosin, M.P. and Lam, W.L., 2003. Use of complete coverage array comparative genomic hybridization to define copy number alterations on chromosome 3p in oral squamous cell carcinomas. Cancer Res, 63(24): 8582-5.

Garnis, C., Buys, T.P.H. and Lam, W.L., 2004a. Genetic alteration and gene expression modulation during cancer progression. Mol Cancer, 3(1): 9.

Garnis, C., Campbell, J., Zhang, L., Rosin, M.P. and Lam, W.L., 2004b. OCGR array: an oral cancer genomic regional array for comparative genomic hybridization analysis. Oral Oncol, 40(5): 511-9.

Garnis, C. et al., 2004c. Novel regions of amplification on 8q distinct from the MYC locus and frequently altered in oral dysplasia and cancer. Genes, Chromosomes Cancer, 39(1): 93-8.

Garnis, C., Coe, B.P., Zhang, L., Rosin, M.P. and Lam, W.L., 2004d. Overexpression of LRP12, a gene contained within an 8q22 amplicon identified by high-resolution array CGH analysis of oral squamous cell carcinomas. Oncogene, 23(14): 2582-6.

Garnis, C., MacAulay, C., Lam, S. and Lam, W., 2004e. Genetic alteration on 8q distinct from MYC in bronchial carcinoma in situ lesions. Lung Cancer, 44(3): 403-4.

Gasparian, A.V. et al., 1998. Allelic imbalance and instability of microsatellite loci on chromosome 1p in human non-small-cell lung cancer. Br J Cancer, 77(10): 1604-11.

Gazdar, A.F. et al., 1994. Molecular genetic changes found in human lung cancer and its precursor lesions. Cold Spring Harb Symp Quant Biol, 59: 565-72.

Girard, L., Zochbauer-Muller, S., Virmani, A.K., Gazdar, A.F. and Minna, J.D., 2000. Genome-wide allelotyping of lung cancer identifies new regions of allelic loss, differences between small cell lung cancer and non-small cell lung cancer, and loci clustering. Cancer Res, 60(17): 4894-906.

Giri, D., Ropiquet, F. and Ittmann, M., 1999. FGF9 is an autocrine and paracrine prostatic growth factor expressed by prostatic stromal cells. J Cell Physiol, 180(1): 53-60.

Goeze, A. et al., 2002. Chromosomal imbalances of primary and metastatic lung adenocarcinomas. J Pathol, 196(1): 8-16.

Grandis, J.R. and Tweardy, D.J., 1993. Elevated levels of transforming growth factor alpha and epidermal growth factor receptor messenger RNA are early markers of carcinogenesis in head and neck cancer. Cancer Res, 53(15): 3579-84.

Gras, E. et al., 2001. Loss of heterozygosity on chromosome 13q12-q14, BRCA-2 mutations and lack of BRCA-2 promoter hypermethylation in sporadic epithelial ovarian tumors. Cancer, 92(4): 787-95.

Gray, J.W. et al., 1991. Applications of fluorescence in situ hybridization in biological dosimetry and detection of disease-specific chromosome aberrations. Prog Clin Biol Res, 372: 399-411.

Greshock, J., Naylor, T.L. and Margolin, A., 2004. 1-Mb resolution array-based comparative genomic hybridization using a BAC clone set optimized for cancer gene analysis. Genome Res, 14(1): 179-87.

Gugger, M. et al., 2001. Alterations of cell cycle regulators are less frequent in advanced non-small cell lung cancer than in resectable tumours. Lung Cancer, 33(2-3): 229-39.

Gupta, V.K., Schmidt, A.P., Pashia, M.E., Sunwoo, J.B. and Scholnick, S.B., 1999. Multiple regions of deletion on chromosome arm 13q in head-and-neck squamous-cell carcinoma. Int J Cancer, 84(5): 453-7.

Ha, P.K. and Califano, J.A., 2003. The molecular biology of mucosal field cancerization of the head and neck. Crit Rev Oral Biol Med, 14(5): 363-9.

Hainaut, P. et al., 1998. IARC Database of p53 gene mutations in human tumors and cell lines: updated compilation, revised formats and new visualisation tools. Nucleic Acids Res, 26(1): 205-13.

Han, S. et al., 1999. Infrequent somatic mutations of the p73 gene in various human cancers. Eur J Surg Oncol, 25(2): 194-8.

Harris, G. et al., 1992. Identification and selective inhibition of an isozyme of steroid 5 alpha-reductase in human scalp. Proc Natl Acad Sci U S A, 89(22): 10787-91.

He, X., Semenov, M., Tamai, K. and Zeng, X., 2004. LDL receptor-related proteins 5 and 6 in Wnt/beta-catenin signaling: arrows point the way. Development, 131(8): 1663-77.

Henderson, L.J. et al., 2004. Genomic and gene expression profiling of minute alterations of chromosome arm 1p in small cell lung carcinoma cells. British Journal of Cancer., submmitted.

Hermsen, M.A. et al., 1998. Genetic analysis of 53 lymph node-negative breast carcinomas by CGH and relation to clinical, pathological, morphometric, and DNA cytometric prognostic factors. J Pathol, 186(4): 356-62.

Herz, J. and Bock, H.H., 2002. Lipoprotein receptors in the nervous system. Annu Rev Biochem, 71: 405-34.

Herz, J. and Strickland, D.K., 2001. LRP: a multifunctional scavenger and signaling receptor. J Clin Invest, 108(6): 779-84.

Hoang, B.H. et al., 2004. Expression of LDL receptor-related protein 5 (LRP5) as a novel marker for disease progression in high-grade osteosarcoma. Int J Cancer, 109(1): 106-11.

Hogg, R.P. et al., 2002. Frequent 3p allele loss and epigenetic inactivation of the RASSF1A tumour suppressor gene from region 3p21.3 in head and neck squamous cell carcinoma.[comment]. European Journal of Cancer., 38(12): 1585-92.

Huang, Q. et al., 2002. Genetic differences detected by comparative genomic hybridization in head and neck squamous cell carcinomas from different tumor sites: construction of oncogenetic trees for tumor progression. Genes Chromosomes Cancer, 34(2): 224-33.

Ikegawa, S., Isomura, M., Koshizuka, Y. and Nakamura, Y., 1999. Cloning and characterization of ASH2L and Ash2l, human and mouse homologs of the Drosophila ash2 gene. Cytogenet Cell Genet, 84(3-4): 167-72.

Ishkanian, A.S. et al., 2004. A tiling resolution DNA microarray with complete coverage of the human genome. Nat Genet, 36(3): 299-303.

Ito, Y. et al., 2003. Overexpression of human tumor-associated antigen, RCAS1, is significantly linked to dedifferentiation of thyroid carcinoma. Oncology, 64(1): 83-9.

Jemal, A. et al., 2003. Cancer statistics, 2003. CA Cancer J Clin, 53(1): 5-26.

Jiang, Y., Woronicz, J.D., Liu, W. and Goeddel, D.V., 1999. Prevention of constitutive TNF receptor 1 signaling by silencer of death domains. Science, 283(5401): 543-6.

Johnson, B.E. et al., 1996. MYC family DNA amplification in 126 tumor cell lines from patients with small cell lung cancer. J Cell Biochem Suppl, 24: 210-7.

Jong, K., Marchiori, E., Meijer, G., Van Der Vaart, A. and Ylstra, B., 2004a. Breakpoint identification and smoothing of array comparative genomic hybridization data. Bioinformatics.

Jong, K.E. et al., 2004b. Remoteness of residence and survival from cancer in New South Wales. Med J Aust, 180(12): 618-22.

Jung, J., Zheng, M., Goldfarb, M. and Zaret, K.S., 1999. Initiation of mammalian liver development from endoderm by fibroblast growth factors. Science, 284(5422): 1998-2003.

Kakinuma, R. et al., 1999. Detection failures in spiral CT screening for lung cancer: analysis of CT findings. Radiology, 212(1): 61-6.

Kallioniemi, O.P., 2001. Biochip technologies in cancer research. Ann Med, 33(2): 142-7.

Kashiwagi, H. and Uchida, K., 2000. Genome-wide profiling of gene amplification and deletion in cancer. Human Cell, 13(3): 135-41.

Kayahara, H., Yamagata, H., Tanioka, H., Miki, T. and Hamakawa, H., 2001. Frequent loss of heterozygosity at 3p25-p26 is associated with invasive oral squamous cell carcinoma. J Hum Genet, 46(6): 335-41.

Kaye, F. et al., 1988. Structure and expression of the human L-myc gene reveal a complex pattern of alternative mRNA processing. Mol Cell Biol, 8(1): 186-95.

Kennedy, T.C., Miller, Y. and Prindiville, S., 2000. Screening for lung cancer revisited and the role of sputum cytology and fluorescence bronchoscopy in a high-risk group. Chest, 117(4 Suppl 1): 72S-79S.

Kiechle, M. et al., 2000. Genetic imbalances in precursor lesions of endometrial cancer detected by comparative genomic hybridization. Am J Pathol, 156(6): 1827-33.

Kirchhoff, M. et al., 1999. Comparative genomic hybridization reveals a recurrent pattern of chromosomal aberrations in severe dysplasia/carcinoma in situ of the cervix and in advanced-stage cervical carcinoma. Genes, Chromosomes Cancer, 24(2): 144-50.

Kirchhoff, M. et al., 2001. Comparative genomic hybridization reveals non-random chromosomal aberrations in early preinvasive cervical lesions. Cancer Genet Cytogenet, 129(1): 47-51.

Kitamura, E. et al., 2000. A transcription map of the minimally deleted region from 13q14 in B-cell chronic lymphocytic leukemia as defined by large scale sequencing of the 650 kb critical region. Oncogene, 19(50): 5772-80.

Klingensmith, J. and Nusse, R., 1994. Signaling by wingless in Drosophila. Dev Biol, 166(2): 396-414.

Kolligs, F.T., Bommer, G. and Goke, B., 2002. Wnt/beta-catenin/tcf signaling: a critical pathway in gastrointestinal tumorigenesis. Digestion, 66(3): 131-44.

Korinek, V. et al., 1997. Constitutive transcriptional activation by a beta-catenin-Tcf complex in APC-/- colon carcinoma. Science, 275(5307): 1784-7.

Kraus, J., Pantel, K., Pinkel, D., Albertson, D.G. and Speicher, M.R., 2003. High-resolution genomic profiling of occult micrometastatic tumor cells. Genes, Chromosomes Cancer, 36(2): 159-66.

Krzywinski, M. et al., 2004. A set of BAC clones spanning the human genome. Nucleic Acids Res, 32(12): 3651-60.

Kuo, M.Y., Lin, C.Y., Hahn, L.J., Cheng, S.J. and Chiang, C.P., 1999. Expression of cyclin D1 is correlated with poor prognosis in patients with areca quid chewing-related oral squamous cell carcinomas in Taiwan. Journal of Oral Pathology & Medicine., 28(4): 165-9.

Lam, S., MacAulay, C., leRiche, J.C. and Palcic, B., 2000. Detection and localization of early lung cancer by fluorescence bronchoscopy. Cancer, 89(11 Suppl): 2468-73.

Lark, A.L. et al., 2003. Overexpression of focal adhesion kinase in primary colorectal carcinomas and colorectal liver metastases: immunohistochemistry and real-time PCR analyses. Clin Cancer Res, 9(1): 215-22.

Lee, A.Y. et al., 2004. Expression of the secreted frizzled-related protein gene family is downregulated in human mesothelioma. Oncogene, 23(39): 6672-6.

Lee, J.I. et al., 2001. Loss of Fhit expression is a predictor of poor outcome in tongue cancer. Cancer Research., 61(3): 837-41.

Lese, C.M. et al., 1995. Visualization of INT2 and HST1 amplification in oral squamous cell carcinomas. Genes Chromosomes Cancer, 12(4): 288-95.

Levine, A.J., 1997. p53, the cellular gatekeeper for growth and division. Cell, 88(3): 323-31.

Li, X. et al., 1994. Allelic loss at chromosomes 3p, 8p, 13q, and 17p associated with poor prognosis in head and neck cancer. J Natl Cancer Inst, 86(20): 1524-9.

Li, Z. et al., 2002. Genome-wide allelotyping of a new in vitro model system reveals early events in breast cancer progression. Cancer Res, 62(20): 5980-7.

Lindblad-Toh, K. et al., 2000. Loss-of-heterozygosity analysis of small-cell lung carcinomas using single-nucleotide polymorphism arrays. Nat Biotechnol, 18(9): 1001-5.

Lingfei, K., Pingzhang, Y., Zhengguo, L., Jianhua, G. and Yaowu, Z., 1998. A study on p16, pRb, cdk4 and cyclinD1 expression in non-small cell lung cancers. Cancer Lett, 130(1-2): 93-101.

Lippman, S.M. and Hong, W.K., 2001. Molecular markers of the risk of oral cancer. N Engl J Med, 344(17): 1323-6.

Lisitsyn, N. and Wigler, M., 1993. Cloning the differences between two complex genomes. Science, 259(5097): 946-51.

Locker, J., 1991. Gene amplification during stages of carcinogenesis. Basic Life Sci, 57: 157-66; discussion 166-70.

Lu, D. et al., 2004. Activation of the Wnt signaling pathway in chronic lymphocytic leukemia. Proc Natl Acad Sci U S A, 101(9): 3118-23.

Lucito, R. et al., 2003. Representational oligonucleotide microarray analysis: a high-resolution method to detect genome copy number variation. Genome Res, 13(10): 2291-305.

Luk, C., Tsao, M.S., Bayani, J., Shepherd, F. and Squire, J.A., 2001. Molecular cytogenetic analysis of non-small cell lung carcinoma by spectral karyotyping and comparative genomic hybridization. Cancer Genet Cytogenet, 125(2): 87-99.

Lumerman, H., Freedman, P. and Kerpel, S., 1995. Oral epithelial dysplasia and the development of invasive squamous cell carcinoma. Oral Surg Oral Med Oral Pathol Oral Radiol Endod, 79(3): 321-9.

Lynch, T.J. et al., 2004. Activating mutations in the epidermal growth factor receptor underlying responsiveness of non-small-cell lung cancer to gefitinib. N Engl J Med, 350(21): 2129-39.

Mabuchi, H. et al., 2001. Cloning and characterization of CLLD6, CLLD7, and CLLD8, novel candidate genes for leukemogenesis at chromosome 13q14, a region commonly deleted in B-cell chronic lymphocytic leukemia. Cancer Res, 61(7): 2870-7.

Macfarlane, G.J., McCredie, M. and Coates, M., 1994. Patterns of oral and pharyngeal cancer incidence in New South Wales, Australia. J Oral Pathol Med, 23(6): 241-5.

Macoska, J.A. et al., 2000. Genetic characterization of immortalized human prostate epithelial cell cultures. Evidence for structural rearrangements of chromosome 8 and i(8q) chromosome formation in primary tumor-derived cells. Cancer Genet Cytogenet, 120(1): 50-7.

Maestro, R. et al., 1996. Chromosome 13q deletion mapping in head and neck squamous cell carcinomas: identification of two distinct regions of preferential loss. Cancer Res, 56(5): 1146-50.

Mahdy, E. et al., 1999. Comparison of comparative genomic hybridization, fluorescence in situ hybridization and flow cytometry in urinary bladder cancer. Anticancer Res, 19(1A): 7-12.

Maier, H., De Vries, N. and Snow, G.B., 1991. Occupational factors in the aetiology of head and neck cancer. Clin Otolaryngol, 16(4): 406-12.

Maitra, A. et al., 2001. High-resolution chromosome 3p allelotyping of breast carcinomas and precursor lesions demonstrates frequent loss of heterozygosity and a discontinuous pattern of allele loss. Am J Pathol, 159(1): 119-30.

Mao, L. et al., 1996. Frequent microsatellite alterations at chromosomes 9p21 and 3p14 in oral premalignant lesions and their value in cancer risk assessment. Nat Med, 2(6): 682-5.

Marchio, A. et al., 2001. Chromosomal abnormalities in liver cell dysplasia detected by comparative genomic hybridisation. Mol Pathol, 54(4): 270-4.

Marra, M.A. et al., 1997. High throughput fingerprint analysis of large-insert clones. Genome Res, 7(11): 1072-84.

Matsuzaki, H. et al., 2004. Parallel genotyping of over 10,000 SNPs using a one-primer assay on a high-density oligonucleotide array. Genome Res, 14(3): 414-25.

McWilliams, A., MacAulay, C., Gazdar, A.F. and Lam, S., 2002. Innovative molecular and imaging approaches for the detection of lung cancer and its precursor lesions. Oncogene, 21(45): 6949-59.

Melamed, M.R. and Flehinger, B.J., 1984. Screening for lung cancer. Chest, 86(1): 2-3.

Merlo, A. et al., 1995. 5' CpG island methylation is associated with transcriptional silencing of the tumour suppressor p16/CDKN2/MTS1 in human cancers. Nat Med, 1(7): 686-92.

Michalides, R. et al., 1995. Overexpression of cyclin D1 correlates with recurrence in a group of forty-seven operable squamous cell carcinomas of the head and neck. Cancer Res, 55(5): 975-8.

Michalides, R.J. et al., 1997. Overexpression of cyclin D1 indicates a poor prognosis in squamous cell carcinoma of the head and neck. Archives of Otolaryngology -- Head & Neck Surgery., 123(5): 497-502.

Minna, J.D., Roth, J.A. and Gazdar, A.F., 2002. Focus on lung cancer. Cancer Cell, 1(1): 49-52.

Mitelman, F., Johansson, B. and Mertens, F., 2003. Mitelman Database of Chromosome Aberrations in Cancer.

Miyamoto, R., Uzawa, N., Nagaoka, S., Hirata, Y. and Amagasa, T., 2003. Prognostic significance of cyclin D1 amplification and overexpression in oral squamous cell carcinomas. Oral Oncol, 39(6): 610-8.

Muller, D. et al., 1997. Amplification of 11q13 DNA markers in head and neck squamous cell carcinomas: correlation with clinical outcome. European Journal of Cancer., 33(13): 2203-10.

Nau, M.M. et al., 1985. L-myc, a new myc-related gene amplified and expressed in human small cell lung cancer. Nature, 318(6041): 69-73.

Navarro, J.M. and Jorcano, J.L., 1999. The use of arbitrarily primed polymerase chain reaction in cancer research. Electrophoresis, 20(2): 283-90.

Nawroz, H. et al., 1994. Allelotype of head and neck squamous cell carcinoma. Cancer Res, 54(5): 1152-5.

Nishida, N. et al., 2002. Prognostic impact of multiple allelic losses on metastatic recurrence in hepatocellular carcinoma after curative resection. Oncology, 62(2): 141-8.

Nomoto, S. et al., 2000. Frequent allelic imbalance suggests involvement of a tumor suppressor gene at 1p36 in the pathogenesis of human lung cancers. Genes Chromosomes Cancer, 28(3): 342-6.

Nusse, R. and Varmus, H.E., 1992. Wnt genes. Cell, 69(7): 1073-87.

Odero, M.D. et al., 2001. Comparative genomic hybridization and amplotyping by arbitrarily primed PCR in stage A B-CLL. Cancer Genet Cytogenet, 130(1): 8-13.

Oga, A. et al., 2002. New perspectives for tumor pathology provided by comparative genomic hybridization. Int J Clin Oncol, 7(3): 133-7.

Ogawara, K. et al., 1998. Allelic loss of chromosome 13q14.3 in human oral cancer: correlation with lymph node metastasis. Int J Cancer, 79(4): 312-7.

Ohkubo, N. et al., 2003. Apolipoprotein E and Reelin ligands modulate tau phosphorylation through an apolipoprotein E receptor/disabled-1/glycogen synthase kinase-3beta cascade. FASEB Journal, 17(2): 295-7.

Ohtani, N., Yamakoshi, K., Takahashi, A. and Hara, E., 2004. The p16INK4a-RB pathway: molecular link between cellular senescence and tumor suppression. J Med Invest, 51(3-4): 146-53.

Oizumi, S. et al., 2002. RCAS1 expression: a potential prognostic marker for adenocarcinomas of the lung. Oncology, 62(4): 333-9.

Oliver, C.J. and Shenolikar, S., 1998. Physiologic importance of protein phosphatase inhibitors. Front Biosci, 3: D961-72.

Osoegawa, K. et al., 2001. A bacterial artificial chromosome library for sequencing the complete human genome. Genome Res, 11(3): 483-96.

Ozawa, F., Friess, H., Zimmermann, A., Kleeff, J. and Buchler, M.W., 2000. Enhanced expression of Silencer of death domains (SODD/BAG-4) in pancreatic cancer. Biochem Biophys Res Commun, 271(2): 409-13.

Paez, J.G. et al., 2004. EGFR mutations in lung cancer: correlation with clinical response to gefitinib therapy. Science, 304(5676): 1497-500.

Palcic, B., Lam, S., Hung, J. and MacAulay, C., 1991. Detection and localization of early lung cancer by imaging techniques. Chest, 99(3): 742-3.

Paris, P.L. et al., 2003. High-resolution analysis of paraffin-embedded and formalin-fixed prostate tumors using comparative genomic hybridization to genomic microarrays. Am J Pathol, 162(3): 763-70.

Parkin, D.M., Pisani, P. and Ferlay, J., 1999. Global cancer statistics. CA Cancer J Clin, 49(1): 33-64, 1.

Partridge, M., Emilion, G., Pateromichelakis, S., Phillips, E. and Langdon, J., 1999. Location of candidate tumour suppressor gene loci at chromosomes 3p, 8p and 9p for oral squamous cell carcinomas. Int J Cancer, 83(3): 318-25.

Partridge, M., Pateromichelakis, S., Phillips, E., Emilion, G. and Langdon, J., 2001. Profiling clonality and progression in multiple premalignant and malignant oral lesions identifies a subgroup of cases with a distinct presentation of squamous cell carcinoma. Clin Cancer Res, 7(7): 1860-6.

Pekarsky, Y. et al., 2004. Fhit is a physiological target of the protein kinase Src. Proc Natl Acad Sci U S A, 101(11): 3775-9.

Penkov, D. et al., 2000. Cloning of a human gene closely related to the genes coding for the c-myc single-strand binding proteins. Gene, 243(1-2): 27-36.

Piboonniyom, S.O., Timmermann, S., Hinds, P. and Munger, K., 2002. Aberrations in the MTS1 tumor suppressor locus in oral squamous cell carcinoma lines preferentially affect the INK4A gene and result in increased cdk6 activity. Oral Oncol, 38(2): 179-86.

Pinkel, D. et al., 1998. High resolution analysis of DNA copy number variation using comparative genomic hybridization to microarrays. Nat Genet, 20(2): 207-11.

Pirvola, U. et al., 2002. FGFR1 is required for the development of the auditory sensory epithelium. Neuron, 35(4): 671-80.

Pollack, J.R. et al., 2002. Microarray analysis reveals a major direct role of DNA copy number alteration in the transcriptional program of human breast tumors. Proc Natl Acad Sci USA, 99(20): 12963-8.

Qing, J., Wei, D., Maher, V.M. and McCormick, J.J., 1999. Cloning and characterization of a novel gene encoding a putative transmembrane protein with altered expression in some human transformed and tumor-derived cell lines. Oncogene, 18(2): 335-42.

Radtke, F. and Raj, K., 2003. The role of Notch in tumorigenesis: oncogene or tumour suppressor? Nat Rev Cancer, 3(10): 756-67.

Ragnarsson, G. et al., 1999. Loss of heterozygosity at chromosome 1p in different solid human tumours: association with survival. Br J Cancer, 79(9-10): 1468-74.

Raschke, S., Balz, V., Efferth, T., Schulz, W.A. and Florl, A.R., 2005. Homozygous deletions of CDKN2A caused by alternative mechanisms in various human cancer cell lines. Genes Chromosomes Cancer, 42(1): 58-67.

Reed, A.L. et al., 1996. High frequency of p16 (CDKN2/MTS-1/INK4A) inactivation in head and neck squamous cell carcinoma. Cancer Research., 56(16): 3630-3.

Renan, M.J., 1993. How many mutations are required for tumorigenesis? Implications from human cancer data. Mol Carcinog, 7(3): 139-46.

Richardson, G.E. and Johnson, B.E., 1993. The biology of lung cancer. Semin Oncol, 20(2): 105-27.

Ried, T. et al., 1994. Mapping of multiple DNA gains and losses in primary small cell lung carcinomas by comparative genomic hybridization. Cancer Res, 54(7): 1801-6.

Rijsewijk, F. et al., 1987. The Drosophila homolog of the mouse mammary oncogene int-1 is identical to the segment polarity gene wingless. Cell, 50(4): 649-57.

Rodriguez, S. et al., 2003. Expression profile of genes from 12p in testicular germ cell tumors of adolescents and adults associated with i(12p) and amplification at 12p11.2-p12.1. Oncogene, 22(12): 1880-91.

Rosin, M.P. et al., 2000. Use of allelic loss to predict malignant risk for low-grade oral epithelial dysplasia. Clin Cancer Res, 6(2): 357-62.

Rowley, H., Jones, A., Spandidos, D. and Field, J., 1996. Definition of a tumor suppressor gene locus on the short arm of chromosome 3 in squamous cell carcinoma of the head and neck by means of microsatellite markers. Archives of Otolaryngology -- Head & Neck Surgery., 122(5): 497-501.

Roylance, R., 2002. Methods of molecular analysis: assessing losses and gains in tumours. Mol Pathol, 55(1): 25-8.

Roz, L. et al., 1996. Allelic imbalance on chromosome 3p in oral dysplastic lesions: an early event in oral carcinogenesis. Cancer Res, 56(6): 1228-31.

Rubin, E., Tamrakar, S. and Ludlow, J.W., 1998. Protein phosphatase type 1, the product of the retinoblastoma susceptibility gene, and cell cycle control. Front Biosci, 3: D1209-19.

Ruddon, R.W., 1995. Cancer Biology. Oxford University Press, New York.

Sanchez-Cespedes, M., Okami, K., Cairns, P. and Sidransky, D., 2000. Molecular analysis of the candidate tumor suppressor gene ING1 in human head and neck tumors with 13q deletions. Genes Chromosomes Cancer, 27(3): 319-22.

Sanchez-Izquierdo, D. et al., 2003. MALT1 is deregulated by both chromosomal translocation and amplification in B-cell non-Hodgkin lymphoma. Blood, 101(11): 4539-46.

Saranath, D., Bhoite, L.T., Mehta, A.R., Sanghavi, V. and Deo, M.G., 1991. Loss of allelic heterozygosity at the harvey ras locus in human oral carcinomas. J Cancer Res Clin Oncol, 117(5): 484-8.

Saretzki, G., Petersen, S., Petersen, I., Kolble, K. and von Zglinicki, T., 2002. hTERT gene dosage correlates with telomerase activity in human lung cancer cell lines. Cancer Lett, 176(1): 81-91.

Sattler, H.P., Rohde, V., Bonkhoff, H., Zwergel, T. and Wullich, B., 1999. Comparative genomic hybridization reveals DNA copy number gains to frequently occur in human prostate cancer. Prostate, 39(2): 79-86.

Saura, C.A. et al., 2000. The nonconserved hydrophilic loop domain of presenilin (PS) is not required for PS endoproteolysis or enhanced abeta 42 production mediated by familial early onset Alzheimer's disease-linked PS variants. J Biol Chem, 275(22): 17136-42.

Scarpa, A., Moore, P.S., Rigaud, G. and Menestrina, F., 2001. Genetic alterations in primary mediastinal B-cell lymphoma: an update. Leukemia & Lymphoma, 41(1-2): 47-53.

Schillace, R.V. and Scott, J.D., 1999. Association of the type 1 protein phosphatase PP1 with the A-kinase anchoring protein AKAP220. Curr Biol, 9(6): 321-4.

Schillace, R.V., Voltz, J.W., Sim, A.T., Shenolikar, S. and Scott, J.D., 2001. Multiple interactions within the AKAP220 signaling complex contribute to protein phosphatase 1 regulation. J Biol Chem, 276(15): 12128-34.

Schleger, C., Arens, N., Zentgraf, H., Bleyl, U. and Verbeke, C., 2000. Identification of frequent chromosomal aberrations in ductal adenocarcinoma of the pancreas by comparative genomic hybridization (CGH). J Pathol, 191(1): 27-32.

Schneider, G.B. et al., 2002. Elevated focal adhesion kinase expression facilitates oral tumor cell invasion. Cancer, 95(12): 2508-15.

Schneider, W.J. and Nimpf, J., 2003. LDL receptor relatives at the crossroad of endocytosis and signaling. Cell Mol Life Sci, 60(5): 892-903.

Scholes, A.G. et al., 1998. Synchronous oral carcinomas: independent or common clonal origin? Cancer Res, 58(9): 2003-6.

Sekido, Y., Fong, K.M. and Minna, J.D., 1998. Progress in understanding the molecular pathogenesis of human lung cancer. Biochim Biophys Acta, 1378(1): F21-59.

Selim, A.G., Ryan, A., El-Ayat, G. and Wells, C.A., 2002. Loss of heterozygosity and allelic imbalance in apocrine metaplasia of the breast: microdissection microsatellite analysis. J Pathol, 196(3): 287-91.

Sengelov, L. et al., 2000. Loss of heterozygosity at 1p, 8p, 10p, 13q, and 17p in advanced urothelial cancer and lack of relation to chemotherapy response and outcome. Cancer Genet Cytogenet, 123(2): 109-13.

Serrano, M., Hannon, G.J. and Beach, D., 1993. A new regulatory motif in cell-cycle control causing specific inhibition of cyclin D/CDK4.[comment]. Nature., 366(6456): 704-7.

Shafer, W.G. and Waldron, C.A., 1975. Erythroplakia of the oral cavity. Cancer, 36(3): 1021-8.

Shin, D.M. et al., 1996. p53 expressions: predicting recurrence and second primary tumors in head and neck squamous cell carcinoma. J Natl Cancer Inst, 88(8): 519-29.

Shintani, S. et al., 2002. Expression of cell cycle control proteins in normal epithelium, premalignant and malignant lesions of oral cavity. Oral Oncology., 38(3): 235-43.

Silverman, S., Jr. and Gorsky, M., 1990. Epidemiologic and demographic update in oral cancer: California and national data--1973 to 1985. J Am Dent Assoc, 120(5): 495-9.

Simpson, D.J. et al., 2003. Genome-wide amplification and allelotyping of sporadic pituitary adenomas identify novel regions of genetic loss. Genes, Chromosomes Cancer, 37(3): 225-36.

Siwoski, A. et al., 2002. An efficient method for the assessment of DNA quality of archival microdissected specimens. Modern Path, 15(8): 889-92.

Slaughter, D.P., Southwick, H.W. and Smejkal, W., 1953. Field cancerization in oral stratified squamous epithelium; clinical implications of multicentric origin. Cancer, 6(5): 963-8.

Snaith, M.R. et al., 1996. Genomic structure and chromosomal mapping of the mouse nov gene. Genomics, 38(3): 425-8.

Snijders, A.M. et al., 2001. Assembly of microarrays for genome-wide measurement of DNA copy number. Nat Genet, 29(3): 263-4.

Solinas-Toldo, S. et al., 1997. Matrix-based comparative genomic hybridization: biochips to screen for genomic imbalances. Genes Chromosomes Cancer, 20(4): 399-407.

Sone, S., 2000. [Treatment of lung cancer: recent progress]. Nippon Naika Gakkai Zasshi, 89(3): 560-4.

Soriano, S. et al., 2001. Presenilin 1 negatively regulates beta-catenin/T cell factor/lymphoid enhancer factor-1 signaling independently of beta-amyloid precursor protein and notch processing. J Cell Biol, 152(4): 785-94.

Steen, H.B., 2000. Flow cytometry of bacteria: glimpses from the past with a view to the future. J Microbiol Methods, 42(1): 65-74.

Steiner, T. et al., 2002. Gain in chromosome 8q correlates with early progression in hormonal treated prostate cancer. Eur Urol, 41(2): 167-71.

Sturgis, E.M. and Miller, R.H., 1995. Second primary malignancies in the head and neck cancer patient. Ann Otol Rhinol Laryngol, 104(12): 946-54.

Su, J.M., Gui, L., Zhou, Y.P. and Zha, X.L., 2002. Expression of focal adhesion kinase and alpha5 and beta1 integrins in carcinomas and its clinical significance. World J Gastroenterol, 8(4): 613-8.

Suarez, P., Batsakis, J.G. and el-Naggar, A.K., 1998. Leukoplakia: still a gallimaufry or is progress being made?--A review. Adv Anat Pathol, 5(3): 137-55.

Sugio, K., Kishimoto, Y., Virmani, A.K., Hung, J.Y. and Gazdar, A.F., 1994. K-ras mutations are a relatively late event in the pathogenesis of lung carcinomas. Cancer Res, 54(22): 5811-5.

Sun, P.C., el-Mofty, S.K., Haughey, B.H. and Scholnick, S.B., 1995. Allelic loss in squamous cell carcinomas of the larynx: discordance between primary and metastatic tumors. Genes Chromosomes Cancer, 14(2): 145-8.

Suzuki, H. et al., 2004. Epigenetic inactivation of SFRP genes allows constitutive WNT signaling in colorectal cancer. Nat Genet, 36(4): 417-22.

Tachdjian, G., Aboura, A., Lapierre, J.M. and Viguie, F., 2000. Cytogenetic analysis from DNA by comparative genomic hybridization. Ann Genet, 43(3-4): 147-54.

Takahashi, M., 2001. The GDNF/RET signaling pathway and human diseases. Cytokine Growth Factor Rev, 12(4): 361-73.

Taketo, M.M., 2004. Shutting down Wnt signal-activated cancer. Nat Genet, 36(4): 320-2.

Tamai, K. et al., 2000. LDL-receptor-related proteins in Wnt signal transduction. Nature, 407(6803): 530-5.

Testa, J.R. et al., 1994. Cytogenetic analysis of 63 non-small cell lung carcinomas: recurrent chromosome alterations amid frequent and widespread genomic upheaval. Genes, Chromosomes & Cancer, 11(3): 178-94.

Thayer, S.P. et al., 2003. Hedgehog is an early and late mediator of pancreatic cancer tumorigenesis. Nature, 425(6960): 851-6.

Trask, B.J., 1991. Fluorescence in situ hybridization: applications in cytogenetics and gene mapping. Trends Genet, 7(5): 149-54.

Travis, W.D., Travis, L.B. and Devesa, S.S., 1995. Lung cancer. Cancer, 75(1 Suppl): 191-202.

Tsuneizumi, M., Nagai, H., Harada, H., Kazui, T. and Emi, M., 2002. A highly polymorphic CA repeat marker at the EBAG9/RCAS1 locus on 8q23 that detected frequent multiplication in breast cancer. Ann Hum Biol, 29(4): 457-60.

Uematsu, K. et al., 2003a. Activation of the Wnt pathway in non small cell lung cancer: evidence of dishevelled overexpression. Oncogene, 22(46): 7218-21.

Uematsu, K. et al., 2003b. Wnt pathway activation in mesothelioma: evidence of Dishevelled overexpression and transcriptional activity of beta-catenin. Cancer Res, 63(15): 4547-51.

Ullmann, R. et al., 1998. Unbalanced chromosomal aberrations in neuroendocrine lung tumors as detected by comparative genomic hybridization. Hum Pathol, 29(10): 1145-9.

Uthoff, S.M., Eichenberger, M.R., McAuliffe, T.L., Hamilton, C.J. and Galandiuk, S., 2001. Wingless-type frizzled protein receptor signaling and its putative role in human colon cancer. Mol Carcinog, 31(1): 56-62.

Uzawa, N. et al., 2001. Homozygous deletions on the short arm of chromosome 3 in human oral squamous cell carcinomas. Oral Oncology., 37(4): 351-6.

van der Riet, P. et al., 1994. Frequent loss of chromosome 9p21-22 early in head and neck cancer progression. Cancer Res, 54(5): 1156-8.

van Oijen, M.G., van de Craats, J.G. and Slootweg, P.J., 1999. p53 overexpression in oral mucosa in relation to smoking. J Pathol, 187(4): 469-74.

Veltman, J.A. et al., 2003. Array-based Comparative Genomic Hybridization for Genome-Wide Screening of DNA Copy Number in Bladder Tumors. Cancer Res, 63(11): 2872-80.

Vermeulen, K., Van Bockstaele, D.R. and Berneman, Z.N., 2003. The cell cycle: a review of regulation, deregulation and therapeutic targets in cancer. Cell Prolif, 36(3): 131-49.

Viswanathan, M., Sangiliyandi, G., Vinod, S.S., Mohanprasad, B.K. and Shanmugam, G., 2003. Genomic Instability and Tumor-specific Alterations

in Oral Squamous Cell Carcinomas Assessed by Inter- (Simple Sequence Repeat) PCR. Clin Cancer Res, 9(3): 1057-1062.

Vizcarra, E. et al., 2001. Identification of two subgroups of mantle cell leukemia with distinct clinical and biological features. Hematol J, 2(4): 234-41.

Wada, T. et al., 2000. Bladder cancer: allelic deletions at and around the retinoblastoma tumor suppressor gene in relation to stage and grade. Clin Cancer Res, 6(2): 610-5.

Wallace-Brodeur, R.R. and Lowe, S.W., 1999. Clinical implications of p53 mutations. Cell Mol Life Sci, 55(1): 64-75.

Wang, D.G. et al., 1998. Large-scale identification, mapping, and genotyping of single-nucleotide polymorphisms in the human genome. Science, 280(5366): 1077-82.

Welsh, J. and McClelland, M., 1990. Fingerprinting genomes using PCR with arbitrary primers. Nucleic Acids Res, 18(24): 7213-8.

Wesley, C.S., 1999. Notch and wingless regulate expression of cuticle patterning genes. Mol Cell Biol, 19(8): 5743-58.

Wiebe, J.P. and Lewis, M.J., 2003. Activity and expression of progesterone metabolizing 5alpha-reductase, 20alpha-hydroxysteroid oxidoreductase and 3alpha(beta)-hydroxysteroid oxidoreductases in tumorigenic (MCF-7, MDA-MB-231, T-47D) and nontumorigenic (MCF-10A) human breast cancer cells. BMC Cancer, 3(1): 9.

Wieland, I. and Bohm, M., 1994. Frequent allelic deletion at a novel locus on chromosome 5 in human lung cancer. Cancer Res, 54(7): 1772-4.

Wieland, I. et al., 1996. Allelic deletion mapping on chromosome 5 in human carcinomas. Oncogene, 12(1): 97-102.

Wilhelm, M. et al., 2002. Array-based comparative genomic hybridization for the differential diagnosis of renal cell cancer. Cancer Res, 62(4): 957-60.

Williams, J.G., Kubelik, A.R., Livak, K.J., Rafalski, J.A. and Tingey, S.V., 1990. DNA polymorphisms amplified by arbitrary primers are useful as genetic markers. Nucleic Acids Res, 18(22): 6531-5.

Wissmann, C. et al., 2003. WIF1, a component of the Wnt pathway, is down-regulated in prostate, breast, lung, and bladder cancer. J Pathol, 201(2): 204-12.

Wistuba, II et al., 2000. High resolution chromosome 3p allelotyping of human lung cancer and preneoplastic/preinvasive bronchial epithelium reveals multiple,

discontinuous sites of 3p allele loss and three regions of frequent breakpoints. Cancer Res, 60(7): 1949-60.

Wistuba, II et al., 2002. High resolution chromosome 3p, 8p, 9q and 22q allelotyping analysis in the pathogenesis of gallbladder carcinoma. Br J Cancer, 87(4): 432-40.

Wolf, S. et al., 2001. B-cell neoplasia associated gene with multiple splicing (BCMS): the candidate B-CLL gene on 13q14 comprises more than 560 kb covering all critical regions. Hum Mol Genet, 10(12): 1275-85.

Xia, W. et al., 1999. Combination of EGFR, HER-2/neu, and HER-3 is a stronger predictor for the outcome of oral squamous cell carcinoma than any individual family members. Clinical Cancer Research., 5(12): 4164-74.

Yakushiji, T. et al., 2001. Analysis of a role for p16/CDKN2 expression and methylation patterns in human oral squamous cell carcinoma. Bull Tokyo Dent Coll, 42(3): 159-68.

Yamada, T. et al., 2000. Frequent chromosome 8q gains in human small cell lung carcinoma detected by arbitrarily primed-PCR genomic fingerprinting. Cancer Genet Cytogenet, 120(1): 11-7.

Yamamoto, F. et al., 2001. NotI-MseII methylation-sensitive amplied fragment length polymorhism for DNA methylation analysis of human cancers. Electrophoresis, 22(10): 1946-56.

Yamashita, K., Dai, T., Dai, Y., Yamamoto, F. and Perucho, M., 2003. Genetics supersedes epigenetics in colon cancer phenotype. Cancer Cell, 4(2): 121-31.

Yarbrough, W.G. et al., 1994. ras mutations and expression in head and neck squamous cell carcinomas. Laryngoscope, 104(11 Pt 1): 1337-47.

Yin, X.Y. et al., 1991. Gene amplification and gene dosage in cell lines derived from squamous cell carcinoma of the head and neck. Genes Chromosomes Cancer, 3(6): 443-54.

Yoo, G.H. et al., 1994. Infrequent inactivation of the retinoblastoma gene despite frequent loss of chromosome 13q in head and neck squamous cell carcinoma. Cancer Res, 54(17): 4603-6.

Yuan, L. et al., 1999. Isolation of a novel gene, TSP50, by a hypomethylated DNA fragment in human breast cancer. Cancer Research., 59(13): 3215-21.

Zabarovsky, E.R., Lerman, M.I. and Minna, J.D., 2002. Tumor suppressor genes on chromosome 3p involved in the pathogenesis of lung and other cancers. Oncogene., 21(45): 6915-35.

Zajac-Kaye, M., 2001. Myc oncogene: a key component in cell cycle regulation and its implication for lung cancer. Lung Cancer, 34 Suppl 2: S43-6.

Zhang, L. et al., 1997a. Molecular analysis of oral lichen planus. A premalignant lesion? Am J Pathol, 151(2): 323-7.

Zhang, L. et al., 1997b. Gene expression profiles in normal and cancer cells. Science, 276(5316): 1268-72.

Zhao, L., Hayes, K., Khan, Z. and Glassman, A., 2001. Spectral karyotyping study of chromosome abnormalities in human leukemia. Cancer Genet Cytogenet, 127(2): 143-7.

Zheng, M. et al., 2004. TRIO amplification and abundant mRNA expression is associated with invasive tumor growth and rapid tumor cell proliferation in urinary bladder cancer. Am J Pathol, 165(1): 63-9.

Zhu, C.Q. et al., 2004. Skp2 gene copy number aberrations are common in non-small cell lung carcinoma, and its overexpression in tumors with ras mutation is a poor prognostic marker. Clin Cancer Res, 10(6): 1984-91.